Effet de l'hétérogénéité du peuplement sur les charges imposées par le vent

Thèse

Marine Duperat

Doctorat en sciences forestières
Philosophiæ doctor (Ph. D.)

Québec, Canada

Effet de l'hétérogénéité du peuplement sur les charges imposées par le vent

Thèse de Doctorat

Marine Duperat

Sous la direction de :

Jean-Claude Ruel, directeur de recherche

Barry Gardiner, codirecteur de recherche

Résumé

Depuis une vingtaine d'années, la gestion forestière tend à augmenter l'utilisation de coupes partielles dans les peuplements régénérés naturellement, laissant les arbres résiduels sujets à un risque accru de dommages éoliens durant leurs premières années d'acclimatation. Largement répandu au Québec, le sapin baumier (*Abies balsamea* (L.) Mill.) est une essence connue pour être particulièrement vulnérable aux dommages éoliens. Afin de mitiger les pertes dans les sapinières naturellement régénérées, il est important de comprendre comment réagissent les sapins baumiers face aux charges de vent, et de trouver des paramètres sylvicoles spécifiques à intégrer dans les modèles de gestion des risques de chablis. Ceci permettrait d'aider les gestionnaires à mitiger les risques lors du choix de prescription sylvicole. Le principal objectif de cette thèse était d'étudier les charges de vents interceptées par un échantillon de sapin baumier en conditions estivales, hivernales et à la suite d'un retrait des compétiteurs proches.

Pour réaliser cet objectif, un réseau de capteurs et d'acquisiteurs de données a été mis en place dans une sapinière à bouleau blanc de la Forêt Montmorency (Forêt expérimentale de l'Université Laval) pour avoir une prise de données continue durant trois saisons : l'été 2018, l'hiver 2019, et l'été 2019 à la suite d'une coupe partielle. Une tour aluminium équipée de deux anémomètres placés à hauteur et mi-hauteur de la canopée et de sondes de températures (air et sol) a été installée en bordure de peuplement pour suivre en continu les événements météorologiques. En parallèle, des jauges de contrainte fixées aux troncs de sapins baumiers ont permis de mesurer les moments de flexion induits par le vent sur un échantillon d'arbres. Durant l'hiver, un suivi continu de la quantité de neige sur les houppiers a été réalisé à l'aide d'une caméra de chasse pour évaluer l'effet additionnel de la neige sur la charge de vent. Au début de l'été 2019, une éclaircie localisée a été réalisée pour retirer l'ensemble des compétiteurs dans un rayon de 3.5m autour de 2/3 des arbres étudiés.

Les principaux résultats de cette thèse démontrent (1) l'importance de l'utilisation d'indices de compétition, notamment C_{BAL}, dans la modélisation des risques de chablis en peuplement hétérogène ; (2) l'impact global de l'hiver sur l'augmentation des moments de force appliqués sur les troncs et cela indépendamment de l'épaisseur de neige sur les houppiers ; et (3) l'effet local mais en même temps global d'une coupe partielle sur l'augmentation des moments de forces appliqués sur les arbres d'un peuplement, les arbres les moins compétitifs étant les plus affectés.

Abstract

Over the past twenty years, forest management has tended to increase the use of partial cutting in naturally regenerated stands, leaving residual trees at increased risk of wind damage during their first years of acclimation. Widespread in Quebec, balsam fir (*Abies balsamea* (L.) Mill.) is a species known to be particularly vulnerable to wind damage. To mitigate losses in naturally regenerated balsam fir stands, it is important to understand how balsam fir trees bend under wind loads, and to find specific silvicultural parameters to be integrated into wind risk management models. This should help managers mitigate risks when choosing silvicultural prescriptions. The main objective of this thesis was to study the wind loads experienced by balsam fir trees under summer and winter conditions and following the removal of nearby competitors.

For this purpose, a network of sensors and data loggers was set up in a white birch-balsam fir stand in the Montmorency Forest (Laval University's experimental forest) for continuous data collection over three seasons: summer 2018, winter 2019, and summer 2019 following partial cutting. An aluminium tower equipped with two anemometers placed at the height and mid-height of the canopy and temperature sensors (air and soil) was installed at the edge of the stand to continuously monitor weather events. At the same time, strain gauges attached to balsam fir trunks made it possible to measure wind induced bending moments on a sample of trees. During the winter, continuous monitoring of the amount of snow on tree crowns was carried out using a hunting camera to assess the additional effect of snow on wind load. At the beginning of summer 2019, a localised thinning was carried out to remove all competitors within a radius of 3.5m around 2/3 of the trees studied.

The main results of this thesis demonstrate (1) the importance of using competition indices, in particular C_{BAL}, in modelling the risk of wind damages in heterogeneous stands; (2) the global impact of winter on the increase in the turning moments experienced by the trunks, regardless of the thickness of snow on the canopies; and (3) the local, but also global, effect of partial cutting on the increase in the turning moments experienced by all the trees in a stand, with the most suppressed trees being the most at risk.

Table des matières

Liste des figures

Liste des tables

Liste des abréviations

AIC Akaike Information Criterion
BA basal area | *Surface basale*
C_x Competition index |*Indice de compétition*
CD Crown Depth | *Longueur de houppier* (m)
CR Crown Radius | *Largeur de houppier* (m)
CrownD Crown Depth | *Longueur de houppier* (m)
CrownW Crown Width | *Largeur de houppier* (m)
CWS Critical Wind Speed | *Vitesse de vent critique* ($m \cdot s^{-1}$)
CWS_{break} Critical Wind Speed for breakage | *Vitesse de vent critique pour le bris* ($m \cdot s^{-1}$)
CWS_{over} Critical Wind Speed for overturning | *Vitesse de vent critique pour le déracinement* ($m \cdot s^{-1}$)
DBH Diameter at Breast Height ~130cm |*Diamètre à hauteur de poitrine ~130cm*
D_{cs} Distance competitor-subject | *Distance compétiteur - sujet* (m)
FG_TMC ForestGALES + TMC model
FG_TMC_BAL ForestGALES + TMC + BAL competition index model
H Tree height | *Hauteur de l'arbre* (m)
M Known applied turning moment | *Moment de force connu appliqué* (Nm)
M_{Max} Maximal hourly turning moment |*Moment de force maximum horaire* (Nm)
MOR Modulus of Rupture | *Module de rupture* (Pa)
STS Strain Transducer Signal | *Signal des jauges de contraintes* (mV/V)
SW Stem Weight | *Poids de la tige* (kg)
TMC Turning Moment Coefficient | *Coefficient de moment de flexion* (kg)
TMC_{invivo} Turning moment coefficient measured on field | *Coefficient de moment de flexion mesuré sur le terrain* (kg)
WAsP Wind Atlas Analysis and Application Program
WS Wind Speed | *Vitesse du vent* ($m \cdot s^{-1}$)

Dédicace

À mes parents qui m'ont toujours poussée et soutenue autant moralement que financièrement pendant ces dix longues années d'études universitaires. À mes sœurs et mes grands-parents, qui ont accepté la distance et ont continué à croire en moi et à me soutenir. À Roman qui malgré notre récente séparation m'a épaulé durant les 8 dernières années et a accepté de me suivre à travers le monde. À François et Nathalie, mes 'parents de cœur' québécois, qui ont su me donner une famille dans un pays où je n'en avais pas. À Olivier et Emilie, Caroline, Pierre-Yves, Isolde, Karelle, Amandine, Louis-Philippe, et tous ceux que j'oublie car la liste est longue ! Pour votre soutien moral, pour les soirées jeux et les sorties plein air, et pour m'avoir aidé à m'intégrer rapidement et faire de Québec ma nouvelle maison. À Heidi et sa bonne humeur contagieuse, toujours présente pour m'aider et me remonter le moral en me donnant un morceau de chocolat ou en improvisant une pause-café virtuelle.

Et plus légèrement, à mon chat Minicrotte, qui malgré une lutte permanente pour l'utilisation du clavier d'ordinateur, m'a permis de ne pas 'virer folle' pendant ces mois d'isolement, de télétravail et de pandémie.

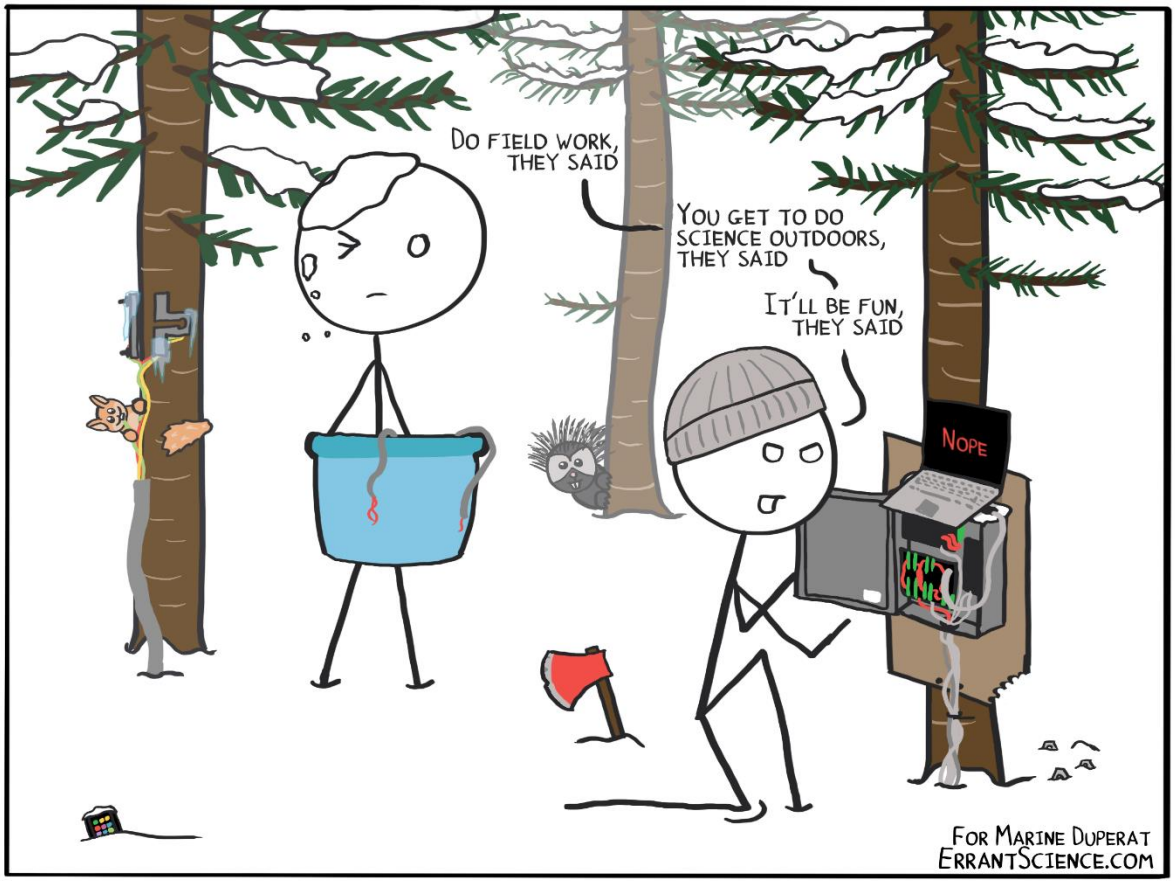
DO FIELD WORK, THEY SAID
YOU GET TO DO SCIENCE OUTDOORS, THEY SAID
IT'LL BE FUN, THEY SAID
NOPE
FOR MARINE DUPERAT
ERRANTSCIENCE.COM

Remerciements

Je tiens tout d'abord à remercier mes directeurs de recherche, Jean-Claude Ruel et Barry Gardiner, pour leurs bons conseils et leur soutien moral dans les bons comme dans les mauvais moments ; pour leur soutien financier tout au long de l'aventure et pour m'avoir permis de voyager à plusieurs reprises pour des conférences, ateliers et stages internationaux. Merci de m'avoir fait confiance et de ne pas m'avoir laissé abandonner en cours de route.

Je souhaite également remercier mon comité d'encadrement, Sylvain Jutras et Alexis Achim, tous deux professeurs à l'Université Laval, qui ont été de bons conseils et d'un bon soutien au gré des rencontres annuelles et des rencontres de couloir.

Merci à Alain Cloutier (Université Laval, Québec, Canada), Thièry Constant (INRA, Champenoux, France) et Alexia Stokes (INRA, Montpellier, France) qui ont accepté leur mission en tant que membres du jury, et ont pris le temps de corriger et d'évaluer mon travail.

Bien entendu, je remercie aussi la Faculté de Foresterie, de Géographie et de Géomatique et toute l'équipe de la Forêt Montmorency, les « travailleurs de l'ombre », notamment Julie Bouliane et Robert Côté pour leur soutien logistique permanent. Je souhaite aussi mentionner la plus-value importante qu'apporte le Centre d'Étude de la Forêt, pour leurs nombreuses bourses de soutien aux étudiants gradués, mais surtout pour avoir pris l'initiative de financer la prolongation de mon stage en Nouvelle-Zélande lorsque j'étais bloquée à cause de la pandémie.

Merci à Evelyne Thiffault pour m'avoir fait confiance dans l'encadrement du cours d'Écologie Forestière deux années de suite, et pour m'avoir remise dans les rails lorsque je doutais de mes capacités. Merci à Yan Boulanger qui a été un support virtuel extraordinaire durant ces longues semaines d'isolement, de rédaction et de recherche d'emploi. Et merci aux nombreux étudiants qui sont venus aider ponctuellement sur mon projet de recherche, et notamment Philippe Leblanc qui a passé un été entier avec moi lors de ma première saison de terrain.

Et finalement : un ENORME merci à François Larochelle, pour son aide dans le laboratoire et pour les interminables heures passées sur le terrain été comme hiver à galérer, à rire et à « pogner les nerfs ». Merci pour ton support et pour les innombrables connaissances que tu m'as apportées, le projet n'aurait clairement pas été réalisable sans toi.

Avant-propos

Cette thèse par insertion d'articles scientifiques a été rédigée à l'aide de mes co-auteurs et encadrants de doctorat : Jean-Claude Ruel (*Pr., PhD et Ing. F., Centre d'Étude de la Forêt, Département des Sciences du Bois et de la Forêt, Faculté de Foresterie, de Géographie et de Géomatique, Université Laval, Québec, QC, Canada*) et Barry Gardiner (*PhD, Institut Européen de la Forêt Cultivée, Site de Recherche Forêt – Bois, Cestas, France*). L'utilisation des articles mentionnés ci-dessous a été préalablement approuvée par mes co-auteurs et par les éditeurs des journaux scientifiques concernés.

Mon rôle dans l'écriture de ces articles a été la mise en place de l'expérimentation nécessaire à l'acquisition de données, l'ajout d'idées au design expérimental à la base de cette thèse, le traitement et l'analyse des données, ainsi que la rédaction des articles. Le tout a été fait sous la supervision de mes co-auteurs et en bénéficiant de leur aide et commentaires. Leur apport a été non-négligeable dans l'ensemble de mes travaux de recherche.

Chapitre 1

Duperat, M., Gardiner, B., & Ruel, J. C. (2021). Testing an individual tree wind damage risk model in a naturally regenerated balsam fir stand: potential impact of thinning on the level of risk. *Forestry: An International Journal of Forest Research*, 94(1), 141-150. DOI: 10.1093/forestry/cpaa023

Chapitre 2

Duperat, M., Gardiner, B., & Ruel, J. C. (2020). Wind and Snow Loading of Balsam Fir during a Canadian Winter: A Pioneer Study. *Forests, 11*(10), 1089. DOI: 10.3390/f11101089

Chapitre 3

Duperat, M., Gardiner, B., & Ruel, J. C. (*unsubmitted*). Effects of a localized thinning on wind loading in a naturally regenerated balsam fir stand.

Introduction Générale

Contexte

Depuis les années 90, de nombreuses tempêtes ont fait rage en Europe et Amérique du Nord remodelant totalement les paysages forestiers. Les plus dommageables sont sans conteste Martin et Lothar qui se sont abattues en Europe fin décembre 1999 et dont les dégâts ont été estimés à 176 millions de mètres cubes sur le territoire français et 25 millions sur le territoire allemand, transformant entièrement le marché du bois et engendrant d'énormes pertes économiques pour les gestionnaires forestiers (Gardiner et al., 2010). Ces tempêtes ont laissé derrière elles des forêts totalement dévastées et un travail titanesque pour récolter le bois tombé et rétablir de nouveaux peuplements. Cet exemple reste parmi les plus dramatiques ayant eu lieu depuis les années 90, mais de nombreux dégâts éoliens, plus couramment appelés chablis, arrivent chaque année à plus petite échelle, causant des dommages directs sur la production et la qualité du bois. Les chablis font partie des perturbations naturelles abiotiques qui touchent les peuplements forestiers. Ils peuvent être aggravés par des facteurs météorologiques additionnels au vent, tels que de fortes de chutes de neige, de pluie ou des températures fortement négatives (Peltola et al., 2000; Silins et al., 2000); par des facteurs biotiques, tels que des dégâts causés par des insectes ou champignons qui viendraient fragiliser la structure de l'arbre (Silva, 1996; Bergeron et al., 2007); ou encore par des facteurs anthropiques lorsqu'on a affaire à un peuplement cultivé. Il existe de nombreuses façons de cultiver des peuplements forestiers, allant de structure simples et homogènes telles que les plantations équiennes monospécifiques, à des structures hétérogènes plus complexes telles que des peuplements inéquiennes et plurispécifiques (Larouche et al., 2013). Cependant, toutes les prescriptions sylvicoles n'ont pas le même impact sur les dégâts éoliens. Ainsi, il est important d'étudier et de comprendre au mieux ces phénomènes, pour développer des outils d'aides à la prévention des chablis et permettre aux gestionnaires forestiers de réduire ou d'anticiper ces risques lors du choix de prescription sylvicole à appliquer.

Des modèles d'estimation de ces risques ont d'ailleurs été développés en se basant sur la compréhension des mécanismes induisant le chablis (Quine, 1994). Les travaux initiaux portaient sur des peuplements monospécifiques de structure simple (Seidl et al., 2014) et se positionnaient à l'échelle du peuplement. Dans les modèles déjà existants tels que le modèle finlandais HWind (Peltola et al., 1999) et le modèle britannique ForestGALES (Gardiner et al., 2008), la charge appliquée par le vent est répartie de façon égale entre les arbres du peuplement en considérant un arbre « moyen » défini grâce à des inventaires forestiers. Cependant, les méthodes de sylviculture actuelles tendent à faire la promotion d'opérations sylvicoles menant à des peuplements plus complexes (Puettmann et

al., 2008), rendant impossible l'utilisation d'un arbre moyen pour décrire l'ensemble du peuplement. Il devient donc nécessaire de passer la modélisation au niveau de l'arbre individuel (Gardiner et al., 2008; Seidl et al., 2014), prenant en compte la complexité de l'hétérogénéité spatiale et structurelle des arbres et peuplements, et favorisant la création d'un modèle plus proche de la réalité. Deux approches de modélisation fonctionnelle dérivées du modèle ForestGALES ont été utilisées jusqu'à présent. La première, ForestGALES_BC, est une version adaptée aux conifères de Colombie Britannique (Canada) par l'ajout des propriétés mécaniques des essences locales et de résultat d'études en soufflerie (Mitchell, 2008). La seconde, ForestGALES-TMC, réside en l'ajout d'indices de compétition (Hale et al., 2012). C'est sur cette seconde version que se basent les travaux de cette thèse.

Les indices de compétition sont « des indices permettant de pondérer la croissance d'un arbre en fonction de l'intensité de la compétition qu'il subit par rapport à un arbre en croissance libre. De tels indices peuvent être calculés à partir des dimensions et de la localisation des arbres voisins ou des caractéristiques de l'ensemble du peuplement » (Bastien and Gauberville, 2011). Les indices de compétition en foresterie peuvent être de deux natures : les indices indépendants de la distance, pour lesquels la dimension des arbres et la description du peuplement sont des facteurs importants ; et les indices dépendants de la distance, pour lesquels la distance et la position des arbres au sein du peuplement permettent de déterminer leur état de compétition vis-à-vis de leur entourage direct (Prévosto, 2005).

Selon le modèle ForestGALES – TMC de Hale et al. (2012, 2015), la charge appliquée par le vent sur chaque arbre d'un peuplement est répartie en fonction de leurs critères morphologiques propres et de leur niveau de compétition. Le comportement du vent à l'échelle de l'arbre individuel demeure difficile à prédire, cependant leur modèle propose de distribuer l'énergie éolienne selon la taille des arbres via la relation qui suit :

$$M_{Max} = TMC \times u_h^2 \qquad \text{Eq. 0.1}$$

Avec M_{Max} (Nm) le moment de force maximal appliqué à la base de l'arbre, *TMC* (*Turning Moment Coefficient*, kg) le coefficient de moment de flexion directement lié au diamètre des arbres et à la compétition locale ; et u^2_h ($m^2 \cdot s^{-2}$) le carré de la vitesse du vent au sommet de la canopée. Le diamètre à 130cm (*DBH*) est lié à la hauteur de l'arbre et à la taille du houppier. Plus l'arbre est haut, plus il est lourd et plus le bras de levier qui contribue au moment de force est important. Additionnellement, la dimension et structure du houppier sont des paramètres importants à considérer dans l'interception du vent (Kamimura et al., 2017). Le fait que cette méthode de calcul prenne en compte la compétition

locale, et donc l'implication des autres arbres, permet de modéliser l'effet du vent sur les arbres individuels en peuplement hétérogène et de recalculer rapidement la nouvelle structure spatiale du peuplement à la suite d'une perturbation telle qu'une éclaircie. Il est important d'inclure cette compétition locale car l'espacement des arbres et la structure du peuplement ont un effet important sur la vitesse et le flux du vent au sein de la canopée, et donc, sur la charge appliquée sur chacun des arbres (Gardiner et al., 1997).

Cas du Québec

Dans la province de Québec (Canada), les sapins baumiers (*Abies balsamea* (L.) Mill, Figure 0.1) sont connus pour être une essence particulièrement vulnérable au chablis (Ruel, 2000). Ces chablis sont liés à la gestion forestière (Ruel, 1995) et peuvent être considérés comme une source importante de perturbations et de pertes économiques (Meunier, 2002). Afin d'améliorer la gestion forestière dans ces peuplements et d'atténuer le risque de dommages causés par le vent, la stabilité et la vulnérabilité des sapins baumiers ont été étudiées en condition estivale, et ont permis d'agrémenter le modèle ForestGALES de variables mécaniques propres à cette essence (Achim et al., 2005a, 2005b).

Figure 0.1: Bris des deux têtes d'un sapin baumier. De nombreux troncs de sapins ayant été brisés ou déracinés par le vent jonchent le sol des sapinières à bouleaux blancs de la Forêt Montmorency. Québec, Canada (Octobre 2019).

Figure 0.2: Aperçu des changements structurels dus à l'hiver. A gauche, photo estivale, les branches sont horizontales et s'entrecroisent. A droite, photo hivernale, le niveau du sol est surélevé par la couche de neige, les branches sont alourdies par la neige.

La particularité du Québec est que le climat boréal engendre un hiver pouvant durer 6 mois. Les conditions hivernales consistent en de fortes précipitations neigeuses pouvant mener à des accumulations de plus de 2m au sol, et des températures fortement négatives. D'après des études scandinaves, les conditions hivernales viennent changer la structure du peuplement (Figure 0.2) et la réaction mécanique des arbres. La présence de neige augmente la masse des houppiers, le froid augmente la rigidité du tronc, le gel du sol et dans certains cas l'épaisse couverture de neige viennent bloquer le système racinaire (Nykänen et al., 1997), et modifier le flux de vent dans la canopée (Lundqvist, 1996). Le tout crée ainsi un cocktail explosif augmentant les risques de rupture des troncs (Peltola et al., 2000; Silins et al., 2000). Le modèle ForestGALES permet pour l'instant de prendre en compte les précipitations neigeuses comme variable additionnelle aux risques de chablis. La neige est alors simplement représentée comme un poids supplémentaire sur le houppier, ce qui modifie la masse en surplomb de la couronne et lorsque l'arbre est plié par le vent, augmente le moment de force appliqué sur le tronc.

Limite des connaissances et objectifs de travail

Il est actuellement possible de modéliser facilement un peuplement homogène, cependant les recherches sont relativement nouvelles et encore peu nombreuses sur les peuplements hétérogènes du fait de leur grande variabilité et complexité. La majorité des études concernant directement les perturbations post-coupes partielles se basent sur des inventaires forestiers, la plupart du temps dans les années ayant suivi la coupe. Il n'existe que peu de connaissances de l'effet d'une perturbation partielle sur la réaction mécanique directe des arbres individuels face à ce changement rapide de compétition locale, et au Québec, l'impact direct d'une coupe partielle sur le risque de chablis reste à établir pour assurer une gestion appropriée de ce type de peuplement. Additionnellement, les conditions hivernales boréales modifient totalement la structure des peuplements, créant des situations bien plus complexes qu'une simple addition de masse sur le houppier. Aucune étude sur l'impact direct de l'hiver sur la réaction mécanique des arbres n'a pour le moment été réalisée dans ce contexte à l'échelle de l'arbre individuel.

L'objectif à la base de cette thèse était d'observer l'effet de l'hétérogénéité du peuplement sur les charges imposées par le vent au niveau des arbres individuels. Le terme hétérogénéité désigne ici à la fois l'hétérogénéité spatiale du peuplement (répartition des arbres, changement de la structure en hiver) mais également l'hétérogénéité dans la morphologie des arbres étudiés et de leurs compétiteurs. Les objectifs dérivés de ce projet sont les suivants :

i) Mesurer l'effet de l'hétérogénéité du peuplement sur la répartition de la charge du vent au niveau de l'arbre individuel ;

ii) Evaluer l'impact du climat boréal sur la répartition de la charge du vent au niveau de l'arbre individuel ;

iii) Étudier l'effet immédiat d'une coupe partielle sur la répartition de la charge du vent à l'échelle de l'arbre individuel et du peuplement.

Chacun de ces objectifs sera développé dans un chapitre dédié.

Démarche méthodologique

Pour répondre à ces objectifs, un dispositif de recherche (Figure 0.3) a été mis en place à la Forêt Montmorency (Forêt d'enseignement et de recherche de l'Université Laval) pour toute la durée de l'étude. Le peuplement utilisé est une petite sapinière à bouleau blanc régénérée naturellement à la

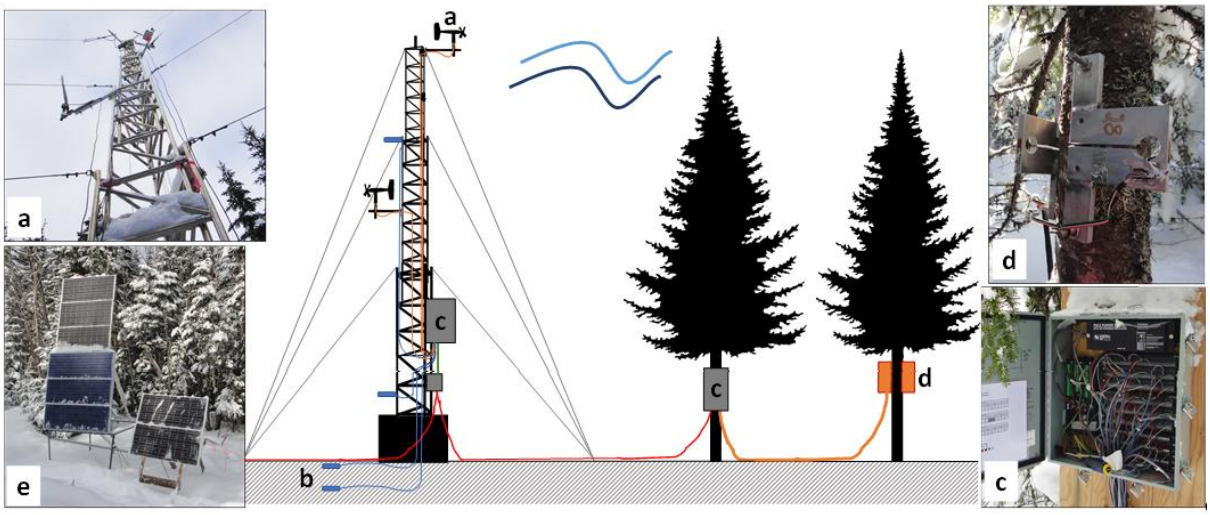

Figure 0.3: Dispositif expérimental. Avec a) anémomètres, b) sondes de températures, c) acquisiteurs de données, d) jauges de contraintes, et e) panneaux solaires

suite d'une coupe à blanc (1982) et ayant subi une éclaircie pré-commerciale (1992). Des jauges de contrainte fixées aux troncs de sapins baumiers ont permis de mesurer les moments de flexion induits par le vent sur quinze arbres études. En parallèle, une tour aluminium équipée de deux anémomètres placés à hauteur et mi-hauteur de la canopée et des sondes de températures (air et sol) ont été installés en bordure de peuplement pour suivre en continu les événements météorologiques. L'ensemble de l'expérimentation a été alimentée à l'aide de 8 panneaux solaires placés dans une clairière à 140m du peuplement, permettant une prise de données continue durant trois saisons : l'été 2018, l'hiver 2019, et l'été 2019. Un suivi continu de la quantité de neige sur les houppiers a été réalisé à l'aide d'une caméra de chasse durant l'hiver 2019. Une éclaircie localisée a été réalisée au début de l'été 2019 pour simuler un changement brusque du niveau de compétition. Cette éclaircie localisée a consisté à retirer tous les compétiteurs dans un rayon de 3.5m autour de 8 des arbres étudiés.

Le premier chapitre de cette thèse (Figure 0.4a) sert de base de compréhension des réactions mécaniques propres à notre peuplement de sapin baumier. Il consiste à trouver des valeurs de paramètres spécifiques à cette essence et à tester deux approches différentes du modèle ForestGALES, la version de base (Gardiner et al., 2008) et la version *TMC* suivant l'approche de Hale et al (2012, 2015) afin de simuler l'impact de différents types d'éclaircies commerciales sur le risque de chablis, et de déterminer laquelle permet de minimiser potentiellement le risque dans un peuplement naturellement régénéré.

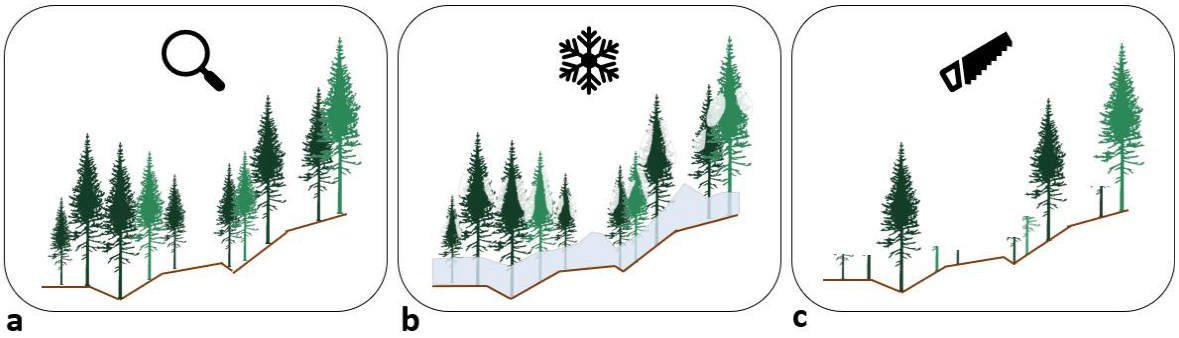

Figure 0.4: Illustration des 3 chapitres abordés dans cette thèse. Avec a) le chapitre 1 concernant la situation initiale du peuplement, b) le chapitre 2 concernant les conditions hivernales et c) le chapitre 3 concernant les conditions post-coupe partielle.

Le second chapitre de cette thèse (Figure 0.4b) est une étude pionnière concernant les conditions hivernales. Il offre une première évaluation de l'effet additionnel de l'interception de la neige, et des températures négatives sur la réaction mécanique des sapins baumiers. Cette étude sert de premier pas vers une compréhension des mécanismes hivernaux dans le but d'orienter les futures études vers les principales variables à prendre en compte pour un modélisation hivernale des risques de chablis.

Le troisième et dernier chapitre de cette thèse (Figure 0.4c) concerne l'étude de la réaction mécanique des sapins baumiers avant et après un retrait total de la compétition avoisinante. Cette étude est la première dans son genre et nous a permis d'attester un changement du profil du vent dans le peuplement à la suite d'une éclaircie localisée et d'observer l'impact de l'éclaircie localisée, non seulement à l'échelle de l'arbre, mais également du peuplement.

Chapitre 1 : Test d'un modèle de prévision des risques de dégâts éoliens à l'échelle de l'arbre individuel dans une sapinière naturellement régénérée : impact potentiel de l'éclaircie commerciale sur le niveau de risque

Testing an individual tree wind damage risk model in a naturally regenerated balsam fir stand: potential impact of thinning on the level of risk

Résumé

Largement répandu au Québec, le sapin baumier (*Abies balsamea* (L.) Mill.) est une essence vulnérable aux dommages causés par le vent. Les tendances récentes de gestion forestière tendent à augmenter l'utilisation de coupes partielles dans les peuplements qui se régénèrent naturellement, exposant les arbres restants à un risque accru de dommages causés par le vent. Afin de limiter les dommages causés par le vent après une coupe partielle, il est donc important de trouver des pratiques sylvicoles qui minimisent le risque de dommages causés par le vent dans ce type de peuplement. L'objectif principal de cette étude était de trouver des valeurs de paramètres spécifiques au sapin baumier à intégrer dans le modèle de risque de vent ForestGALES, afin de simuler l'impact de différents types d'éclaircies commerciales sur le risque de dommages par le vent, et de déterminer quelle pratique permet de minimiser potentiellement le risque dans un peuplement naturellement régénéré. Un anémomètre placé à hauteur de la canopée et des jauges de contrainte fixées aux troncs de sapins baumiers nous ont permis de mesurer les moments de flexion induits par le vent subis par un échantillon de sapins baumiers. Cela a permis de calculer les coefficients de moment de flexion spécifiques à chacun des arbres afin de les comparer aux prévisions du modèle ForestGALES et d'adapter le modèle aux sapins baumiers. Le modèle a d'abord été testé avec uniquement le diamètre et la hauteur des arbres comme variables d'entrée pour calculer le coefficient de moment de flexion, puis avec l'ajout d'un indice de concurrence, et enfin avec l'ajout des dimensions de la couronne. Les paramètres du climat éolien pour la prévision de la probabilité de dommages ont été calculés à l'aide du modèle de flux d'air du Programme d'analyse et d'application de l'Atlas des vents. Le modèle le plus précis a ensuite été utilisé pour simuler deux types d'éclaircies et déterminer l'impact sur le risque de dommages dus au vent pour chaque arbre du peuplement. Selon les prévisions du modèle, l'éclaircie par le bas présente un risque réduit de dommages dus au vent par rapport à l'éclaircie par le haut.

Abstract

Widely distributed in Quebec, balsam fir (*Abies balsamea* (L.) Mill.) is highly vulnerable to wind damage. Recently, there has been a trend in forest management to increase the use of partial cuttings in naturally regenerating stands, leaving the remnant trees at increased risk of wind damage. In order to limit wind damage after partial cuttings, it is therefore important to find silvicultural practices that minimize the risk of wind damage in these fir stands. Our main objective was to find balsam fir-specific values of parameters to integrate into the wind risk model ForestGALES, in order to simulate the impact of different types of commercial thinning on wind damage risk, and to determine which practice potentially minimizes the risk in a naturally regenerated stand. An anemometer placed at canopy height and strain gauges attached to the trunks of balsam firs allowed us to measure the wind-induced bending moments experienced by a sample of balsam fir trees. This enabled the calculation of the turning moment coefficients specific to each of the trees in order to compare them with the ForestGALES model predictions and to adapt the model for balsam fir stands. The model was tested first with only tree diameter and height as input variables to calculate the turning moment coefficient, then with the addition of a competition index, and finally with the addition of crown dimensions. Wind climate parameters for prediction of the probability of damage were calculated using the Wind Atlas Analysis and Application Program airflow model. The model with the highest accuracy was then used to simulate two types of thinning and determine the impact on wind damage risk for each tree in the stand. According to the model's predictions, thinning from below has a reduced risk of wind damage compared with thinning from above.

1.1 Introduction

Increasingly, forest management tends to promote complex and more natural stands in an attempt to increase forest resilience (Puettmann et al., 2008). In Québec (Canada), most stands are naturally regenerated from advance regeneration, leading to some heterogeneity in the new stands. In this context, there is an increased use of partial cutting either to maintain or to recreate the structures typically created by natural disturbances (Bergeron et al., 2007). One type of partial cutting that could be included in such a strategy is commercial thinning in which commercially valuable trees are removed in order to promote the individual growth of the remaining trees and to increase stand quality (Bastien and Gauberville, 2011). After commercial thinning or other types of partial cuttings, the susceptibility of residual trees to be damaged by wind increases, because of the abrupt change in exposure to the wind of trees that have always grown sheltered by neighbouring trees (Mitchell, 2013). Therefore, it is important to use thinning methods that promote the retention of trees that are likely to live through the next cutting cycle. The two most common types of commercial thinning are thinning from below, where suppressed trees are removed, and thinning from above, where dominant trees from the upper canopy are removed (Bastien and Gauberville, 2011). The choice of thinning type is complex and depends on many variables specific to the stand and also on the return on investment for the forest manager (Larouche et al., 2013). In the boreal forest, balsam fir trees are known to be vulnerable to windthrow (Ruel, 2000) but have not yet been subjected to large scale partial cutting. Therefore, the potential impact of different forms of commercial thinning on windthrow risk remains to be established to ensure proper management of this type of stand. Since the 1990s, models have been developed as tools to estimate wind damage risk based on the understanding of mechanisms that induce windthrow (Quine, 1994). Initial work focused on monospecific stands of simple structure and was only applicable at the stand level (Peltola et al., 1999; Gardiner et al., 2000). The ForestGALES model is a hybrid mechanistic-empirical model developed in the United Kingdom (UK) as a tool to help forest managers avoid or minimize wind damage to a stand. The first version was designed to calculate the critical wind speed (CWS) and the return period for damage at stand level in homogeneous and even-aged stands (Gardiner et al., 2008). The model worked by allocating the wind load equally among the trees within a stand, using an average tree defined from field measurements. The equations are described in detail in Quine and Gardiner (2007) and Hale et al. (2015). To model windthrow risk in complex stands, it becomes necessary to work at the individual tree level (Gardiner et al., 2008; Hale et al., 2012; Seidl et al., 2014). Wind behavior at the individual tree scale remains difficult to predict, but a recent study (Hale et al., 2012) found that the wind loading on individual trees in acclimated stands was a strong function of tree size. It is therefore possible to adapt ForestGALES for more heterogeneous natural-like stands

by predicting the wind load as a function of tree size within a stand. The turning moment coefficient (*TMC*) is defined as the turning moment at the base of the tree during a wind event divided by the square of mean wind speed at canopy top (u^2_h, m^2s^{-2}). Canopy top (h, m) is defined as $1.05 * $ top height (mean height of 100 largest diameter trees per hectare) based on the measured heights in Hale et al. (2012). This new functional modelling approach, called ForestGALES turning moment coefficient (FG_TMC), is based on a *TMC* value specific to each tree in the forest (Hale et al., 2015a). In addition to tree size, neighbouring trees affect the wind loading on a subject tree. Using competition indices could therefore improve the model's predictions in heterogeneous forests. The FG_TMC version allows the addition of competition indices and tree morphology indices into its input (Hale et al., 2012; Seidl et al., 2014; Kamimura et al., 2015). This addition should increase the model's capacity to predict wind damage, especially in the case of commercial thinning, which involves an abrupt change of stand density and shelter for the remaining trees. Therefore, in this paper, the parameterization and application of the FG_TMC model is used to better understand the impact of wind on balsam fir stands in the Canadian boreal forest, and to compare the impact of thinning practices on wind damage risk. The hypotheses for the study were as follows:

1. The relationship between maximum turning moment and canopy top wind speed squared established in Hale et al. (2012) in planted forests in the UK is also applicable to naturally regenerated balsam fir stands in Quebec.

2. The inclusion of a competition index increases the accuracy of FG_TMC predictions for naturally regenerated balsam fir stands.

3. The FG_TMC model is able to differentiate between the impacts of different thinning methods on the vulnerability of residual trees to wind damage in naturally regenerated balsam fir stands.

1.2 Methods

1.2.1 Climate and stand

The study was conducted in the Université Laval Montmorency Experimental Forest (47°16'13.0''N, 71°09'24.1''W), 80 km north of Québec City in the Laurentian Hills of the Canadian Shield. Average annual air temperature, total precipitation and snowfall precipitation are, respectively, 0.5°C, 1583 mm and 619 cm. Average annual wind speed is 6.9 km/h, and wind direction is mainly from the North-West (Normales climatiques canadiennes, 2011). Typical of a polar subcontinental climate,

snow cover persists from mid-October to the end of May. The study area is located in the eastern section of the balsam fir-white birch bioclimatic domain of central Québec (Robitaille and Saucier, 1998). The selected study area was a 36-year-old-balsam-firdominated stand originating from natural regeneration after clear-cutting in 1982. It was treated by pre-commercial thinning in 1992. It is composed of balsam fir, black spruce (*Picea mariana* (Mill.)) and white birch (*Betula papyrifera* Marshall). Mean stand height is around 8 m and mean diameter at breast height (DBH) measured at 1.3 m above ground level is 12 cm. The study is concentrated on a 0.13-ha circular plot located near the centre of the stand. Tree stocking density in this area is 1450 stems per hectare. The trees are heterogeneously distributed, and an intermittent stream crosses the stand near its centre, creating a treeless linear gap. The stand is located on a north-facing gentle slope with minor variations in the surface of 1–2 m creating dips and raised areas where the trees can be located. Elevation is around 745 m, and soil is a glacial till with a sandy loam texture. The site is mesic and has moderate drainage. The field work for this study was carried out between summer 2017 and autumn 2018. The stand studied was selected according to logistical constraints: (1) stand height had to be slightly under 10 m so that the additional growth that will take place over time will make it possible to use a 10-m mast to monitor wind speed at canopy top; (2) the site had to be easily accessible, given the material to transport and the frequency of visits required and (3) an open area was needed very close to the site to install the solar panels that provide power to the equipment.

1.2.2 Wind loading on trees: TMC method

Hale et al. (2012) suggested that each tree has a consistent relationship between the turning moment experienced by the tree and the square of the canopy top wind speed. They define this in vivo response in terms of *TMC*. *TMC* is highly dependent of the squared *DBH* (m) of the tree multiplied by the tree height, *H* (m), noted DBH^2H (m^3), which is also well correlated with resistance to overturning (Peltola et al., 2000). Hale et al. (2012) described this relationship as follows:

$$M_{max} = TMC_{invivo} \times u_h^2 \qquad \text{Eq.1.1}$$

where *Mmax* (Nm) is the maximum hourly turning moment, TMC_{invivo} (kg) is the *TMC* measured in vivo and u^2_h (m^2s^{-2}) is the squared mean hourly wind speed at canopy top. This relationship can be incorporated in the ForestGALES model to provide predictions at the individual tree scale. However, this relationship only holds for trees already acclimated to the wind, and adjustment to the equation is needed if modelling wind loading immediately after a thinning and for a few years afterwards (Hale et al., 2015a).

1.2.3 Wind speed and air temperature measurements

To measure weather conditions within the stand, a 10-m-high aluminum tower (T35, Aluma Tower Company, Vero Beach, Florida, USA) was installed in the forest at the edge of our sampling area. Wind speed and direction were measured at a frequency of 5 Hz by a 05103-L Wind Monitor Young anemometer (Campbell Scientific, Edmonton, Canada) fixed at canopy height. Air temperature was measured with a T107 sensor (Campbell Scientific, Edmonton, Canada) at 30-min intervals. Data from the anemometer and temperature sensor were recorded using a CR5000 datalogger (Campbell Scientific, Edmonton, Canada).

1.2.4 Sample trees

During the summer of 2017, DBH and H were measured on every tree of the study area. Among these trees, we selected, as sample trees, 15 balsam firs showing no visible symptoms of disease or crown

Table 1.1: Experimental tree ID, tree *DBH*, tree height (*H*), crown radius (*CR*), crown depth (*CD*), turning moment coefficient (*TMC*), *P-value* and the adjusted coefficient of determination (*Adj. R^2)* of the linear relationship between the maximum hourly turning moment (Nm) and squared average hourly canopy top wind speed (m^2s^{-2}). 2056 hours of data were recorded for each tree.

Tree ID	*DBH* (cm)	*H* (m)	*CR* (m)	*CD* (m)	*TMC* (kg)	*P-value*	*Adj. R^2*
a1	11.7	9.1	1.6	5.9	7.3	< 0.01	0.98
a2	10.6	6.7	0.9	1.9	0.5	< 0.01	0.98
a3	11.0	9.2	1.5	5.7	3.9	< 0.01	0.97
a4	10.8	8.2	1.3	5.2	7.9	< 0.01	0.97
a5	17.5	12.5	1.8	9.0	39.2	< 0.01	0.99
a6	13.1	9.3	1.6	5.0.	11.5	< 0.01	0.99
a7	11.0	9.0	1.1	5.4	2.3	< 0.01	0.9
a8	9.9	7.8	1.1	4.3	0.7	< 0.01	0.98
a9	11.5	8.7	1.5	5.3	0.2	< 0.01	0.99
a11	17.1	8.9	1.7	5.8	25.1	< 0.01	0.99
a12	10.3	7.4	1.4	4.4	9.0	< 0.01	0.97
a13	14.2	9	1.5	6.0	22.0	< 0.01	0.98
a14	10.8	7.2	1.1	3.5	0.4	< 0.01	0.98
a15	10.9	8.8	1.1	5.0	6.2	< 0.01	0.98

Notes: Tree a10 is missing because one of the strain gauges broke and we were not able to repair it quickly enough to incorporate the data from this tree into our analyses.

discoloration and sufficiently spaced from the other sample trees to prevent competition between sample trees. Within the possibilities left by the location constraints, the 15 trees have been selected to represent the whole range of sizes present in the stand. H, crown radius (*CR* (m)), crown depth (*CD* (m)) and *DBH* were measured to characterize sample tree morphology. The value of *CR* corresponds to the average length of branches measured in the first green whorl. The value of *CD* corresponds to the height difference between the top of the crown and the first green whorl. Data from the sample trees are summarized in Table 1.1. Neighbouring trees for calculating distance-dependent competition indices were defined as each tree standing within a 4-m radius around a sample tree. *H, DBH* and distance (D_{cs}) to the sample tree were recorded for all neighbouring trees. The study trees were used to model how the wind load is distributed at the individual tree level, whereas the whole plot inventory (134 trees) was used to simulate the effect of thinning at the plot scale.

1.2.5 Turning moments

Wind loads on the tree trunks were recorded on the sample trees during 89 days in the summer of 2018. On each sample tree, two strain transducers were orthogonally fixed on the trunk at 2-m height on the north and east sides to minimize the thermal effects of the sun. The strain transducers were manufactured in aluminum following an existing design (Blackburn, 1997; Moore et al., 2005) and use two 350-Ω strain gauges attached to the transducer and two precision 1000 Ω resistances to create a Wheatstone half-bridge. The transducers allow measurement of the strain on the surface of the tree trunk when trees bend. The strain is defined by: $\varepsilon = \Delta L/L$, where ΔL (m) is the change in distance and L (m) the total distance between the attachment points on the tree. Bending of the tree under wind loading creates a change in electrical resistance of the strain gauges mounted on the transducer creating a voltage across the bridge, which is recorded as mV/V by the datalogger. To record the strain transducer signal (STS), we used a CR1000 datalogger (Campbell Scientific, Edmonton, Canada) and two CDM-A116 multiplexors (Campbell Scientific, Edmonton, Canada). Recording frequency was 5 Hz. The whole experiment was powered by eight solar panels (5 PowerMax Ultra 80-P, Shell, The Hague, The Netherlands and 3 SX80U, Solarex, Frederick, USA) installed facing south in a clearcut located 70m south from the tower. To convert measured strain to turning moment, the strain transducers mounted on the sample trees had to be individually calibrated by step pulling (Blackburn, 1997; Gardiner et al., 1997). The method used to correctly carry out the pulling and calibration is fully described in Wellpott (2008). The method consists of attaching a cable to the trunk at 2/3 H, and step pulling the tree in the direction of the strain transducer axis with a known force measured by a heavy duty spring scale (Pesola, Schindellegi, Switzerland) with a maximum capacity of 100 kg. The relationship between turning moment and STS (mV/V) is linear. Knowing the cable

attachment height, the angle between the cable and the ground, the angle of the pulling relative to the strain transducer and the force applied to pull the tree, we can obtain a linear conversion equation to transform the measured STS into a known applied turning moment (M (Nm)). See Appendix 1.1 in the Supplementary Material section for additional information. STS data were converted into turning moment with the calibration value obtained from the pulling test. A major problem with strain transducers is daily drifts caused by thermal variations during the day (Blackburn, 1997) and trunk diameter variations due to sap flow, circadian rhythms in trees and weather (Offenthaler et al., 2001; Deslauriers et al., 2003). To zero the data and avoid these daily drifts, we applied a Butterworth highpass filter (Butterworth, 1930) using the « butter » function of the R package « signal » (signal developers, 2014). Parameters chosen for the Butterworth filter were filter order n=2 and critical frequency of the filter W = 0.01666 * 2/5, equivalent to a time period of 1 min. See Appendix 1.3 in the Supplementary Material Section for additional information. Once the data had the thermal and diurnal drifts removed, orthogonal turning moments were combined to produce a single turning moment for each tree. To calculate the maximum hourly turning moment and find the most probable extreme value experienced during each hour, we used the Gumbel method (Cook, 1985). As described in Hale et al. (2012), the 5-Hz turning moment data were divided into one-hour periods. Each hour-long period was further divided into 20 periods of 3 min and the maximum turning moment for each 20 periods was identified. The absolute maximum and minimum values were removed to avoid any artifacts from the datalogger, then the statistical mode of the 18 remaining values was taken as the maximum turning moment for the hour. To calculate TMC_{invivo}, Equation (1.1), for our 14 balsam firs, days with a daily mean air temperature above 0°C were selected to prevent changes in trunk mechanical properties at freezing (Silins et al., 2000). For each sample tree, we ran a linear regression forced through zero between squared hourly mean wind speed and maximum hourly turning moment. The squared hourly mean speed was averaged by 1 m^2s^{-2} class. TMC_{invivo} is equal to the regression coefficient and is specific to each tree. 2056 hours of STS data were used to calculate the TMC_{invivo} value for each tree.

1.2.6 Parameterizing the FG_TMC model for balsam fir stands

Equation (2) adapted from Hale et al. (2015) shows the FG_TMC method to calculate *TMC* values based on DBH^2H:

$$TMC_{FG\_TMC} = 126.01 \times DBH^2H - 7.91 \quad \text{Eq.1.2}$$

Equation 1.2 is a linear regression calculated with TMC_{invivo} measured on our balsam fir trees as dependent variable and DBH^2H as explanatory variables (*P-value <0.01; adj.* R^2 *= 0.88*). The

Table 1.2: Competition indices and crown ratios. *P-value*, adjusted coefficient of determination (*Adj. R²*) and AIC corresponding to the linear relationship between TMC_{invivo} and these indices. g_c (m^2) is the basal area of the competitor; y =1 for competitor with diameter (d_c) larger than the subject (d_s) tree, otherwise y = 0; D_{cs} (m) is distance between subject and competitor; CR_c (m) is crown radius of the competitor, CR_s (m) is crown radius of the subject and N_c is the number of competitors.

Index type	Index formula	References/Definition	*P-value*	*Adj. R²*
Distance-independent	$C_{BAL} = \sum g_c * y$	(Biging and Dobbertin, 1995)	<0.01	0.703
	$C_{DR} = \sum \frac{d_c}{d_s}$	(Kiernan et al., 2008)	0.060	0.202
	$C_{DRL} = \sum \frac{d_c}{d_s} * y$	(Kiernan et al., 2008)	0.018	0.338
Distance-dependent	$C_{Hegyi} = \sum_{c=1}^{n} \frac{d_c/d_s}{D_{cs}}$	(Hegyi, 1974)	0.052	0.217
	$C_{11} = \sum_{c=1}^{n} \frac{d_c/d_s}{D^2_{cs}}$	(Rouvinen and Kuuluvainen, 1997)	0.089	0.157
	$C_{12} = \sum_{c=1}^{n} \frac{(d_c/d_s)^2}{D_{cs}}$	(Rouvinen and Kuuluvainen, 1997)	0.014	0.357
Mean crown ratio	$\frac{\sum CR_s/CR_c}{N_c}$	All competitors within a 4m radius	0.090	0.143
Mean crown ratio with crown touching	$\frac{\sum CR_s/CR_c}{N_c}$ when $D_{cs} < CR_s + CR_c$	All competitors who have a crown touching the subject	0.015	0.353
Mean crown ratio with North-West competitor	$\frac{\sum CR_s/CR_c}{N_c}$	All competitors in a 4m radius perimeter in the North-West direction (dominant wind)	0.113	0.129

regression coefficient (126.01) is specific to our stand and close to the coefficient of 111.7 initially found by Hale et al. (2015). In order to improve our capacity to model CWS for individual trees, it is possible to integrate competition indices (Table 1.2) into the FG_TMC calculation method (Seidl et al., 2014). The choice of competition index type differs from one study to another. An earlier study (Hale et al., 2012) suggested that distance-independent competition indices are efficient in describing the local environment. Conversely, another study (Kamimura et al., 2015) suggested that distance-independent indices are not useful explanatory variables for single-tree damage. To establish which competition index provides the best fit in our study, we built linear regressions between TMC_{invivo}

values and six competition indices. Among these indices, three were distance-dependent, and three were distance-independent. In addition to these indices and based on an idea of Kamimura et al. (2017), we tested the relationship between TMC_{invivo} and various crown ratios to see if a close competitor relationship can improve the prediction. To find specific input for each model, we looked at the competition indices and crown ratios that had a significant linear relationship with *TMC*. Among them, the one with the lowest Akaike information criterion (*AIC*) was selected. Competition indices, crown ratios and results are detailed in Table 1.2. The C_{BAL} index appeared to be the competition index most closely correlated with *TMC*. Including C_{BAL} in the prediction of *TMC* gives the following equation:

$$TMC_{FG\_TMC\_BAL} = 102.14 \times DBH^2H - 0.50 \times C_{BAL} \quad \text{Eq.1.3}$$

The interaction term was not included as it increased the *AICc* value. Regression coefficients in this equation were calculated using a forced through zero linear regression, with TMC_{invivo} as a dependent variable and DBH^2H and C_{BAL} as explanatory variables ($P_{value} < 0.01$; *adj.* $R^2 = 0.929$). We then tested the ability of the models to evaluate TMC values for our stand by comparing the predicted and in vivo values. FG_TMC is the model with no competition index (Equation (1.2)) used in the calculation of CWS (similar to Hale et al., 2015). FG_TMC_BAL is the model using DBH^2H and C_{BAL} (Equation (1.3)) to predict CWS. FG_TMC_{invivo} is the model which directly uses the TMC_{invivo} values for each tree to calculate CWSs. The first two models are almost equivalent, but FG_TMC_BAL includes a competition index that will vary after a partial cut, while FG_TMC uses only DBH^2H, which will change gradually after a partial cutting as the remaining trees reacclimate to their wind environment (Nicoll et al., 2019). The FG_TMC_BAL model is therefore the most useful for studying the impact of thinning on the risk of wind damage.

1.2.7 Calculating CWSs and risk of wind damage

CWS for overturning (CWS_{over}) and CWS for breakage (CWS_{break}) at canopy top for each balsam fir within our stand were calculated using Equation (1.4) and (1.5) below, respectively. Equation (1.6) was then used to convert these values to the respective CWSs values at 10 m above the height of zero-plane displacement (d) (CWS_{Calc}) using the methodology of Raupach (1994). Equations (1.4) and (1.5) are adaptations of equations (11) and (12) in Hale et al. (2015) to incorporate the C_{BAL} competition index by modifying the denominator of the first term. Equation (1.3) is equivalent to equation (8) in Hale et al. (2015)

$$u_{h,over} = \left(\frac{C_{reg} \times SW}{102.14 \times DBH^2H - 0.50 \times C_{BAL}}\right)^{1/2} \times \left(\frac{1}{1.136}\right)^{1/2} \times \left(\frac{1}{TMC\_Ratio}\right)^{1/2} \quad \text{Eq.1.4}$$

$$u_{h,over} = \left(\frac{C_{reg} \times SW}{102.14 \times DBH^2H - 0.50 \times C_{BAL}}\right)^{1/2} \times \left(\frac{1}{1.136}\right)^{1/2} \times \left(\frac{1}{TMC\_Ratio}\right)^{1/2} \quad \text{Eq.1.5}$$

$$0u_{Calc} = u_h \times \frac{ln\ (10/z_0)}{ln\ ((h-d)/z_0)} \quad \text{Eq.1.6}$$

In these equations, C_{reg} (Nm kg−1) is a coefficient obtained from tree pulling experiments and is a function of species, soil type and rooting depth (Achim et al., 2005a); *SW* (kg) is the weight of the bole of the tree; TMC_Ratio is a variable used to account for the change in wind loading following a thinning equal to 0.99 multiplied by the ratio of the mean spacing before and after a thinning (Hale et al., 2015a); MOR is the modulus of rupture (Pa) for balsam fir (Jessome, 1977); d^3 is the cube of the stem diameter at the tree base (m^3). The ratio 1/1.136 accounts for the additional turning moment due to the displaced tree crown (Hale et al., 2015). To establish how silvicultural practices affect CWS at the individual tree scale, two types of thinning were simulated: thinning from above and thinning from below. Thinning from above was simulated by sequentially removing the biggest trees within the stand, based on DBH^2H values, while thinning from below was simulated by removing the smallest trees within the stand. In both cases, we removed trees without consideration of the spatial distribution of trees or the species until the target basal area removal of 28 percent of stand basal area was reached. Using the simulation of the CWS of the individual balsam fir trees before and after thinning and the topography and climate of the area, we modelled wind damage risk for each tree. The Wind Atlas Analysis and Application Program WAsP (Mortensen et al., 1993a), a computational linearized fluid dynamics model, was used to calculate the wind climate at the location of the experiment. The wind climate data used as input for WAsP were the past 20 years of wind data from the weather station of the Montmorency Forest located 5.6 km north of our experiment. LIDAR data providing topography and forest canopy height for this area were obtained from the Montmorency Forest database and incorporated into WAsP. Evolution of wind damage risk after thinning was calculated by combining the FG_TMC_BAL CWS results with the WAsP-derived wind climate result. More details of the WAsP calculations are

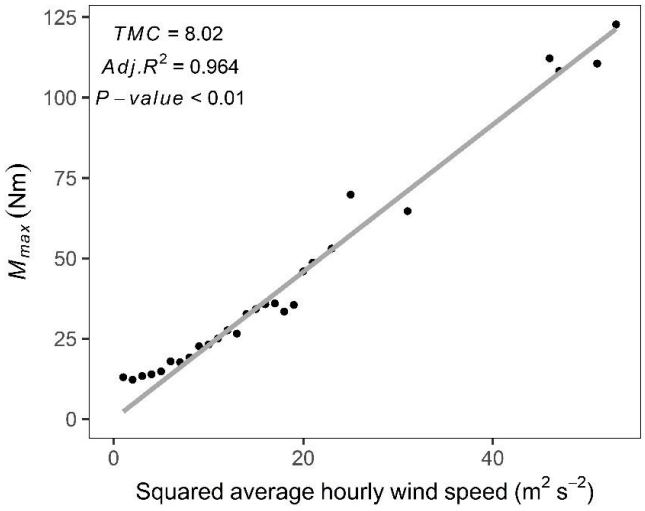

Figure 1.1: Maximum hourly turning moment (*Mmax*) plotted against the squared average hourly wind speed class measured at canopy top for tree a7. *Adjusted R²* shows a good relationship between *Mmax* and squared average hourly wind speed class.

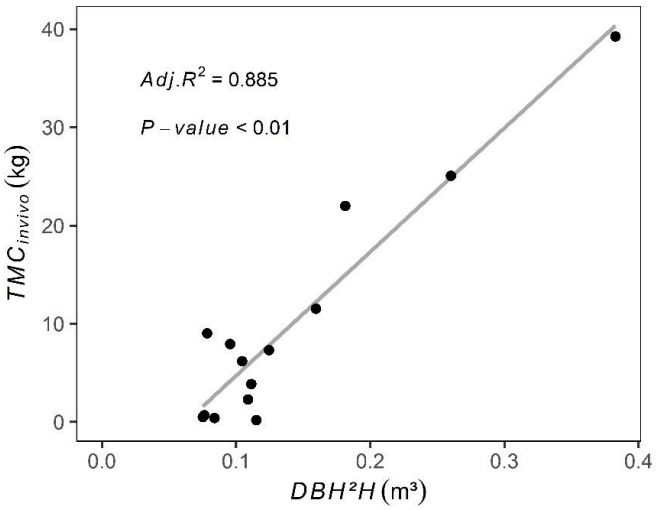

Figure 1.2: TMC of each experimental tree measured in vivo (kg) plotted against *DBH²H* (m^3).

provided in the Appendix 1.3 in the Supplementary Material section. The use of WAsP results to predict the probability of damage from CWS can be found in Hale et al. (2015) and Kamimura et al. (2015). The loess regression function of the ggplot2 R package (Wickham, 2016; R Core Team, 2018) was used to plot the trending curves in Figures 1.5 and 1.6 for visual purposes only. This function uses local weighted regression to fit a smooth curve through points in a scatter plot, allowing for easy visualization of intrinsic trends in the displayed data. All the results presented for these figures have been calculated from actual data and not from these trend curves. All data were analyzed within the R program (R Core Team, 2018).

1.3 Results

1.3.1 Modelling wind load at the individual tree level

For each sample tree, M_{max} showed a very close linear relationship with squared average hourly wind speed class measured at canopy top (Table 1.1). We did not make any discrimination in terms of wind direction, and all linear regressions were forced through zero, because with a wind speed of zero, there must be zero turning moment. *TMC* and correlation coefficients are given for each tree in Table 1.1. An example of a linear regression is shown in Figure 1.1 for tree a7. The relationship between *TMC* and DBH^2H was linear: larger trees had a higher *TMC* than smaller trees. However, there was more scatter in *TMC* value for the smallest trees with DBH^2H between 0.075 and 0.115 (Figure 1.2). The three crown ratios tested did not show a strong relationship with TMC_{invivo}. As discussed in the Methods section, C_{BAL} out of all the competition indices had the most significant relationship with TMC_{invivo} (P_{value} *<0.01, adj.* R^2 *= 0.703, AIC= 105,* Table 1.2) and was used to modify and improve the TMC model. Figure 1.3 shows the comparison of the linear regression between TMC_{invivo} and theoretical *TMC* calculated with the FG_TMC and FG_TMC_BAL models. Theoretical *TMC* values calculated with FG_TMC_BAL (*AIC= 89, Adj.* R^2 *= 0.902,* P_{value} *< 0.01*) are slightly closer to TMC_{invivo} than the ones calculated with FG_TMC (*AIC= 90, Adj.* R^2 *= 0.898,* P_{value} *< 0.01*). However, even if the FG_TMC_BAL method displayed generally equivalent results to the TMC_{invivo} values, the model gives less accurate estimates for the smaller trees with a DBH^2H value between 0.075 and 0.115. We ran the three models FG_TMC, FG_TMC_BAL and FG_TMC_{invivo} to evaluate the impact of the different calculation methods on CWS predictions. The models have good agreement in the prediction of CWS at canopy top for overturning and breaking for the largest trees (DBH^2H>0.15 m^3) but showed disparity for the smallest trees (Figure 1.4).

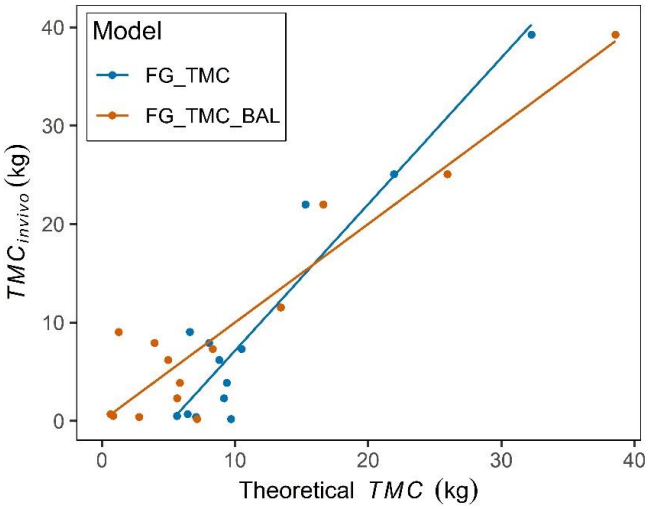

Figure 1.3: Comparison of the linear regression between TMC_{invivo} and theoretical *TMC* calculated with FG_TMC and FG_TMC_BAL models.

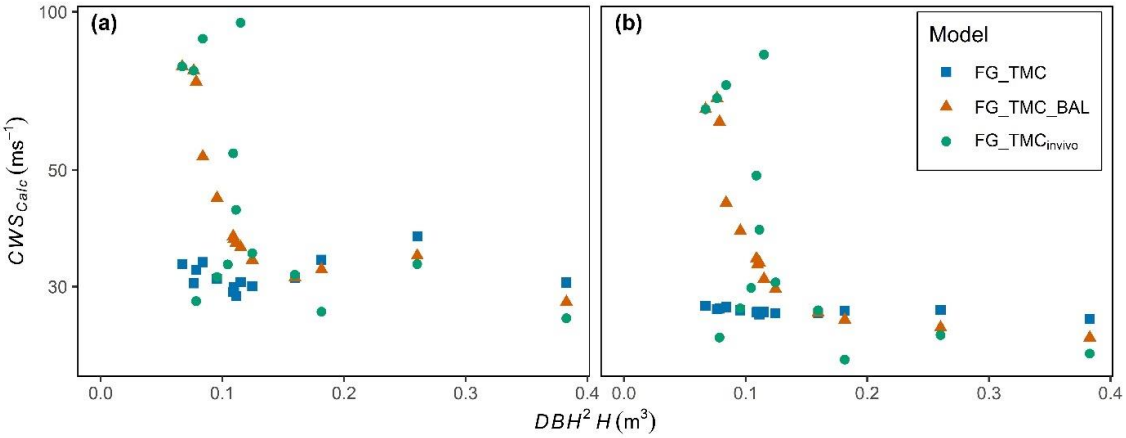

Figure 1.4: Comparison of CWS 10 m above zero-plane displacement (CWS_{Calc}) for breakage (a) and overturning (b) of the different FG models tested for our 14 sample trees. Note that y-axis is in logarithm scale.

1.3.2 Vulnerability of individual trees to wind damage risk following a simulated commercial thinning

For breakage and overturning, there is a high variability in the CWS of small trees. However small trees seemed generally to have CWS higher than large trees (Figure 1.5). Thinning from below only decreased CWS for overturning for the smallest trees left after thinning. However, their CWS still remained higher than CWS of large trees, even unthinned ones. CWS for breakage is larger than CWS for overturning for all tree sizes and in all thinning conditions. The thinning which had the biggest impact on CWS is the thinning from above which decreased CWS for breakage by up to 34 m s^{-1} and for overturning by up to 27.3 m s^{-1}. For trees with $DBH^2H < 0.115$, the results might not fully reflect the actual variation as indicated by the variations in TMC_{invivo} that was observed in Figure 1.3. Both types of simulated thinning increased wind damage risk for breakage and overturning for the biggest trees within the stand (Figure 1.6). Thinning from below increased the probability that CWS will be reached within the year up to a value of 0.04% for breakage (Figure 1.6a) and 0.42% for overturning (Figure 1.6b), while thinning from above increased the probability up to a value of 0.12% for breakage (Figure 1.6a) and 0.02% for overturning (Figure 1.6b). In contrast, the maximum level of risk with no thinning was predicted to be 0.51% and 0.24% for breakage and overturning, respectively. These calculations are based on the predicted wind climate at the experimental site calculated using WAsP and subject to the accuracy of those calculations. See Appendix 1.3, in the Supplementary Materials section for additional information on the WAsP calculations.

1.4 Discussion

1.4.1 Methodology choices and limitations

The results show that the relationship between maximum turning moment and canopy top wind speed squared established by Hale et al. (2012) in planted forests is also applicable to naturally regenerated balsam fir stands in Quebec even though the forest types are very different. It provides evidence that the TMC method of Hale et al. (2012, 2015a) can be applied in forest types other than plantation forests, and thus confirms our first hypothesis. Further measurements in forests with more complex structure would be extremely valuable. Our results also support our second hypothesis: the inclusion of a competition index increases the accuracy of FG_TMC predictions for a naturally regenerated balsam fir stand and allows us to take a further step forward in understanding and modelling the risk of wind damage in the boreal forest environment. This confirms the ideas of Hale et al. (2012) and

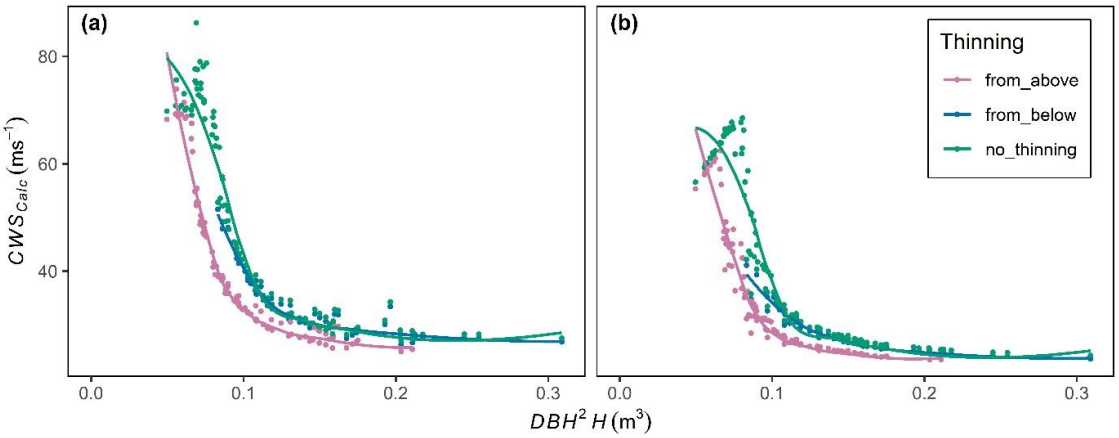

Figure 1.5: Effect of thinning from above and below on changes in *CWS* for breakage (a) and overturning (b) 10 m above zero-plane displacement (CWS_{Calc}). Calculated for all the trees in the stand, using FG_TMC_BAL method.

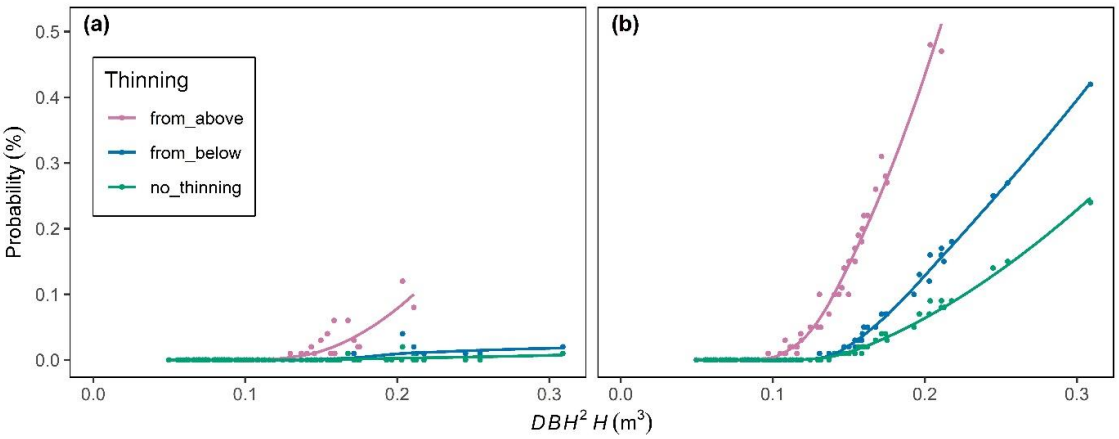

Figure 1.6: Probability (%) for breakage (a) and overturning (b) that the *CWS* will be reached within a year as a function of thinning method. The wind damage probability is calculated for each tree within the stand.

supports the results of Seidl et al. (2014). The inclusion of the BAL competition index helps to calculate the TMC for a variety of tree sizes and levels of competitiveness. This approach has the potential to describe the impact of any partial cutting treatment or other forest disturbance on the risk of wind damage. The choice of the competition index was not straightforward. Seidl et al. (2014). proposed using the distance-dependent index C_{Heygi} to improve the Hale et al. (2012) model by including local neighbour sheltering. Kamimura et al. (2015) then tested Seidl's idea but with the addition of a distance-independent index in very homogeneous maritime pine stands. They determined that including distance-dependent competition index did not improve the prediction of single-tree damage. The discussion about the usefulness of competition indices has also been taking place for a long time in growth modelling for which these indices were initially developed (Alemdag, 1978; Mugasha, 1989). Distance dependent indices provide a more detailed description of the tree local environment but usually cannot be computed from operational sample plots. According to Mugasha (1989), distance-independent indices should perform well in homogeneous stands such as plantations but distance-dependent ones might be preferable in more complex stands. Our stand was naturally regenerated and then treated by precommercial thinning. Even though this treatment may have simplified stand structure, the stand remained relatively heterogeneous. The performance of C_{BAL} may indicate that the structure of the whole stand has a major influence on individual tree wind load in comparison with fine-scale variations in canopy structure. The coherent structures known to cause wind damage to forest stands (Kamimura et al., 2019) have the scale of several tree heights in the along wind direction and a single tree height across the wind direction. Their structure and scale are determined by the shape of the wind profile created by the stand as a whole (Raupach et al., 1996). We also found that TMC for a few small commercial trees was not well estimated by FG_TMC_BAL, and results for this kind of tree were always variable. Competition indices and crown ratio did not help us to improve the model for these trees, so caution is required when using trees with a DBH^2H lower than 0.115 m^3. The FG_TMC CWSs are almost invariant with DBH^2H. This is a reflection of the fact that wind loading is a function of DBH^2H, and the resistance to overturning is a function of SW (well correlated to DBH^2H) and the resistance to breakage is a function of DBH^3 (also correlated to DBH^2H) so that the wind loading and the tree resistance tend to balance for all tree sizes. Only when the variable C_{BAL} is added in the FG_TMC_BAL model is there a clear change in CWS with tree size, and this is another reason for preferring this form of the model. In addition, the FG_TMC_{invivo} model results for some of the smallest trees give extremely high and unrealistic CWSs. This is a reflection of the fact that some of the small trees in the stand were extremely well sheltered from the wind and when using their TMC measured in vivo values they appear to be incapable of being damaged. In an actual storm, as surrounding trees become damaged and fall over, these small trees

would become increasingly exposed and vulnerable as shelter is lost. Additional research is required to better understand the reaction of these small trees under wind loading. Previous studies have found a relationship between the abundance of saplings and the amount of wind damage (Riopel et al., 2010; Lavoie et al., 2012). Gardiner et al. (2005) and Wellpott (2008) have shown that small stems can reduce the wind load on dominant trees, and saplings could therefore play a similar role in our stand. Given that saplings were only slightly smaller than our small trees, this effect may be significant. However, it would not be captured by C_{BAL} that only considers trees larger than the subject tree. Even though our predictions were less precise for small trees, these were least at risk during storms, and disparities observed for the smallest trees are not, in our opinion, a major problem for predicting damage risk in similar stands. They also represent a small volume of low value, meaning that their loss would have less impact on the management of these stands.

1.4.2 Types of thinning and limitations

The choice of type of thinning in a mature stand is not easy because the forest manager has to consider many aspects, including an increased risk of wind damage. Many criteria have to be taken into account to reduce damage: dominant species, stand age, silvicultural treatment history, soil, wind exposure and rooting characteristics (Ruel, 1995). Because of the variability and complexity of criteria, the literature provides different opinions between the risks associated with type of thinning. For example, according to Cremer et al. (1982), thinning from below would be preferable to thinning from above because the height/diameter ratio of the trees left after a thinning from below would be favorable to resisting wind damage. On the contrary, according to Busby (1965), thinning from above would be preferable to thinning from below because the retained trees would be shorter. Based on our results, and to confirm our third hypothesis, removing the biggest trees in a balsam fir stand induces an important decrease of the CWS for breakage and overturning and increases the risk of damage especially for the largest trees left in the stand. Thinning from below appears to be the least risky thinning of the two thinning approaches tested for naturally regenerated balsam fir stands with much lower increases in the level of risk for the remaining trees. These ForestGALES predictions constitutes a case study that shed some light about the choice of commercial thinning in balsam fir stands. They suggest that silvicultural practices for the most vulnerable balsam fir stands should aim to remove trees from the upper canopy during commercial thinning. Other factors, such as expected growth response and economical profitability, must also be considered when developing partial cutting strategies in these stands. Even though we simulated thinning only for a single stand, the relative impact of the two types of thinning should apply for other stands since the effect on the competition index would operate in the same manner. The probability of damage remained rather low

in our case for two main reasons. First, the stand was rather young, and trees were short, height being an important variable in tree vulnerability. Even though our stand was slightly young to apply a commercial thinning, the ranking of thinning types should apply in older stands. Second, the stand was precommercially thinned, and previous research has shown that acclimation after such treatment reduces the vulnerability to subsequent commercial thinning (Achim et al., 2005a). The limits of interpretation of these results are mostly due to the consideration of the local environment which is highly spatially heterogeneous. Variability of tree density and soil moisture are also important in such a small area, and we assumed that all the trees studied were under similar conditions. We also assumed that wind speed was constant over the experimental site when we know that is an imperfect approximation due to small-scale variations in topography. It is important to stress here that these small variations (1–2 m scale) are important relative to mean stand height (8 m).

1.5 Conclusions

Our study showed that the FG_TMC method coupled with the distance-independent C_{BAL} competition index has good potential for developing methodologies for predicting wind damage risk in balsam fir stands in Québec. Predictions regarding commercial thinning are promising despite problems in modelling wind damage risks for small commercial trees. However, the predictions remain theoretical, and field tests need to be conducted to verify the reliability of the approach in predicting the increase of turning moment applied to the base of the trees after thinning. It would also be useful to look at how trees acclimate over time to these new growing and wind exposure conditions.

Acknowledgments

The authors thank François Larochelle for technical support and help conducting field work, James Gardiner for help filtering the strain gauge data, the 15 students who worked punctually on the fieldwork, Université Laval Montmorency Experimental Forest for all the proximity services, Julie Bouliane for her help in the logistical organization, as well as the two anonymous Reviewers and the two Editors, Gary Kerr and Elisabeth Poetzelsberger, for their time and help in improving this paper.

Funding

This research was funded by Natural Sciences and Engineering Research Council of Canada, grant number RGPIN-2016-05119 and by the Canadian Wood Fibre Centre, grant CWFC1820-009.

Supplementary Materials

Appendix 1.1: Strain gauge calibration by tree pulling

Each strain gauge (Figure 1.7) has its own characteristics, and each tree has its own rigidity. Once fixed on the tree, an individual calibration of the sensors is required to translate the stress measured by the strain transducer signal (STS, in mV/V) into a moment of force (M, in Nm) (Wellpott, 2008).

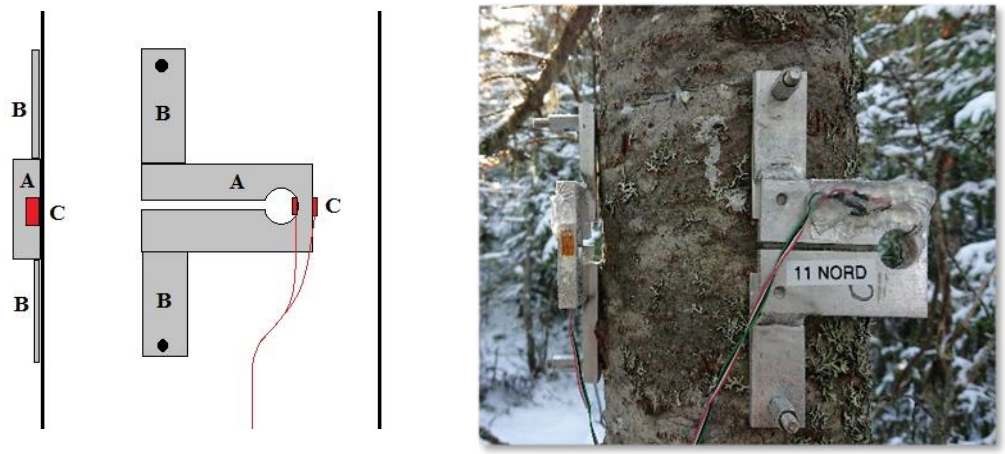

Figure 1.7: Sensors fixed on a balsam fir, following the design of Moore et al. (2005). With A the aluminum bracket; B the two anchor wings; and C the two strain gauges glued on the bracket.

To calibrate the sensors, an artificial moment of force is applied to the trunk with a winching system (Figure 1.8). The winching system is made of a cable, a spring balance and a manual winch, and is attached between the subject tree and an anchor tree. To avoid any risk, the distance between the two trees must be at least equal to the height of the subject tree. The anchor tree must be aligned as much as possible with the sensor axis. The force is applied manually with the winch and is measured with the spring balance attached between the winch and the subject tree. Winching consists of the application by steps of an increasing and then decreasing force (Figure 1.9). Each step must last at least 30 seconds to avoid tree oscillations due to the change in applied force.

To transform the force applied (F, in N) into a moment of force (M, in Nm), we need to apply the following equation: $M = F \times h \times \cos(\alpha) \times \cos(\beta)$. The calibration coefficient corresponds to the coefficient of the linear regression between M (Nm) and STS (mV/V).

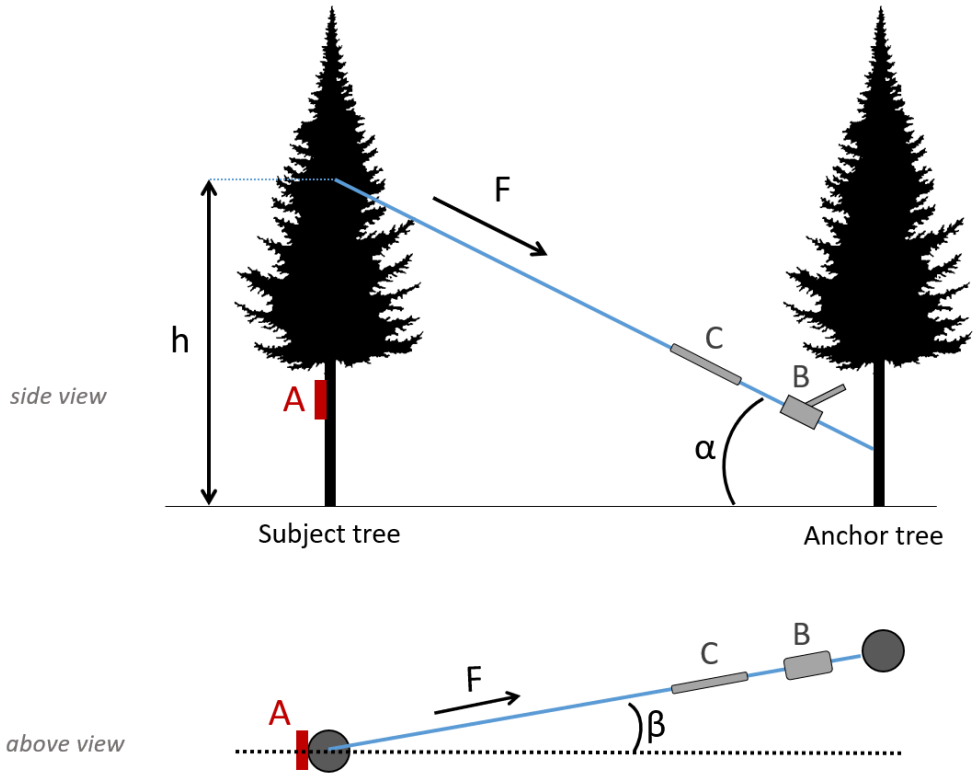

Figure 1.8: Sensor calibration diagram. With A the sensor to calibrate; B the manual winch; C the spring balance; F the force applied ; h the attachment height ; α the angle of winching ; and β the anchorage deviation angle, based on Wellpott (2008).

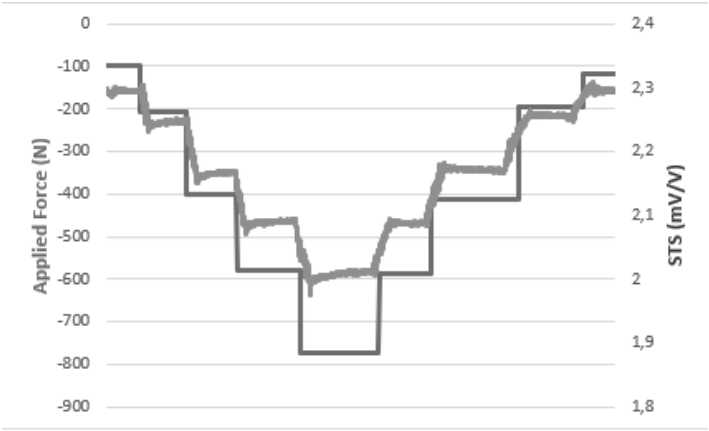

Figure 1.9: Example of tree pulling data: Tree 15, East gauge. The applied force (N) was recorded manually using a spring balance. The Strain Transducer Signal (*STS*, in mV/V) is the strain gauge reaction during the tree pulling. The curves are reversed because for practical reasons the tree has been pulled on the opposite side to the strain gauge.

Appendix 1.2: An example of the use of the Butterworth filter

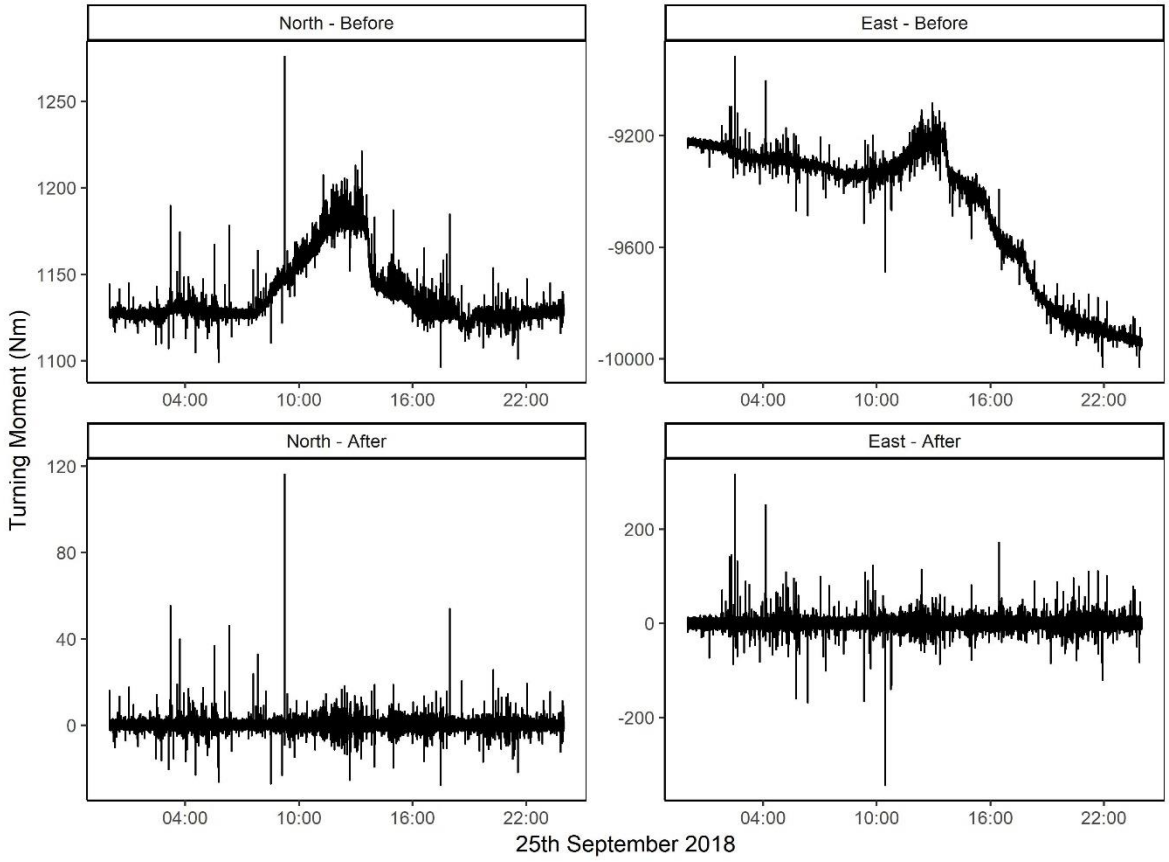

Figure 1.10: North and East gauges of Tree 15 for the 25th September 2018, before and after the use of the Butterworth filter (Butterworth, 1930).

Filter parameters: Highpass filter; order: n=2; critical frequency: W= 0.01666*2/5

R line code, package « signal » (signal developers, 2013; R Core Team, 2018):

data$STS <- filtfilt (butter(2, 0.1666*2/5, 'high') data$STS)

Appendix 1.3: WAsP Wind Climate Calculations for Experimental Site in Montmorency Forest

In order to calculate the probability of the calculated critical wind speeds being exceeded at the experimental site it is necessary to have information on the wind climate at the site, specifically the Weibull A and Weibull k values. Unfortunately, there is no long term wind monitoring at the experimental site, but there is long term wind climate data from the climate station located near the main offices of the Montmorency Experimental Forest (47.32 N, 71.15 W, Altitude 640 m). The WAsP (Wind Atlas Analysis and Application Program; (Mortensen et al., 1993b)) is a computer package that can extrapolate wind climate data from one location to another, taking into account local roughness, obstacles and topography at both locations, and assuming that both locations are subject to essentially the same wind climate. The distance between the climate station and the experimental site is 5.8 km.

The wind data used as input for the WAsP simulations were based on the measured wind speeds at a height of 2.5 m at the Montmorency climate station between 1981 to 2010 obtained from Environment and Climate Change Canada[1]. The terrain data and the tree height (h) data were obtained from a detailed LiDAR scan of the whole forest. This data had a horizontal resolution of 1 m but was resampled at 20 m resolution in order to run WAsP. The horizontal extent of the area used for the WAsP simulation was 14.3 km in a north-south direction and 9.3 km in a west-east direction. The calculation area around the experimental site had a spatial extent of 1.5 km in a north-south direction and 1 km in an east-west direction and the predictions were made at a spatial resolution of 5 m. The height of the prediction at the experimental site was set to 10 m to correspond to the height at which ForestGALES predicts the critical wind speed. The aerodynamic roughness values (z_0) in the WAsP simulations were calculated using the ratio z0 = 0.0895*h obtained in ForestGALES for the forest at the experimental site based on (Raupach, 1994). This is a similar but slightly higher ratio than the average for dense coniferous forests in (Jarvis et al., 1976).

The predicted Weibull A value was 3.1 ms^{-1} and the predicted Weibull k value was 1.06 at the experimental site. However, note that there are rapid variations over short distances so that the wind

[1] https://climat.meteo.gc.ca/climate_normals/results_1981_2010_f.html?searchType=stnName&txtStationName=Montmorency&searchMethod=contains&txtCentralLatMin=0&txtCentralLatSec=0&txtCentralLongMin=0&txtCentralLongSec=0&stnID=5682&dispBack=1

climate will vary across the experimental site and the predictions of probability of damage to trees can only be taken as indicative.

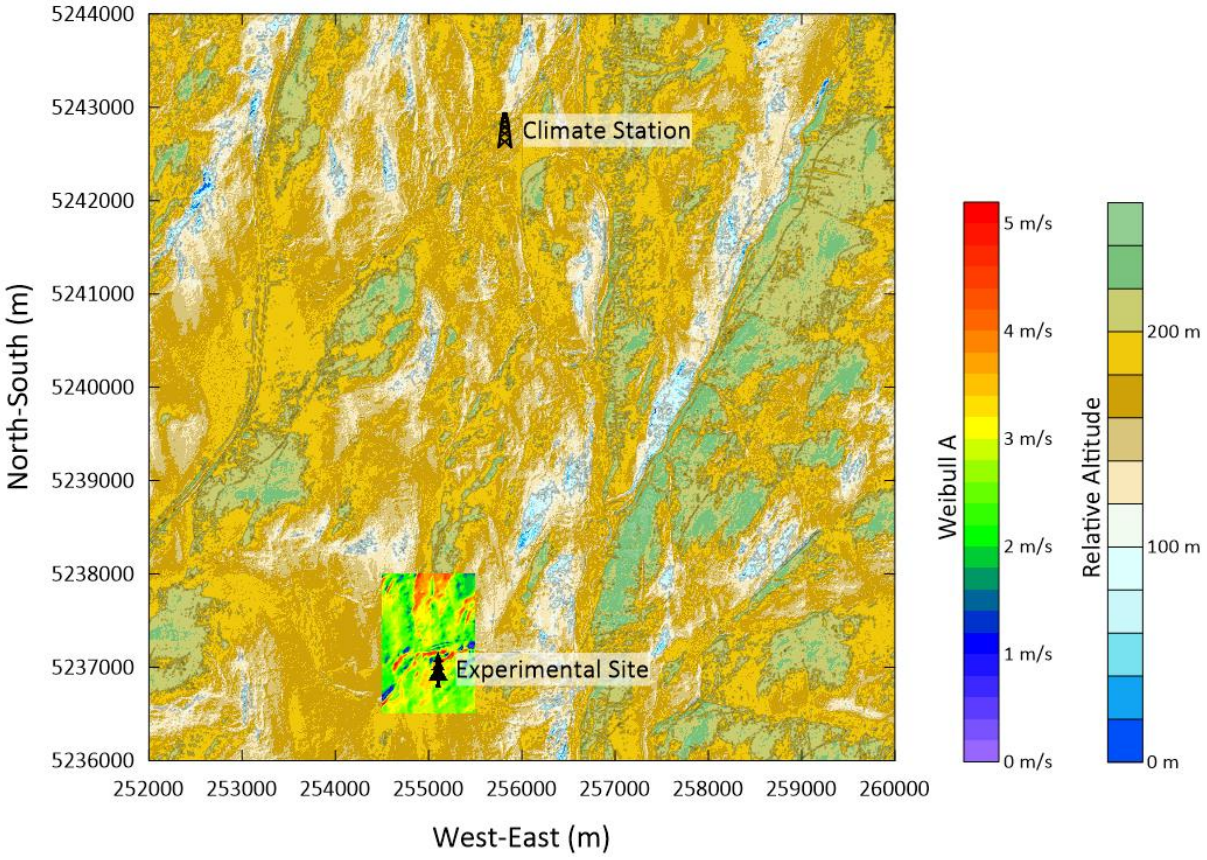

Figure 1.11: Part of the WAsP simulation area showing the location of the climate station, the experimental site and the predicted Weibull A values (ms^{-1}) around the experimental site. The elevation (m) is relative to the lowest point in the calculation domain.

Chapitre 2 : Charge de vent et de neige du sapin baumier pendant un hiver canadien : une étude pionnière

Wind and snow loading of Balsam fir during a Canadian winter: a pioneer study

Résumé

Largement répandu au Québec, le sapin baumier (*Abies balsamea* (L.) Mill) est très vulnérable aux dommages causés par le vent. Les conditions hivernales difficiles, les températures glaciales et la neige constituent un risque supplémentaire. Il est important de comprendre les charges mécaniques subies par les arbres en hiver pour adapter la gestion forestière et minimiser les risques de dégâts éoliens hivernaux. De nombreuses études, principalement basées sur des inventaires des dommages après les tempêtes, ont été menées sur ce types de dommages hivernaux en Europe du Nord. Cependant, aucune étude n'a suivi en continu le moment de force appliqué pendant une période de charge de neige, et aucune étude n'a étudié les charges de vent et de neige sur le sapin baumier. C'est pourquoi notre principal objectif était de mener une étude pionnière pour voir comment les arbres ploient sous la charge du vent en hiver, et pour voir comment l'interception de neige par la canopée contribue à cette charge. Deux anémomètres placés à la hauteur de la canopée et aux 2/3 de celle-ci, des capteurs de température de l'air et du sol, une caméra de chasse et des jauges de contrainte fixées aux troncs de quinze sapins baumiers, nous ont permis de mesurer les moments de flexion des arbres induits par le vent et la neige ainsi que les conditions météorologiques. Les données ont été enregistrées à une fréquence de 5 Hz pendant plus de 2000h durant l'été 2018 et l'hiver 2019. Deux modèles linéaires mixtes ont été utilisés pour déterminer quels paramètres propres aux arbres et au peuplement influencent le moment de force subi par les arbres, et pour évaluer l'effet de l'hiver. Le modèle sélectionné pour les mesures effectuées pendant l'hiver a montré que l'inclusion de l'épaisseur de la neige sur les houppiers était meilleure que les modèles qui ne tenaient pas compte de l'effet de la neige (ΔAICc > 25), mais l'effet de l'épaisseur de la neige sur le moment de flexion semble être mineur. Cependant, dans l'ensemble, le moment de force subi par les arbres en hiver s'est avéré plus élevé que le moment de force subi à la même vitesse de vent en été. Ceci est probablement dû à l'augmentation de la rigidité du tronc et du système racinaire lors de températures négatives et à la modification du flux de vent dans la forêt en raison de la neige sur la canopée et sur le sol lors de la saison hivernale.

Abstract

Widely distributed across Quebec, balsam fir (*Abies balsamea* (L.) Mill) is highly vulnerable to wind damage. The harsh winter conditions, freezing temperatures, and snow pose an additional risk. It is important to find the mechanical loads experienced by trees during winter to adapt forest management and minimize the risk of damage to this species. Many studies have been carried out on wind and snow loading damage risks in Northern Europe, mostly based on post-storm damage inventories. However, no study has continuously monitored the applied turning moment during a period with snow loading, and no study has investigated wind and snow loading on balsam fir. Therefore, our main objective was to conduct a pioneering study to see how trees bend under wind loading during winter, and to see how snow cover on the canopy contributes to the loading. Two anemometers placed at canopy height and 2/3 canopy height, air and soil temperature sensors, a hunting camera, and strain gauges attached to the trunks of fifteen balsam fir trees, allowed us to measure the wind and snow induced bending moments experienced by the trees together with the meteorological conditions. Data were recorded at a frequency of 5 Hz for more than 2000 h during summer 2018 and winter 2019. Two mixed linear models were used to determine which tree and stand parameters influence the turning moment on the trees and evaluate the effect of winter. The selected model for measurements made during winter found that including the snow thickness on crowns was better than those models that did not consider the effect of snow (ΔAICc > 25), but the effect of snow depth on the bending moment appears to be minor. However, overall, the turning moment experienced by trees during winter was found to be higher than the turning moment experienced at the same wind speed in summer. This is probably a result of increases in the rigidity of the stem and root system during freezing temperatures and the change in wind flow through the forest due to snow on the canopy and on the ground during the winter season.

2.1 Introduction

In Québec province, Canada, windthrow events in balsam fir (*Abies balsamea* (L.) Mill) stands can be considered as a significant source of disturbance and economic losses (Meunier, 2002), and are known to be linked to forest management (Ruel, 1995). To improve forest management in these stands and mitigate the wind damage risk, the stability and vulnerability of balsam fir trees has been studied as a consequence of different types of thinning (Achim et al., 2005b; Duperat et al., 2021) and an existing British wind risk model: ForestGALES (Gardiner et al., 2004; Hale et al., 2015b) has been tested, adapted, and improved to provide a decision support tool for forest managers (Ruel, 2000; Achim et al., 2005b; Anyomi et al., 2016; Duperat et al., 2021). During winter, freezing temperatures and snow cover are known to have an additional impact on wind damage. The ForestGALES model allows for the addition of snow in the calculation of the critical wind speed at which a tree will uproot or break. Snow is represented as an additional weight in the crown, changing the moment due to the overhanging crown mass when the tree is bent by the wind, and therefore increasing the turning moment applied to the trunk. However, what happens in a stand during winter is much more complex than this simple representation. In balsam fir forests, winter and snow cover can last for 6 to 7 months and snow can reach more than 200 cm depth. This thick layer of snow and ice produces a change in the wind profile as the snow offers less aerodynamic resistance to wind than ground vegetation and, therefore, the rate of change in wind speed is probably larger at ground level during the winter season (Lundqvist, 1996). In the canopy, snow accumulates on branches and can form large clumps of snow and ice. The weight of the snow pressing on the branches causes a change in the shape of the crowns and a decrease in the canopy porosity likely to influence the stand wind profile as well. This snow loading of tree crowns combined with freezing temperatures can cause severe damages to trees, such as stem bending or stem breakage, but rarely uprooting, as frozen temperatures increases stem stiffness (Peltola et al., 2000; Silins et al., 2000), and as the weight of the snow cover on the soil, and/or frozen soil, reinforce the root system (Nykänen et al., 1997). Most of the studies conducted on wind, snow, and conifers are from Northern Europe, and are based on long-term damage surveys. What is known from these studies is that the factors that most influence winter breakage or uprooting are related to tree shape and stand characteristics (Díaz-Yáñez et al., 2017). More specifically, stem taper (Valinger and Fridman, 1997; Peltola et al., 1999, 2000), crown characteristics (Nykänen et al., 1997), and the number of neighboring trees (Valinger et al., 1993) are the most important factors controlling the stability of trees in winter. In relation to this, the choice of thinning carried out in the stands seems to be crucial in their management with an increase in wind and snow damage risk following thinning in a stand (Valinger, 1996; Wallentin and Nilsson, 2014). There are to date no studies on the impact of snow intercepted by the canopy on the turning moment experienced by trees

during wind loading, or any study of winter impact on wind damage in balsam fir stands, creating a lack of knowledge about winter damages in boreal stands in Northeastern America. This gap in knowledge means that we currently are not able to model what is happening in winter, or to estimate the potential impact of snow on the level of wind damage risk. Therefore, improving knowledge in this area is essential to improve the decision making process for forest management (Díaz-Yáñez et al., 2017). Our measurements are the first to directly measure wind and snow loading on trees during winter. The overall hypotheses for the study were:

1. The additional weight of the snow on the crown will increase the lever arm on the trunk, and trees will experience an increased turning moment at a particular wind speed with an increase of snow thickness in their crowns compared to when there is no snow in the crown.

2. The large negative temperatures will stiffen the trunk because of freezing, therefore trees will experience a globally lower turning moment at a particular wind speed in winter compared to during the summer because the crowns move less.

The first hypothesis deals specifically with the effect of snow and the second hypothesis with the effect of freezing temperatures.

2.2 Materials and Methods

This article was written as a continuation of a previous study at the same site for summer only conditions (Duperat et al., 2021). To reduce the length of the text and avoid redundancy, we refer to Duperat et al. (2021) when additional information on methods is required. All data were treated and analyzed within the R program (R Core Team, 2018) with the help of the Tidyverse packages (Wickham, 2016). The key R packages are mentioned in the relevant paragraphs, the data and R scripts are available and linked to this article.

2.2.1. Stand and Climate

The study was conducted in the Université Laval Montmorency Experimental Forest (47°16013.0”N 71°09024.1”W), 80 km north of Québec City in the Laurentian Hills of the Canadian Shield. Average annual temperature, total precipitation, and snowfall precipitation are respectively 0.5°C, 1583 mm, and 619 cm. Average annual wind speed is 6.9 km/h and wind direction is mainly from the northwest (Normales climatiques canadiennes, 2011). Typical of a polar subcontinental climate, snow cover persists from mid-October to the end of May. The study area is located in the eastern section of the balsam fir/white birch *(Betula papyrifera* Marsh.) bio-climatic domain of central Québec (Robitaille

and Saucier, 1998). The study stand is a 38-year-old balsam fir dominated stand originating from natural regeneration after clearcutting in 1982. It was treated by pre-commercial thinning in 1992. It is composed of balsam fir, black spruce (*Picea mariana* (Mill.)), and white birch. Stand mean height is around 8 m and mean diameter at breast height (*DBH*, in m) measured at 1.3m is 12 cm. The study is concentrated on a 0.13 ha circular portion of the stand. Tree density is 1450 stems per hectare and the trees are heterogeneously distributed within the stand. There is a lot of regeneration and an intermittent stream crosses the stand near its center, creating a treeless linear gap. The stand is located on a north-facing gentle slope with minor variations in the surface of 1–2 m creating dips and raised areas where the trees can be located. Elevation is around 745 m and soil is a glacial till with a sandy loam texture. The site is mesic and has moderate drainage. The field work for this study was carried out between summer 2017 and winter 2019. The stand studied was selected partly according to logistical constraints, as described in Duperat et al. (2021).

2.2.2. Sample Trees

During the summer of 2017, tree height and *DBH* were measured on all the trees within the study area. As sample trees, we selected 15 balsam firs showing no visible symptoms of disease or crown discoloration. The sample trees were sufficiently spaced from each other to avoid direct competition between them. Within the possibilities left by the location constraints, the fifteen trees were chosen across the whole range of diameter present in the stand. Height (*H*, in m), crown width (*CrownW*, in m), crown depth (*CrownD*, in m), and *DBH* were recorded to characterize sample tree morphology.

Two types of competitors, merchantable (*DBH* > 9.8 cm) and non-merchantable (5 < *DBH* < 9.8 cm), were counted when positioned within a 4 m radius from the sample tree. Six competition indices, known to be relevant in the context of wind and snow damage (Hale et al., 2012; Seidl et al., 2014), have been calculated with these parameters (Duperat et al., 2021). In addition, the ratio of the C_{BAL} competition index to the tree basal area (*BA*) = *CIB* was included. All the information concerning morphological criteria, competition indices, and number of close competitors of the sample trees are summarized in Table 2.1, and the competition indices are detailed in Appendix 2.1. Note that trees a10, a13, and a14 are missing. For the a10 tree and a13 tree, one of their strain transducers broke and we were not able to repair it quickly enough to incorporate the data from these trees into our analyses. For the a14 tree, the sensor wires snapped under pressure from the huge amount of snow on the ground. Analyses were therefore conducted with 12 trees instead of 15. Since all the analysis will be made at the individual tree level, each sample tree is effectively an experimental unit.

Table 2.1:. Sample trees variables: morphological criteria, competition indices and number of close competitors.

Tree	Morphological criteria							Distance independent			Distance dependent			Competitors		
ID	*DBH*	*H*	*DBH²H*	*CrownW*	*CrownD*	*BA*	*CIB*	C_{BAL}	C_{dr}	C_{drl}	C_{11}	C_{12}	C_{Hegyi}	N_{COM}	N_{NCOM}	N_{ALL}
a1	0.117	9.1	0.125	1.6	5.9	0.011	804.46	8.65	11.04	2.39	1.79	3.56	3.83	6	13	19
a2	0.106	6.7	0.075	0.8	1.9	0.009	1337.38	11.80	8.32	5.46	1.01	3.62	2.83	7	6	13
a3	0.110	9.2	0.111	1.5	5.7	0.01	1141.81	10.85	10.71	8.89	1.45	4.14	3.86	9	7	16
a4	0.108	8.2	0.096	1.3	5.2	0.009	1249.22	11.44	7.34	2.76	1.32	3.20	3.00	7	4	11
a5	0.175	12.5	0.383	1.8	9.0	0.024	43.61	1.05	7.30	0.00	1.03	1.76	2.55	5	1	6
a6	0.131	9.3	0.160	1.6	5.1	0.013	417.79	5.63	4.92	3.15	0.98	2.04	2.07	4	6	10
a7	0.110	9.0	0.109	1.1	5.4	0.01	1133.81	10.78	13.92	10.25	2.25	5.75	5.06	7	5	12
a8	0.099	7.8	0.076	1.1	4.3	0.008	1832.37	14.11	16.51	12.57	2.04	6.39	5.39	6	6	12
a9	0.115	8.7	0.115	1.5	5.3	0.01	873.12	9.07	8.38	1.11	0.79	2.34	2.52	7	6	13
a11	0.171	8.9	0.260	1.7	5.8	0.023	53.99	1.24	4.73	0.00	0.62	1.13	1.65	8	3	11
a12	0.103	7.4	0.079	1.4	4.4	0.008	1595.24	13.29	11.65	6.87	1.50	4.13	3.93	7	5	12
a15	0.109	8.8	0.105	1.1	5.0	0.009	1202.72	11.22	8.09	4.59	1.08	3.00	2.89	9	7	16

With diameter at 1.3m (*DBH*, m), tree height (*H*, m), crown width (*CrownW*, m), crown depth (*CrownD*, m), subject tree basal area (*BA*, m²), C_{BAL} /*BA* (*CIB*), competition indices : C_{BAL} (Biging and Dobbertin, 1995), C_{11} (Rouvinen and Kuuluvainen, 1997), C_{12} (Rouvinen and Kuuluvainen, 1997), C_{dr} (Kiernan et al., 2008), C_{drl} (Kiernan et al., 2008), C_{Hegyi} (Hegyi, 1974), number of commercial competitors in a radius of 4 meters (N_{COM}), number of non-commercial competitors in a radius of 4 meters (N_{NCOM}), and number of competitors (commercial and non-commercial) in a radius of 4 meters (N_{ALL})

2.2.3. Instrumentation

2.2.3.1 Anemometers and Wind Speed

To measure weather conditions within the stand, a 10-m-high aluminum tower (T35, Aluma Tower Company, Vero Beach, FL, USA) was installed in the forest at the edge of our sampling area. Wind speed and direction were measured at a frequency of 5 Hz by two 05103-L Wind Monitor Young anemometers (Campbell Scientific, Edmonton, AB, Canada), the first one fixed at canopy height, and the second one at 2/3 canopy height. Air temperature and soil temperature were measured with two T107 sensors (Campbell Scientific, Edmonton, AB, Canada) at 30 min intervals. Data from the anemometers and temperature sensors were recorded using a CR5000 datalogger (Campbell Scientific, Edmonton, AB, Canada). Due to the large amount of data collected, and existing literature

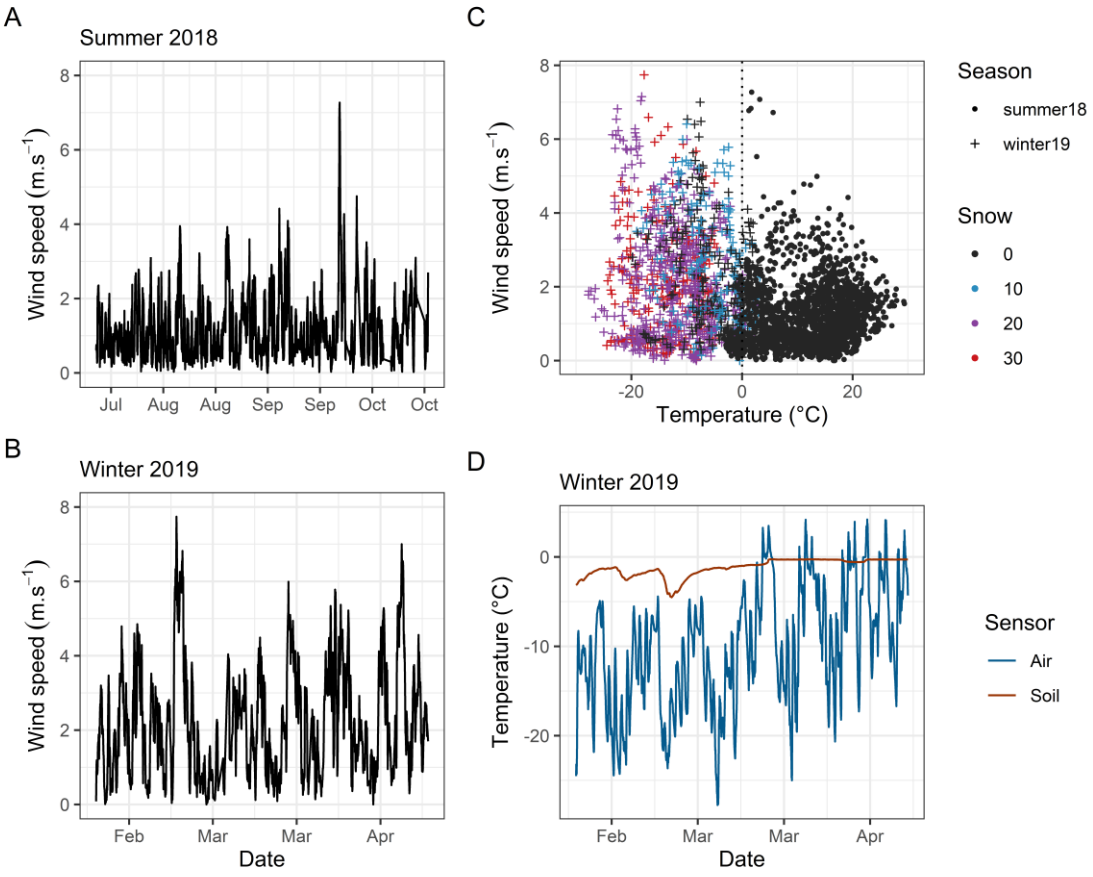

Figure 2.1: Stand meteorological overview, with hourly mean wind speed data for Summer 2018 (A) and Winter 2019 (B), temperature and snow thickness (cm) for both seasons (C), and air and soil temperatures for Winter 2019.

(Hale et al., 2012) and our previous study (Duperat et al., 2021), we decided to work with hourly mean wind speed data (ws, $m \cdot s^{-1}$) (Figure 2.1).

2.2.3.2 Strain Gauges and Turning Moment

Wind loads were recorded on the sample trees during 83 days between July and October 2018 and 56 days between February and April 2019. On each sample tree, two strain transducers were orthogonally fixed on the trunk at two meters height on the north and east sides to minimize the thermal effects of the sun. The stain transducers allow measurement of the strain at the surface of the tree trunk when trees bend and they are described in detail in Duperat et al. (2020). To record the strain transducer signal (STS), we used a CR1000 datalogger (Campbell Scientific, Edmonton, AB, Canada) and two CDM-A116 multiplexors (Campbell Scientific, Edmonton, AB, Canada) connected to datalogger by a SC CPI (Campbell Scientific, Edmonton, AB, Canada). Recording frequency was 5 Hz. The whole experiment was powered by 8 solar panels (5 PowerMax Ultra 80-P, Shell, The Hague, The Netherlands and 3 SX80U, Solarex, Frederick, MD, USA) installed facing south in a clearcut located 70 m south from the tower. To convert measured strain to turning moment, the strain transducers mounted on the sample trees had to be individually calibrated by step pulling (Blackburn, 1997; Gardiner et al., 1997). The method used to correctly carry out the pulling and calibration is fully described in previous studies (Wellpott, 2008; Duperat et al., 2021). Tree pulling calibration was carried out in summer 2018 and in winter 2019 to avoid a bias due to the large difference in temperature and tree trunk stiffness between the two seasons. STS missing values were filled with the previous value, with a maximum of 5 missing values being filled. STS data were then converted into turning moment with the calibration coefficient obtained from the pulling test. Daily drifts caused by thermal variations were removed with a Butterworth highpass filter function from the "signal" package (Butterworth, 1930; signal developers, 2013). Once the data were cleaned, orthogonal turning moments were combined to produce a single turning moment for each tree. Then, we calculated the most probable extreme value experienced during each hour, by calculating the maximum hourly tuning moment (*Mmax*, Nm) with the Gumbel method (Hale et al., 2012; Seidl et al., 2014). Please refer to our previous article (Duperat et al., 2021) for full details of the steps involved in the STS treatment.

2.2.3.3. Hunting Camera and Snow

To measure snow presence or absence on the crown, a HyperFire Reconyx HC500 hunting camera (RECONYX Inc., Holmen, WI, USA) was placed facing a number of crowns. The hunting camera took pictures of the crowns at 1 h intervals during the whole winter season. Each hunting camera

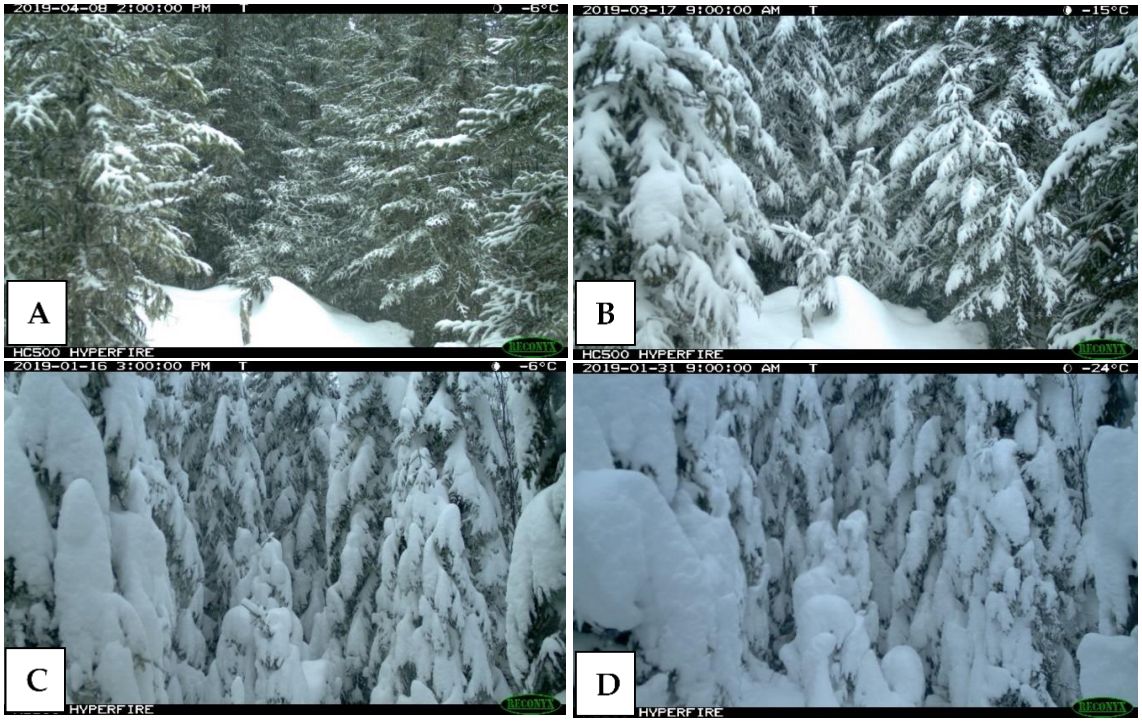

Figure 2.2: Evaluation of the snow thickness on the crowns. A) 0 [0-5 cm] traces of snow on the crowns; B) 10 [5-15cm] the snow sticks to the branches, the branches start to bend; C) 20 [15-25cm] snow clumps everywhere and the branches are fully bent; and D) 30 [>25cm] big snow clumps and bridges between trees.

picture was visually categorized as a function of the snow thickness (*Snow*) on the crown sample. The analysis leads to 4 different categories of *Snow* (0, 10, 20, and 30 cm snow depth) depending on the amount of snow on the branches and the presence of big pieces of snow and snow bridges between trees (Figure 2.1 and 2.2).

2.2.4. Statistical Analysis

2.2.4.1. Effect of snow thickness in the crowns of balsam fir on the overall turning moment

To evaluate the impact of *Snow* on *Mmax*, a linear mixed model selection was made by using the 'nlme' and 'AICcmodavg' packages (Pinheiro et al., 2018; Mazerolle, 2019). Only winter data, from February 2019 to April 2019, were used in this analysis. The response variable (*Mmax*) was log-transformed prior to the analyses to linearize the relation between it and our explanatory variables and to meet the assumptions of homoscedasticity and normality of the residuals. The model selection was made according to 3 steps: determine the best additional variables (Table 2.1) to the basic model,

check the collinearity between the additional variables, and select the best model formulation to consider the relevance of the interaction terms.

Step 1: The variable selection was made by individually adding each available tree variable (all continuous, Table 2.1) to the fixed covariates: *ws* (continuous) and *Snow* (continuous) (Equation 2.1). To consider repeated measurements among trees, *tree* was included as a random intercept in our models. We also included random slopes for *ws* and *Snow* as the effect of these two variables on M_{max} could potentially vary among trees:

$$\log(M_{max}) = ws + Snow + TreeVariable \quad \text{Eq. 2.1}$$

The models were compared using the Akaike information criterion (AICc) (Sakamoto et al., 1986) and the 'AICcmodavg' package (Mazerolle, 2019). The tree variable of the models having a ΔAICc < 2 were kept for the following step. All the models and associated statistics are displayed in Table 2.2.

Step 2: The retained tree variables from step 1 were: C_{BAL}, *DBH*, *CIB*, *CrownW*, *BA*, and DBH^2H. To verify the collinearity between these variables, they were tested two by two with a Pearson correlation test. As they were all correlated with each other at more than 50%, only one of these variables could be included in the final model. The variable with the smallest AICc was selected: C_{BAL}.

Step 3: The model selection was made by testing all possible combinations of variables, and rational interactions between the fixed covariates: *ws* (continuous), *Snow* (continuous), and C_{BAL} (continuous). As in step 1, the models were compared using an AICc comparison. The model with the smallest AICc was kept as best. The tested models and associated statistics are displayed in Table 2.2. Once the final model was selected, the model assumptions were verified by plotting residuals versus fitted values. We assessed the residuals for temporal dependency with an autocorrelation function.

2.2.4.2. Seasonal Differences in Wind Loads in Balsam Fir Stands

Due to the high accumulation of snow in winter leading to a rise in ground level, it was decided to investigate if the anemometers recorded changes in the wind profile between the two seasons. The 'openair' package (Carslaw and Ropkins, 2012) was used to treat the wind speed and wind direction data in summer 2018 and winter 2019. The anemometer wind speed ratio between the top and middle anemometer was compared for each season by using the following linear regression:

$$ws_{top} = ws_{middle} + Season + ws_{middle} \times Season \quad \text{Eq. 2.2}$$

Table 2.2: Snow thickness model selection.

Step 1: Tree variable selection						
log(M_{max}) ~ ws + Snow +	***K***	***AICc***	***ΔAICc***	***AICcWt***	***LL***	***Cum.Wt***
C_{BAL}	8	10116.09	0.00	0.18	-5050.04	0.18
DBH	8	10116.38	0.29	0.16	-5050.18	0.34
CIB	8	10116.74	0.64	0.13	-5050.36	0.48
CrownW	8	10116.85	0.76	0.12	-5050.42	0.61
BA	8	10116.89	0.80	0.12	-5050.44	0.73
$DBH^2 H$	8	10117.77	1.68	0.08	-5050.88	0.81
C_{12}	8	10118.13	2.04	0.06	-5051.06	0.88
CrownS	8	10118.53	2.44	0.05	-5051.26	0.93
C_{dr}	8	10120.99	4.89	0.01	-5052.48	0.95
C_{Heqyi}	8	10121.14	5.05	0.01	-5052.56	0.96
H	8	10121.74	5.64	0.01	-5052.86	0.98
CrownD	8	10123.11	7.02	0.00	-5053.55	0.98
C_{11}	8	10123.23	7.13	0.00	-5053.60	0.99
-	7	10123.79	7.69	0.00	-5054.89	0.99
N_{COM}	8	10124.89	8.80	0.00	-5054.44	0.99
N_{ALL}	8	10125.62	9.53	0.00	-5054.80	0.99
N_{NCOM}	8	10125.79	9.70	0.00	-5054.89	1.00
Step 3: Model selection						
log(M_{max}) ~ ws +	***K***	***AICc***	***ΔAICc***	***AICcWt***	***LL***	***Cum.Wt***
Snow + C_{BAL} + *ws:Snow* + *ws:* C_{BAL} + *Snow:* C_{BAL}	11	10081.87	0.00	0.68	-5029.93	0.68
Snow + C_{BAL} + *ws:Snow* + *Snow:* C_{BAL}	10	10084.12	2.25	0.22	-5032.05	0.90
Snow + C_{BAL} + *ws:Snow* + *ws:* C_{BAL}	10	10086.19	4.32	0.08	-5033.09	0.97
Snow + C_{BAL} + *ws:Snow*	9	10088.40	6.53	0.03	-5035.19	1.00
Snow + *ws:Snow*	8	10096.10	14.22	0.00	-5040.04	1.00
Snow + C_{BAL} + *ws:* C_{BAL} + *snow:* C_{BAL}	10	10109.58	27.70	0.00	-5044.78	1.00
Snow + C_{BAL} + *Snow:* C_{BAL}	9	10111.83	29.95	0.00	-5046.91	1.00
Snow + C_{BAL} + *ws:* C_{BAL}	9	10113.88	32.01	0.00	-5047.94	1.00
Snow + C_{BAL}	8	10116.09	34.22	0.00	-5050.04	1.00
Snow	7	10123.79	41.92	0.00	-5054.89	1.00
C_{BAL} + *ws:* C_{BAL}	8	10186.68	104.80	0.00	-5085.33	1.00
C_{BAL}	7	10188.89	107.01	0.00	-5087.44	1.00
-	6	10196.58	114.71	0.00	-5092.29	1.00

Note: AICc is a version of the Akaike Information Criteria which include a correction for small sample sizes, with delta AICc (ΔAIC_c), AICc weight (*AICcWt*), Log Likelihood (*LL*) and cumulated AICc weight (*Cum.Wt*).

Table 2.3: Season model selection**.**

Step 1: Tree variable selection						
log(M_{max}) ~ ws + Season +	***K***	***AICc***	***ΔAICc***	***AICc Wt***	***LL***	***Cum. Wt***
C_{12}	8	61327.43	0.00	0.39	-30655.71	0.39
CrownW	8	61329.18	1.75	0.16	-30656.59	0.55
C_{BAL}	8	61330.60	3.17	0.08	-30657.30	0.63
DBH	8	61330.63	3.20	0.08	-30657.31	0.70
C_{drl}	8	61330.70	3.27	0.08	-30657.35	0.78
Cib	8	61330.90	3.47	0.07	-30657.45	0.85
BA	8	61331.12	3.69	0.06	-30657.56	0.91
DBH^2H	8	61332.65	5.22	0.03	-30568.32	0.94
C_{heqvi}	8	61333.06	5.63	0.02	-30658.53	0.96
C_{dr}	8	61333.22	5.79	0.02	-30658.61	0.98
C_{11}	8	61335.41	7.98	0.01	-30659.70	0.99
CrownD	8	61336.04	8.61	0.01	-30660.02	0.99
H	8	61336.78	9.35	0.00	-30660.39	1.00
-	7	61340.32	12.89	0.00	-30663.16	1.00
N_{NCOM}	8	61341.79	14.36	0.00	-30662.89	1.00
N_{ALL}	8	61341.82	14.39	0.00	-30662.91	1.00
N_{COM}	8	61342.30	14.87	0.00	-30663.15	1.00
Step 3: Model selection						
log(M_{max}) ~ ws +	***K***	***AICc***	***ΔAICc***	***AICc Wt***	***LL***	***Cum. Wt***
Season + C_{12} + *ws:Season*	9	61163.61	0.00	0.54	-30572.80	0.54
Season + C_{12} + *ws:*C_{12} + *ws:Season*	10	61163.96	0.35	0.45	-30571.98	1.00
Season + C_{12}	8	61327.43	163.81	0.0	-30655.71	1.00
Season + C_{12} + *ws:*C_{12}	9	61327.78	164.16	0.0	-30654.89	1.00
Season	7	61340.32	176.70	0.0	-30663.16	1.00
C_{12}	7	65576.69	4413.07	0.0	-32781.34	1.00
-	6	65589.57	4425.95	0.0	-32788.79	1.00

Note: AICc is a version of the Akaike Information Criteria which include a correction for small sample sizes, with delta AICc (ΔAIC_c), AICc weight (*AICcWt*), Log Likelihood (*LL*) and cumulated AICc weight (*Cum.Wt*).

A linear mixed model selection was made to assess the seasonal effect on turning moment. We decided to analyze our data following the same method as for the first hypothesis, by using the covariate *Season* (categorical with two levels), instead of *Snow*. Both Summer 2018 and Winter 2019 data were used in this analysis. In this case, the retained *TreeVariable* from step 1 were: C_{12} and *CrownW* (Table 2.3). Only one variable could be retained, as they were all correlated with each other (*Pearson correlation coefficient >0.5*). The variable with the smallest AICc was selected: C_{12}. The tested models from step 3 and associated statistics are displayed in Table 2.3. Once the final model was selected, the model assumptions were verified by plotting residuals versus fitted values. We assessed the residuals for temporal dependency with an autocorrelation function.

2.3. Results

2.3.1. Hypothesis 1: Effect of Snow Thickness in the Crowns of Balsam Fir on the Overall Turning Moment

The selected model (Table 2.2) is a mixed linear model, *tree* is used as random intercept, *ws* and *Snow* are used as random slope and the fixed covariates are *ws* (continuous), *Snow* (continuous), and C_{BAL} (continuous). The interaction terms are $ws \times Snow$, $ws \times C_{BAL}$, and $Snow \times C_{BAL}$ (Equation 2.3):

$$\log(M_{max}) = 4.3502 + 0.5179 \times ws - 0.0026 \times Snow - 0.1814 \times C_{BAL} - 0.0003 \times ws \times Snow - 0.0066 \times ws \times C_{BAL} - 0.0001 \times Snow \times C_{BAL}) \quad \text{Eq. 2.3}$$

Model validation indicated no violation of assumptions about homoscedasticity and normality of residuals. The selected model results are displayed in the logarithmic original value in Table 2.4. The model presents a better AICc than models that do not consider the snow effect ($\Delta AICc > 104$), meaning that the addition of *Snow* improves the model predictions and help in defining *Mmax*. However, the snow thickness on the crown, as well as the interaction including this covariate, have little influence on the predicted value of the maximum hourly turning moment.

2.3.2. Hypothesis 2: Seasonal Differences in Wind Loads in Balsam Fir Stands

2.3.2.1. Wind Profile

Wind speed during winter 2019 was stronger and the wind events were more frequent than during summer 2018, with a mean *ws* at canopy top of 2.21 $m.s^{-1}$ and a calm percentage of 2%, in comparison to summer 2018 with values of 1.26 $m.s^{-1}$ and 4.2%, respectively (Figure 2.3). The wind direction

Table 2.4: Snow thickness model results.

Log	*CI lower*	*Estimate*	*CI upper*	*Std.Error*	*DF*	*t-value*
Intercept	*4.1587*	*4.3502*	*4.5417*	*0.0976*	*16479*	*44.529*
ws	0.5012	0.5179	0.5347	0.0085	16479	60.624
Snow	-0.0075	-0.0026	0.0022	0.0025	16479	-1.043
C_{BAL}	-0.2027	-0.1814	-0.1600	0.0097	11	-18.688
Ws:Snow	-0.0008	-0.0003	0.0001	0.0002	16479	-1.368
Ws:C_{BAL}	-0.0081	-0.0066	-0.0052	0.0007	16479	-9.139
Snow:C_{BAL}	-0.0003	-0.0001	0.0005	0.0002	16479	0.344

Note: The results are displayed in logarithms, the interaction between variables are shown with a colon between variables names, with lower confidence interval of the estimate (*CI lower*), upper confidence interval of the estimate (*CI upper*), standard error (*Std.Error*), the degree of freedom (*DF*) and the t-statistics

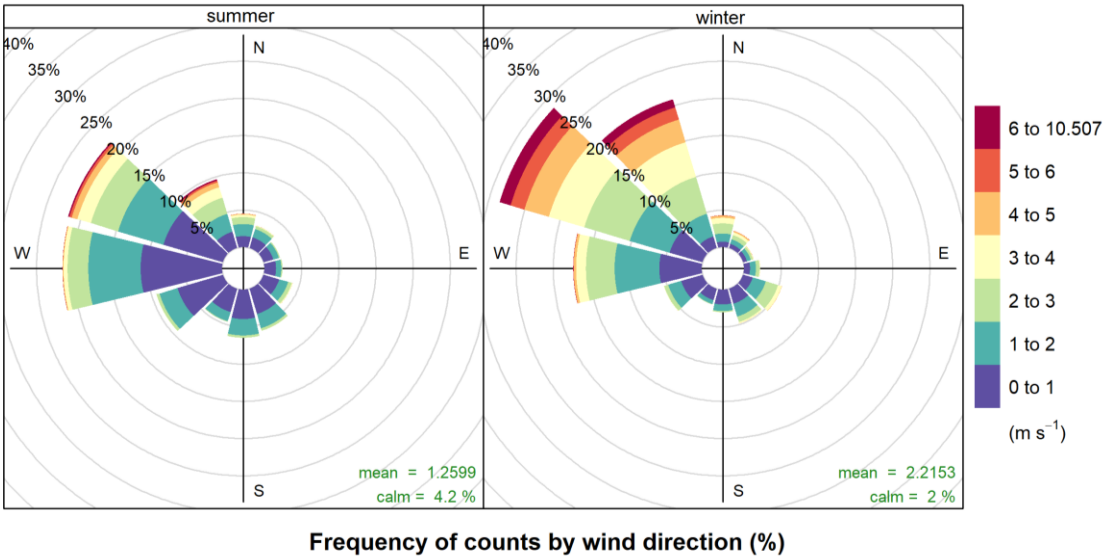

Figure 2.3: Wind rose for summer 2018 and winter 2019 based on hourly mean wind speed and direction data.

was similar, the main winds coming from the northwest. The linear regression carried out on the ratio between the top and middle anemometer shows an increase of 10% (± 0.3, $Adj.R^2 = 0.883$, $p_{value} < 0.01$) of the wind speed ratio during winter, suggesting a clear impact of the snow on the wind profile.

2.3.2.2. Season Model Selection.

The selected model (Table 2.3, Equation 2.4) is a mixed linear model, *tree* is used as random intercept, *ws* and *Season* are used as random slope and the fixed covariates are *ws* (continuous), *Season* (categorical with two levels), and C_{12} (continuous). The interaction term is *ws* × *Season*:

$$\log(M_{max}) = 4.3401 + 0.3268 \times ws + 0.2947 \times Season - 0.5656 \times C_{12} + 0.1199 \times ws \times Season \quad \text{Eq. 2.4}$$

This model gives a much better AICc than models that do not consider the season effect ($\Delta AICc > 176$), meaning that the addition of the variable *Season* increases the model quality. The fixed effects are not correlated with each other. The selected model results are displayed in the logarithmic original value in Table 2.5. Model validation indicated no violation of assumptions about homoscedasticity and normality of residuals. To allow a simpler interpretation of the results, the model's predictions are displayed in Figure 2.4 after back transformation of the logarithms (these values are only provided for illustration purposes because this transformation introduces a bias in the values). As expected, the turning moment increases with the decrease in C_{12}, a low C_{12} representing a tree with little surrounding competition and a high C_{12} representing a tree under a lot of competition. However,

Table 2.5: Season model results.

Log	CI lower	Estimate	CI upper	Std.Error	DF	t-value
Intercept	3.2348	4.3401	5.4455	0.5639	35997	7.694
ws	0.2789	0.3268	0.3747	0.0244	35997	13.373
Season	-0.2792	0.2947	0.8686	0.2928	35997	1.006
C_{12}	-0.8031	-0.5656	-0.3281	0.1065	10	-5.306
ws:Season	0.0903	0.1199	0.1495	0.0151	35997	7.929

Note: The results are displayed in logarithms, the interactions between variables are shown with a colon between variables names, with lower confidence interval of the estimate (*CI lower*), upper confidence interval of the estimate (*CI upper*), standard error (*Std.Error*), the degree of freedom (*DF*) and the t-statistics (*t-value*).

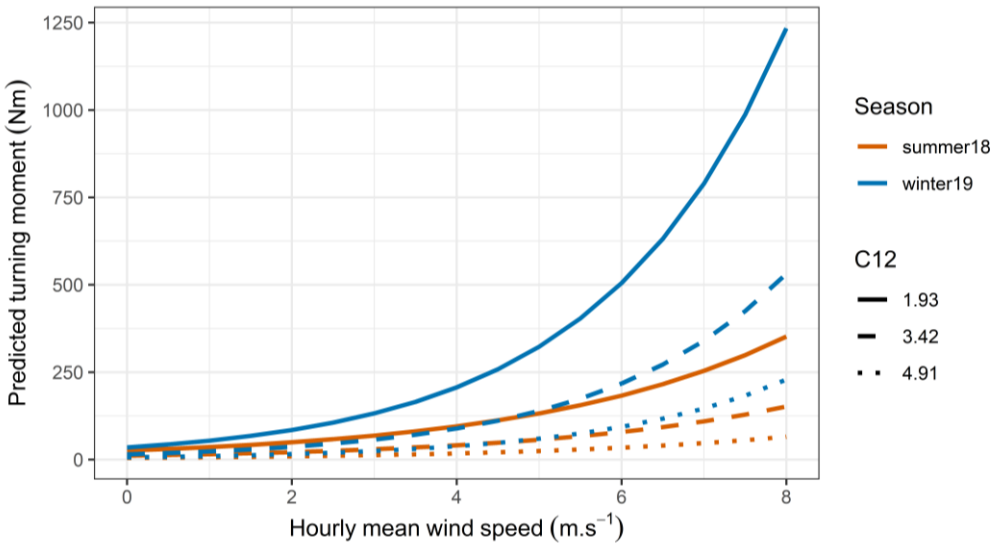

Figure 2.4: Predicted turning moment during winter and summer as a function of C_{12}.

contrary to our hypothesis, the winter season also significantly increases the turning moment experienced by the trees. The turning moment therefore decreases with increasing competition and increases with increasing wind speed.

2.4. Discussion

Our results show that the turning moment experienced by the trees was highly influenced by season, with a turning moment globally higher in winter, but apparently not strongly influenced by the snow thickness on the crowns. These results go against our hypotheses which were that for a similar wind speed, trees experience a higher turning moment when snow is present on their crown, and globally lower turning moment in winter. The *TreeVariables* retained by our model selection also diverge

between the two models. In the first model, including only the winter dataset, at least 4 *TreeVariables* could have been selected instead of the competition index C_{BAL}. However, all these variables are interrelated, based on *DBH*, and relate to the social status of the tree in the forest. In the second model, which combines summer and winter datasets, the distance-dependent competition index C_{12} appears to be the key variable that links the seasons. There is thus a direct dependency of the maximum hourly turning moment on the local competition, which confirms Hale et al. (2012) results, but also shows an influence of close competitors during the winter season. Regarding the effect of snow thickness on the crown, care is needed with the interpretation of the results. The depth of snow on the crown does not seem to make a difference on the turning moment but the model selection for the winter dataset retained snow as a key variable. However, it is important to note that our way of monitoring the presence of snow on the crowns was not optimal. It was a first attempt to evaluate the effect of snow in the canopy on the turning moment in a practical way. Monitoring the presence of snow on the canopy is complicated by the structure of the canopy itself and the great variability in the interception of snow by the branches, as wind and temperature influence the moisture content of snow and therefore the degree of stickiness to the canopy (Nykänen et al., 1997). Therefore, the accumulation of snow on trees sufficient to cause snow damage depends upon the quantity and type of snow (Nykänen et al., 1997) because the same snow thickness could result in two different weights on the branches. As the process of snow interception by trees is complex and involves components of throughfall, adhesion, cohesion, wind removal, sliding, melting, and vapor transport (Keller, 1978), further work is required to evaluate the additional load on trees due to snow. Continuous monitoring of wind at two different heights showed a significant change in the wind profile between summer and winter, with an increase in wind speed at both anemometer heights and reduced calm periods during winter. This is probably due to the presence of snow in winter, which changes the geometrical structure of the stand and therefore the wind profile. This finding supports the fact that deep snow cover also offers less aerodynamic resistance to the wind than ground covered by vegetation and regeneration (Lundqvist, 1996). The accumulation of a large amount of snow on the ground during the winter season, with depths up to 200 cm, also raises the effective level of the ground, while the trees themselves do not change in height and therefore have the same length of lever arm. As observed during fieldwork, the tree trunks remain free to move because their own radiation prevents snow from sticking to the trunk and creates a snow-free sleeve around the trunk down to the ground. The increase of the turning moment experienced by the trees in winter compared to summer for a similar wind speed could be due to several reasons. It might be due to increased stem stiffness due to freezing in the large negative temperatures or to increased root anchorage as the heavy snow depth during our data collection (130–150 cm depth) put a heavy load on the root system. It is quite possible that the

root system in winter is completely locked in place by the snow cover and the frozen soil. The force of the wind on the tree would therefore be mostly applied to the trunk and with very little energy dissipated in the root system. In contrast, in summer, the soil is very wet, and the root system is more flexible, so some of the energy initiated in the trees by the wind is dissipated in the soil. In addition, the higher stiffness of stem and branches during winter decreases the streamlining under wind loads and, combined with a reduced crown porosity, the drag coefficient will be higher in winter. These are probably the two main reasons for the increase of the turning moment during winter.

An increase in the turning moment experienced by the trees, means an increased risk of stem breakage during winter season. With climate change, the relative importance of snow seasons against snow free seasons is likely to change, with an increase of unfrozen soil days during the windiest periods (Saad et al., 2017). If the soil remains unfrozen and without deep snow cover during these windiest periods, this could lead to an increase in overturning during early and late winter, when strong winds are more frequent. It will be important in the near future to have reliable predictions of the future winter climate in Quebec. It will also be useful to study the root anchorage of trees during the pre-winter and winter periods by carrying out destructive tree winching at different temperatures and with different snow cover on the ground, to evaluate if the changes we observed in this study are actually related to changes in root anchorage.

2.5. Conclusions

Wind loading on trees is higher in winter and linked to local competition. It also appears to be strongly related to freezing conditions as differences in snow thickness in the tree crown do not seem to have a major impact on wind loading. However, a single estimate of snow load was applied to all trees and a more precise measurement of the snow load should be examined. The interaction of winter conditions with many factors normally considered in wind damage modeling should also be examined, including the impact of below freezing temperatures on green wood mechanical properties, changes in wind profile, changes in crown shape and porosity, and changes in root/soil stiffness.

Acknowledgments:

The authors thank François Larochelle for technical support and help conducting field work, James Gardiner for help filtering the strain gauge data, François Rousseu from Sherbrooke University for his incredible help with some aspects of the statistics, the 15 students who worked punctually on the fieldwork, but especially Emma Côté for helping with the calibration process, Université Laval Montmorency Experimental Forest for all the proximity services, Julie Bouliane for her help in the

logistical organization, André Desrochers for lending us his snowmobiles, Benjamin Bouchard, Pierre-Erik Isabelle, Maxime Beaudoin-Galaise for introducing us to the snow interception, Sylvain Jutras for providing us with a working lab and support equipment, as well as the anonymous Reviewers and the Editors for their time and help in improving this paper.

Funding

This research was funded by Natural Sciences and Engineering Research Council of Canada, grant number RGPIN-2016-05119, and by the Canadian Wood Fibre Centre, grant CWFC1820-009.

Supplementary Materials

Appendix 2.1: Competition indices

Index type	Index formula	References/Definition
Distance-independent	$C_{BAL} = \sum BA_c * y$	(Biging and Dobbertin, 1995)
	$C_{DR} = \sum \frac{d_c}{d_s}$	(Kiernan et al., 2008)
	$C_{DRL} = \sum \frac{d_c}{d_s} * y$	(Kiernan et al., 2008)
Distance-dependent (DBH)	$C_{Hegyi} = \sum_{c=1}^{n} \frac{d_c/d_s}{D_{cs}}$	(Hegyi, 1974)
	$C_{11} = \sum_{c=1}^{n} \frac{d_c/d_s}{D^2_{cs}}$	(Rouvinen and Kuuluvainen, 1997)
	$C_{12} = \sum_{c=1}^{n} \frac{(d_c/d_s)^2}{D_{cs}}$	(Rouvinen and Kuuluvainen, 1997)
CIB	C_{BAL}/BA	-

Where BA (m^2) is the basal area; y = 1 for competitor with diameter larger than the subject tree, otherwise y = 0; d is DBH; Dcs (m) is distance between subject (s) and competitor (c).

Chapitre 3 : Effet d’une éclaircie localisée sur la charge de vent dans un peuplement de sapin baumier naturellement régénéré.

Effects of a localized thinning on wind loading in a naturally regenerated balsam fir stand.

Resumé

Les tendances récentes en matière de gestion forestière tendent à accroître l'utilisation des coupes partielles dans les peuplements naturellement régénérés, augmentant également le risque de dommages causés par le vent pour les arbres laissés sur place. Pour limiter ces risques, il est important de mieux comprendre l'évolution des charges de vent appliquées aux arbres à la suite d’une coupe partielle. Le sapin baumier (*Abies balsamea* (L.) Mill.) est une essence largement distribuée au Québec et très vulnérable aux dommages causés par le vent, faisant de cette essence une candidate idéale pour l'étude des chablis. Notre principal objectif était d'étudier le comportement mécanique d’un échantillon de sapin baumier soumis à des charges de vent avant et après retrait des compétiteurs environnants. Les objectifs sous-jacents étaient d’attester un potentiel changement du profil de vent dans le peuplement à la suite de l'éclaircie localisée, et de quantifier l'impact de l'éclaircie localisée sur les arbres individuels à l'échelle du peuplement. Deux anémomètres placés à la hauteur de la canopée et aux 2/3 de celle-ci, et des jauges de contrainte fixées sur les troncs de sapins baumiers nous ont permis de mesurer les moments de flexion induits par le vent subis par un échantillon de sapins baumiers. Une éclaircie localisée consistant à retirer tous les compétiteurs proches dans un rayon de 3,5m a été effectuée sur 2/3 des arbres de l'échantillon la deuxième année de l'expérience. Les résultats montrent une augmentation globale du moment de flexion des arbres après le traitement localisé en raison du changement du profil du vent à travers la canopée. Cette augmentation était plus importante pour les arbres traités, mais globalement, les arbres les moins compétitifs (traités ou non) étaient ceux qui subissaient le plus de stress, et étaient donc les plus à risques suite à la coupe. Cette étude démontre la puissance de l'utilisation des indices de compétition pour comprendre les risques de dommages causés par le vent dans les peuplements hétérogènes.

Abstract

Recent trends in forest management tend to increase the use of partial cuttings in naturally regenerated stands, increasing the risk of wind damage to the remnant trees in the first few years after cutting. To limit those risks, it is therefore important to better understand the change in wind loads experienced by the remnant trees following the cutting treatment. Balsam fir (*Abies balsamea* (L.) Mill.) is widely distributed in Eastern Canada and highly vulnerable to wind damage, making it a good candidate for studying wind loads. The main objective was to survey the mechanical response of individual balsam fir under wind loading before and after removing all their surrounding competitors. Secondarily, we wanted to observe the change in wind profile in the stand because of the localized thinning, as well as the impact of the localized thinning on individual trees at the stand scale. Two anemometers placed at canopy height and 2/3 canopy height, and strain gauges attached to the trunks of balsam fir trees allowed us to measure the wind-induced turning moments experienced by a sample of trees. A localized thinning was made around 2/3 of the sample trees the second year of the experiment (described in Chapters 1 and 2). All the close competitors were removed in an area within a 3.5m radius. The results show a global increase in the turning moment experienced by the trees after the localized treatment due to the change in wind profile through the canopy. This increase was greater for the treated trees, but globally, the less competitive trees (treated or not) were the ones experiencing most wind stress, and thus their risk of wind damage was increased the most. This study also demonstrates the value of the use of competition indices in understanding the risks of wind damages in heterogeneous stands.

3.1 Introduction

Following large storm damages in Europe in the 1990s, which had a strong impact on wood markets for several years (Hanewinkel and Peyron, 2013, in Gardiner et al., 2013), forest research on wind damage risks has intensified in order to increase our understanding of wind and tree interactions, and mechanisms that induce windthrow (Quine, 1994). In the last 30 years, the knowledge accumulated by a world-wide group of researchers working on wind and trees has made it possible to develop wind damage risk prediction models and decision-support tools for forest managers (Peltola et al., 1999; Gardiner et al., 2008). Recent trends in forest-management encourage a more heterogeneous composition of cultivated forests, moving from even-aged and homogenous plantations to forests with a more natural structure and complexity (Gauthier, 2009; Vitkova and Dhubháin, 2013). This transformation of the cultivated forests represents a challenge both in terms of silviculture and risk management (Schütz, 2001), but could lead to an increase in stand resilience against wind (Jactel et al., 2017; Morimoto et al., 2019). These new forestry regimes mainly use partial cuts to harvest trees. However, even though partial cuts may increase a stand's resistance to wind over the long term, they also increase the risk of overturning and breakage in the first years of acclimation for the remaining trees (Cremer et al., 1982). The partial cuts change the stand structure and decrease its stability (Gardiner et al., 2005) by increasing wind loads in the canopy, changing the gust and wind behaviour (Poëtte et al., 2017) and by reducing shelter from neighbouring trees (Cameron et al., 1995; Wallentin and Nilsson, 2014; Kamimura et al., 2017). Following a partial cut, the level of wind damage risk increases with the size and frequency of the gaps within the canopy (Gardiner et al., 1997; Kamimura et al., 2017), but also with the proportion of basal area removed (Wallentin and Nilsson, 2014). Another important factor for wind damage risk is the size of the trees left in place (Kamimura et al., 2017). As the bigger trees are more acclimated to wind loads (Kamimura et al., 2017) and are sheltering their neighbors, thinning from below is normally recommended (Cremer et al., 1982; Duperat et al., 2021).

Therefore, models initially developed for stand-level risk in even-aged and homogeneous stands (Peltola et al., 1999; Gardiner et al., 2000), have been modified to calculate tree-level risk in more heterogenous and nature-like stands (Hale et al., 2012; Seidl et al., 2014). The challenge with these new models lies in the complexity and structural variability of heterogeneous stands. Recent studies on wind and trees have focused on finding simple variables and indices, to help the models predicting wind loading in those complex stands. Some studies tend to emphasize the use of simple competition indices to evaluate the wind loading on a single tree (Hale et al., 2012; Seidl et al., 2014; Kamimura et al., 2015). The location of the tree relative to others and the shelter they provide is an important

consideration when looking at the interaction of wind and trees (Gardiner et al., 2016), as trees can be physically supported by neighbors when crowns overlap (Quine, 1994; Rudnicki et al., 2001, 2003, 2008; Schelhaas et al., 2007; Schindler et al., 2012) and as roots can interlock (Savill, 1983; Smith et al., 1987) enhancing the stability of the root anchorage. Therefore, those competition indices could be a useful and easy way of monitoring spatial changes in the stand following a partial cutting, as they directly reflect the number of remaining individuals, their size and in some cases the distance between them, and as most of the variables needed to calculate them are generally listed in stand inventories.

Hale et al. (2012) observed a relationship between various competition indices and the wind load applied on trees in heterogeneous stands. However, they stressed that further studies should be conducted in order to verify whether the relationship is modified by thinning. The only data we could find concerning the monitoring of the direct wind load applied to the trees before and after a partial cut were obtained in a wind tunnel by using 1:75 scaled plastic trees (Gardiner et al., 1997, 2005) and these plastic trees cannot acclimate to the change in wind conditions. To advance the knowledge on wind loads on trees and to refine risk management models, it is necessary to monitor the trees *in situ* before and after a partial cut.

The principal aim of this study is therefore to document how the wind loads on balsam fir (*Abies balsamea* (L.) Mill) trees changes after a partial cutting, by comparing for the first time the wind loading on individual trees before and after partial cutting. In Quebec (Canada), balsam fir trees are widespread and known to be particularly prone to wind damage (Taylor et al., 2019) and particularly to overturning because of their inflexible foliage and their shallow rooting (Achim et al., 2005b). This makes balsam fir an ideal candidate for this study.

To document the changes in wind loads of balsam fir after partial cutting, we focused on the following hypotheses:

1. The wind profile of the stand is influenced by a localized thinning around a sample of trees (Gardiner et al., 1997, 2005; Novak et al., 2000; Zhu et al., 2003).

2. Trees from which close competitors have been removed experience a higher turning moment than trees with competitors, for a similar wind speed (Hale et al., 2012; Seidl et al., 2014).

3. All trees within the stand are affected by a localized thinning, even if their close-competitors remain standing.(Gardiner et al., 1997; Hale et al., 2012).

3.2. Materiel and Methods

3.2.1. Stand and climate

The study was conducted in the Université Laval Montmorency Experimental Forest (47°16'13.0"N 71°09'24.1" W), 80 km north of Québec City in the Laurentian Hills of the Canadian Shield. Average annual temperature, total precipitation, and snowfall precipitation are respectively 0.5°C, 1583 mm, and 619 cm. Average annual wind speed is 6.9 km/h and wind direction is mainly from the northwest (Normales climatiques canadiennes, 2011). Typical of a polar subcontinental climate, snow cover persists from mid-October to the end of May. The study area is located in the eastern section of the balsam fir/white birch *(Betula papyrifera* Marsh.) bio-climatic domain of central Québec (Robitaille and Saucier, 1998). The study stand is a 38-year-old balsam fir dominated stand originating from natural regeneration after clearcutting in 1982. It was treated by pre-commercial thinning in 1992. It is composed of balsam fir, black spruce (*Picea mariana* (Mill.)), and white birch. Stand mean height is around 8 m and mean diameter at breast height (*DBH*, in m) measured at 1.3m is 12 cm. The study is concentrated on a 0.13 ha circular portion of the stand. Initial tree density was 1450 stems per hectare and the trees were heterogeneously distributed within the stand. There is a lot of regeneration and an intermittent stream crosses the stand near its center, creating a treeless linear gap. The stand is located on a north-facing gentle slope with minor variations in the surface of 1–2 m creating dips and raised areas where the trees can be located. Elevation is around 745 m and soil is a glacial till with a sandy loam texture. The site is mesic and has moderate drainage. The field work for this study was carried out between summer 2017 and summer 2019. The stand studied was selected partly according to logistical constraints, as described in Duperat et al. (2021).

3.2.2 Trees

During the summer of 2017, tree height and *DBH* were measured on all the trees within the study area. As sample trees, we selected balsam firs showing no visible symptoms of disease or crown discoloration. The sample trees had to be sufficiently spaced from each other to avoid direct competition between them. Within the possibilities left by these constraints, fifteen trees were chosen across the whole range of diameters present in the stand. Height (*H*, in m), crown width (*CrownW*, in m), crown depth (*CrownD*, in m), and *DBH* were recorded at the beginning of the study to characterize sample tree morphology. Since balsam fir growth is particularly slow under these climatic conditions and manual measurement is subject to experimenter imprecision, these parameters were not subsequently re-measured. Therefore, the very minor growth in the first season after thinning was not accounted for in this study.

Two types of competitors, merchantable (*DBH* > 9.1 cm) and non-merchantable (5 < *DBH* < 9.1 cm), were counted when positioned within a 3.5 m radius from the sample tree. Six competition indices, known to be relevant in the context of wind damage (Hale et al., 2012; Seidl et al., 2014), were calculated with these parameters (Duperat et al., 2021). All the information concerning morphological criteria, competition indices, and number of close competitors of the sample trees is summarized in Table 3.1, and the competition indices are detailed in Appendix 3.1. The distance dependent competition indices and number of competitors were calculated with the close competitors within the 3.5m radius only. Thus, after thinning the distance dependent competition indices and number of close competitors did not change for the Group A (control) and were equal to zero for the Group B. Note that trees a8, a10, and a14 are missing. In each case, one of their strain transducers broke and we were not able to repair it quickly enough to incorporate the data from these trees into our analyses. Analyses were therefore conducted with 12 trees instead of 15.

3.2.3. Instrumentation

3.2.3.1 On site wind and temperature

To measure wind and temperature conditions within the stand, a 10-m-high aluminum tower (T35, Aluma Tower Company, Vero Beach, FL, USA) was installed in the forest at the edge of our sampling area. Wind speed and direction were measured at a frequency of 5 Hz by two 05103-L Wind Monitor Young anemometers (Campbell Scientific, Edmonton, AB, Canada), the first one fixed at canopy height, and the second one at 2/3 canopy height. Air temperature (T, °C) was measured with a T107 sensor (Campbell Scientific, Edmonton, AB, Canada) at 30 min intervals. Data from the anemometers and temperature sensor were recorded using a CR5000 datalogger (Campbell Scientific, Edmonton, AB, Canada). Following existing literature (Hale et al., 2012) and our previous studies (Duperat et al., 2020, 2021), we decided to work with hourly mean wind speed (*ws*, $m \cdot s^{-1}$) and wind direction (*wd*, degree) data. The wind data were treated using the "openair" package (Carslaw and Ropkins, 2012).

3.2.3.2 Strain gauges

Wind loads were recorded during summer 2018 and summer 2019 using custom-made strain transducers. On each sample tree, two strain transducers (Moore et al., 2005) were orthogonally fixed on the trunk at two meters height on the north and east sides to minimize the thermal effects of the sun. The strain transducers allow measurement of the strain at the surface of the tree trunk when trees bend and they are described in detail in Moore et al. (2005) and in Duperat et al. (2020b).

Table 3.1: Sample trees variables: morphological criteria, competition indices, and number of close competitors.

Tree		Morphological criteria						Distance independent						Distance dependent[1,2]			Competitors[1,2]		
								2018			2019								
Group	*ID*	*DBH*	*H*	DBH^2H	*CrownW*	*CrownD*	*BA*	C_{BAL}	C_{dr}	C_{drl}	C_{BAL}	C_{dr}	C_{drl}	C_{11}	C_{12}	C_{Hegyi}	N_{COM}	N_{NCOM}	N_{ALL}
A[1]	a2	0.106	6.7	0.075	0.8	1.9	0.009	12.31	9.29	6.73	8.98	8.66	6.73	$1.09e^{-4}$	0.036	0.026	7	6	13
	a6	0.131	9.3	0.160	1.6	5.1	0.013	6.02	5.95	4.17	4.61	5.95	4.17	$1.23e^{-4}$	0.021	0.021	4	6	10
	a11	0.171	8.9	0.260	1.7	5.8	0.023	1.27	6.64	1.00	0.82	6.64	1.00	$0.68e^{-4}$	0.011	0.015	8	3	11
	a15	0.109	8.8	0.105	1.1	5.0	0.009	11.52	8.44	5.65	8.41	8.44	5.65	$1.16e^{-4}$	0.031	0.028	9	7	16
B[2]	a1	0.117	9.1	0.125	1.6	5.9	0.011	8.94	12.11	4.46	6.52	7.67	3.46	$1.80e^{-4}$	0.022	0.024	6	13	19
	a3	0.110	9.2	0.111	1.5	5.7	0.010	11.14	11.72	9.89	8.03	2.23	2.23	$1.66e^{-4}$	0.041	0.038	9	7	16
	a4	0.108	8.2	0.096	1.3	5.2	0.009	11.74	8.38	3.80	8.55	1.00	1.00	$1.36e^{-4}$	0.033	0.031	7	4	11
	a5	0.175	12.5	0.383	1.8	9.0	0.024	1.08	5.43	1.00	0.62	3.81	1.00	$0.64e^{-4}$	0.007	0.009	5	1	6
	a7	0.110	9.0	0.109	1.1	5.4	0.010	11.07	14.91	11.25	7.96	7.27	5.41	$2.35e^{-4}$	0.045	0.038	7	5	12
	a9	0.115	8.7	0.115	1.5	5.3	0.010	9.36	9.38	2.11	6.94	4.87	2.11	$0.57e^{-4}$	0.014	0.016	7	6	13
	a12	0.103	7.4	0.079	1.4	4.4	0.008	13.73	12.65	7.87	10.07	6.71	6.71	$1.24e^{-4}$	0.025	0.026	7	5	12
	a13	0.142	9.0	0.181	1.5	6.0	0.016	4.26	5.36	2.37	3.08	1.76	1.00	$0.62e^{-4}$	0.015	0.014	6	12	19

With diameter at 1.3 m (*DBH*, m), tree height (*H*, m), crown width (*CrownW*, m), crown depth (*CrownD*, m), subject tree basal area (*BA*, m^2), C_{BAL}/BA (*CIB*), competition indices: C_{BAL} (Biging and Dobbertin, 1995), C_{11} (Rouvinen and Kuuluvainen, 1997), C_{12} (Rouvinen and Kuuluvainen, 1997), C_{dr} (Kiernan et al., 2008), C_{drl} (Kiernan et al., 2008), C_{Hegyi} (Hegyi, 1974), number of commercial competitors in a radius of 3.5 m (N_{COM}), number of non-commercial competitors in a radius of 3.5 m (N_{NCOM}), and number of competitors (commercial and non-commercial) in a radius of 3.5 m (N_{ALL}).

Notes:

[1].Group A: only distance independent competition indices were affected by the 2019 thinning.

[2].Group B: only distance independent competition indices are displayed for 2019, as we removed all the competitors in an area of 3.5m radius, the distance dependent indices and number of competitors were then all equal to zero.

To record the strain transducer signal (STS), we used a CR1000 datalogger (Campbell Scientific, Edmonton, AB, Canada) and two CDM-A116 multiplexors (Campbell Scientific, Edmonton, AB, Canada) connected to datalogger by a SC CPI (Campbell Scientific, Edmonton, AB, Canada). Recording frequency was 5 Hz. The whole experiment was powered by 8 solar panels (5 PowerMax Ultra 80-P, Shell, The Hague, Netherlands and 3 SX80U, Solarex, Frederick, MD, USA) installed facing south in a clearcut located 70 m south from the tower. To convert measured strain to turning moment, the strain transducers mounted on the sample trees had to be individually calibrated by step pulling (Blackburn, 1997; Gardiner et al., 1997). The method used to correctly carry out the pulling and calibration is fully described in previous studies (Wellpott, 2008; Duperat et al., 2021). Tree pulling calibration was carried out in summer 2018. *STS* data were converted into turning moment with the calibration coefficient obtained from the pulling test. Daily drifts caused by thermal variations were removed with a Butterworth highpass filter function from the "signal" package in R (Butterworth, 1930; signal developers, 2014; Duperat et al., 2021). Once the data were cleaned, orthogonal turning moments were combined to produce a single turning moment for each tree. Then, we calculated the most probable extreme value experienced during each hour, by calculating the maximum hourly tuning moment (*Mmax*, Nm) with the Gumbel method (Cook, 1985; Hale et al., 2012). Please refer to the previous article (Duperat et al., 2021) for full details of the steps involved in the *STS* treatment.

3.2.4 Treatment: localized thinning

The 12 sample trees were divided into two groups: A and B. Group A, with n=4 trees distributed across the *DBH* range of the sample trees, serves as the control group. Group B with n=8 trees serves as the treatment group. To study the effect of an abrupt change of competition on tree response to wind loading, a localized thinning (thinning) was carried out around the trees from group B in June 2019 (Figure 3.1). This meant that all the competitors, merchantable and non-merchantable, within a radius of 3.5m around the sample trees were removed to leave the sample trees with no crown support and no local protection against wind loading. Following thinning, the competition indices were recalculated for the 12 sample trees (Table 3.1).

3.2.5 Analyses

The temperature and wind data were checked between the two summers to ensure that the weather conditions were as close as possible and to prevent a yearly bias. The whole dataset was then filtered by hourly mean battery voltage ($V > 11.3$) to prevent datalogger artifacts caused by power outage. A lot of data were discarded by this method, but because artifacts are difficult to detect on such a big

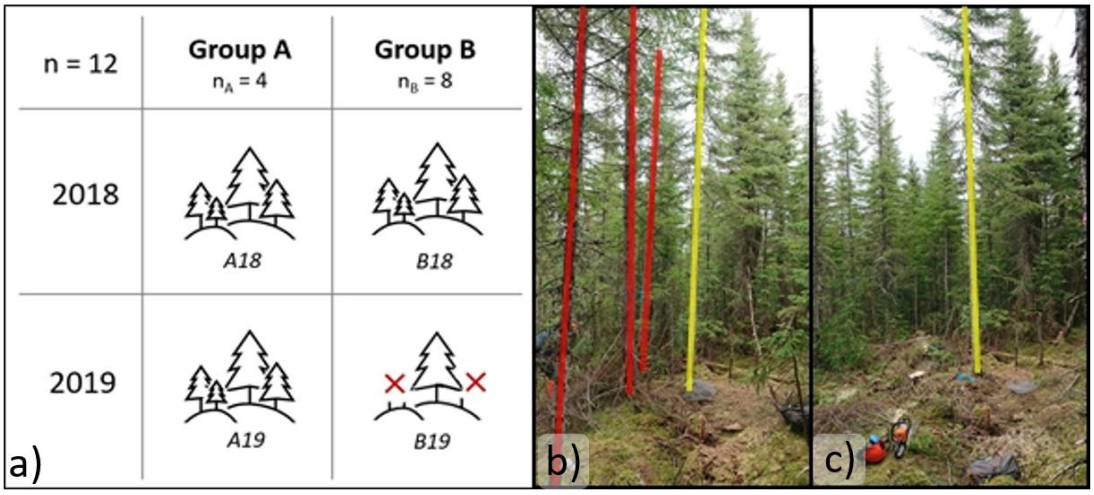

Figure 3.1: Experimental design (a), before (b) and after (c) pictures of one localized thinning. The localized thinning was made in 2019 on the trees from Group B. The red lines (b) represent the competitors that were later cut around the sample tree (yellow lines).

dataset and could potentially bias the Gumbel method, we chose to be restrictive to ensure a good pool of unbiased data.

All the following analyses were then performed on the same pool of post-filtered data: 760 hours recorded over 32 days between the 31st of July and the 31st of August 2018; and 860 hours recorded over 38 days between the 28th of June and 16th of August 2019.

3.2.5.1 Comparison of wind profiles before and after treatment

To evaluate a potential change in the wind profile at the experimental site, wind roses were made with the openair R package (Carslaw and Ropkins, 2012) to visually assess the wind speeds and direction for our two anemometers during the two summers. In addition, a linear model selection was made between *top anemometer* ($m \cdot s^{-1}$) and the covariates *middle anemometer* ($m \cdot s^{-1}$), *Year* (two-levels factor: 2018, 2019) and their interactions. The models were then compared with the Akaike information criterion (AIC). The final linear model chosen was the one with the smallest AIC.

3.2.5.2 Treatment effect by Group – local effect

To evaluate the impact of the localized thinning on *Mmax*, a linear mixed model selection was made by using the 'nlme' and 'AICcmodavg' R packages (Pinheiro et al., 2018; Mazerolle, 2019). The response variable (*Mmax*) was log-transformed prior to the analysis to linearize the relation between it and our explanatory variables and to meet the assumptions of homoscedasticity and normality of

Table 3.2: Treatment effect by groups, model selection by AICc. Maximum hourly turning moment (*Mmax*) in function of wind speed (*ws*, continuous numeric: m.s-1), *Year* (two levels factor: 2018 (reference), 2019) and *Group* (two levels factor: A (reference), B).

log(Mmax) ~ ws +	**K**	**AICc**	**ΔAICc**	**AICcWt**	**AICcCUmwt**	**LL**
Year + Group + ws:Group + Year:Group	10	17585.30	0.00	0.50	0.50	-8782.64
Year + Group + Year:Group	9	17585.30	0.00	0.49	1.00	-8783.64
Year	7	17623.24	37.93	0.00	1.00	-8804.61
Year + Group + ws: Group	9	17624.85	39.54	0.00	1.00	-8803.41
Year + Group	8	17625.23	39.93	0.00	1.00	-8804.61
-	6	19631.33	2046.06	0.00	1.00	-9809.67
Group + ws: Group	8	19633.00	2047.70	0.00	1.00	-9808.49
Group	7	19633.36	2048.05	0.00	1.00	-9809.67

the residuals. The model selection was made by testing all combinations of variables and meaningful interactions between the fixed covariates: *ws* (continuous numeric, $m \cdot s^{-1}$), *Group* (2 levels factor: A, B, with the control group A as reference level), and *Year* (2 levels factor: 2018, 2019, with the control year 2018 as reference level). To consider repeated measurements among trees, *tree* was included as a random intercept in our models. We also included random slope for *ws* as the effect of this variable on *Mmax* could potentially vary among trees. The models were then compared using an Akaike information criterion comparison (AICc, Sakamoto et al., 1986). The model with the smallest AICc was retained. The tested models and associated statistics are displayed in Table 3.2. Once the final model was selected, the model assumptions were verified by plotting residuals vs fitted values. We assessed the residuals for dependency with an autocorrelation function.

3.2.5.3 Treatment effect by trees – global effect

Even if the treatment was localized around the eight selected sample trees, the total area of the localized thinning has fragmented the stand by creating gaps in the canopy, and therefore changed the distance-independent competition indices for all the sample trees. Additionally, the anemometers recorded a change in wind profile after thinning (2019). A second linear model selection was then made to assess a potential effect of the localized thinning treatment on the whole stand. The selection was made in two steps: first, determining the best additional variable to the basic model, then selecting the best model formulation to consider the relevance of the interaction terms.

Step 1: the variable selection was made by individually adding each *tree variable* (all continuous, Table 3.3) to the fixed covariates: *ws* (continuous, $m \cdot s^{-1}$) and *Year* (2 levels factor: 2018, 2019, with the control year 2018 as reference level) (Equation 3.1). To consider repeated measurements among

Table 3.3: Treatment effect by trees in two steps: trees variable selection, then model selection by AICc.

Step 1: Best individual trees variable selection. Model selection by AICc. Maximum hourly turning moment as a function of wind speed (*ws*, continuous numeric: $m \cdot s^{-1}$), *Year* (two levels factor: 2018 (reference), 2019) and different tree variables (continuous numeric).

log(TM) ~ ws +	**K**	**AICc**	**ΔAICc**	**AICcWt**	**AICcCUmwt**	**LL**
Year + C_{BAL}	8	17356.51	0.00	1	1	-8670.25
Year + C_{11}	8	17493.44	136.93	0	1	-8738.71
Year + C_{12}	8	17500.94	144.43	0	1	-8742.47
Year + C_{HEGYI}	8	17505.15	148.64	0	1	-8744.57
Year + C_{DR}	8	17508.72	152.22	0	1	-8746.36
Year + C_{DRL}	8	17527.06	170.56	0	1	-8755.53
Year + DBH^2H	8	17619.01	262.50	0	1	-8801.50
Year + *CrownD*	8	17619.35	262.85	0	1	-8801.67
Year + *BA*	8	17619.46	262.95	0	1	-8801.72
Year + *DBH*	8	17619.49	262.99	0	1	-8801.74
Year + *CrownW*	8	17620.11	263.61	0	1	-8802.05
Year + *H*	8	17620.38	263.87	0	1	-8802.18
Year	7	17623.24	266.73	0	1	-8804.61
Year + N_C	8	17624.10	267.59	0	1	-8804.04
Year + N_A	8	17624.68	268.17	0	1	-8804.33
Year + N_{NC}	8	17625.11	268.61	0	1	-8804.55
-	6	19631.36	2274.86	0	1	-9809.68

Step 2: Model selection by AICc. Maximum hourly turning moment (*Mmax*) as a function of wind speed (*ws*, continuous numeric: $m \cdot s^{-1}$), *Year* (two levels factor: 2018 (reference), 2019) and C_{BAL} (continuous numeric).

log(Mmax) ~ ws + Year + C_{BAL} **+**	**K**	**AICc**	**ΔAICc**	**AICcWt**	**AICcCumwt**	**LL**
ws:C_{BAL} + *Year:*C_{BAL}	10	17298.25	0.00	1	1	-8639.12
Year:C_{BAL}	9	17298.25	24.52	0	1	-8652.38
ws: C_{BAL}	9	17333.25	35.00	0	1	-8657.62
-	8	17356.51	58.25	0	1	-8670.25

Note: The interactions between variables are shown with a colon between variables names, with K, AICc, DeltaAICc,

trees, *tree* was included as a random intercept in our models. We also included random slopes for *ws* as the effect of this variable on *Mmax* could potentially vary among trees.

$$\log(M_{max}) = ws + Year + TreeVariable \qquad \text{Eq. 3.1}$$

The models were then compared using the AICc. The tree variables of the model having the smallest ΔAICc was kept for the following step. All the models and statistics are displayed in Table 3.

Step 2: The model selection was made by testing all possible combination of variables, and meaningful interactions between the fixed covariates: *ws* (continuous, $m \cdot s^{-1}$), *Year* (2 level factors: 2018, 2019, with the control year 2018 as reference level) and C_{BAL} (continuous). As in step 1, the models were compared using an AICc comparison. The model with the smallest AICc was kept as best. The tested models and statistics are displayed in Table 3.3. Once the final model was selected, the model assumptions were verified by plotting residuals against fitted values. We assessed the residuals for temporal dependency with an autocorrelation function.

3.3. Results

3.3.1 Hypothesis 1: effect of the treatment on the wind profile

The wind roses for both on-site anemometers (Figure 3.2) suggest stronger wind speeds and less calm periods in 2019 than in 2018. There was no visible shift in wind directions between the years. Additionally, the linear model selection predicting wind speed at the top anemometer retained the model including the covariates *middle anemometer* ($m.s^{-1}$), *Year* (two-levels factor: 2018 (reference level), 2019), and their interactions ($\Delta AIC > 10$). The model results show a slightly but significant change in the wind profile after thinning (Table 3.4, $p_{value} < 0.01$, $adj.R^2 = 0.851$). The ratio between top anemometer and middle anemometer wind speeds was lower in 2019 as the wind speed increased more in the middle of the canopy than at the top, suggesting an increase in the stand porosity.

3.3.2 Hypothesis 2: local effect of the treatment on the wind loading

The selected model for wind loading (Table 3.2) is a mixed linear model, *tree* is used as random intercept, *ws* is used as random slope and the fixed covariates are *ws* (continuous), *Year* (two-levels factor: 2018, 2019), and *Group* (two-levels factor: A, B). The interaction terms are *ws* x *Group*, and *Year* x *Group* (Equation 3.2):

$$\log(M_{max}) = 2.883 + 0.262 \times ws + 0.197 \times Year - 0.283 \times \text{Group} + 0.065 \times Year \times Group + 0.076 \times ws \times \text{Group} \quad \text{Eq. 3.2}$$

Model validation indicated no violation of assumptions about homoscedasticity and normality of residuals. The selected model results are displayed in the logarithmic original value in Table 3.5. One other model which did not retain the interaction *ws* x *Group* had an equivalent AICc. As the only term that was different between the two models is an interaction term, we decided to not use model averaging (Cade, 2015). We then decided to keep the first model with the interaction term, as the term

seems logical in our opinion and as it offers a more complete model of the stand. The retained model presents a better AICc than all the other models (ΔAICc > 38).

To allow a simpler interpretation of the results, the model's predictions are displayed in Figure 3.3 after back transformation of the logarithms. As expected, the turning moment for Group B increases after the thinning treatment. What we did not expect was that the turning moment would also increase in 2019 for Group A. However, the increase between 2018 and 2019's turning moments is larger for Group B trees than for Group A. Therefore, there is an effect of the localized thinning treatment on the treated trees, but also an effect on the untreated trees in the rest of the stand.

3.3.3 Hypothesis 3: global effect of the treatment on the wind loading

The selected model predicting wind load using a competition index approach (Table 3.3) is a mixed linear model, *tree* is used as random intercept, *ws* is used as random slope and the fixed covariates are ws (continuous), *Year* (two-levels factor: 2018, 2019), and C_{BAL} (continuous). The interaction terms are *Year* x C_{BAL}, and *ws* x C_{BAL} (Equation 3):

$$\log(M_{max}) = 3.018 + 0.338 \times ws + 0.046 \times Year - 0.037 \times C_{BAL} + 0.015 \times Year \times C_{BAL} - 0.03 \times ws \times C_{BAL} \quad \text{Eq. 3.3}$$

This model gives a much better AICc than the other ones (ΔAICc > 24), meaning that the addition of the two interaction terms increases the model quality. The fixed effects are not correlated with each other. The selected model results are displayed in the logarithmic original value in Table 3.6. Model validation indicated no violation of assumptions about homoscedasticity and normality of residuals. To allow a simpler interpretation of the results, the model's predictions are displayed in Figure 3.4 after back transformation of the logarithms. The turning moments increased in 2019 following the localized thinning, at all competition levels. The interaction term between *ws* and C_{BAL} suggests for a given year, a non-linear relationship between M_{max} and *ws* as a function of C_{Bal}. As *ws* increases the M_{max} will increase faster in trees with low C_{Bal} (biggest trees) than trees with high C_{Bal} (smallest trees). Additionally, the interaction term between *Year* and C_{BAL} suggests that the increase in M_{Max} as a result of partial cutting will be greater for the smallest trees (high C_{BAL}) than for the biggest trees (low C_{BAL}).

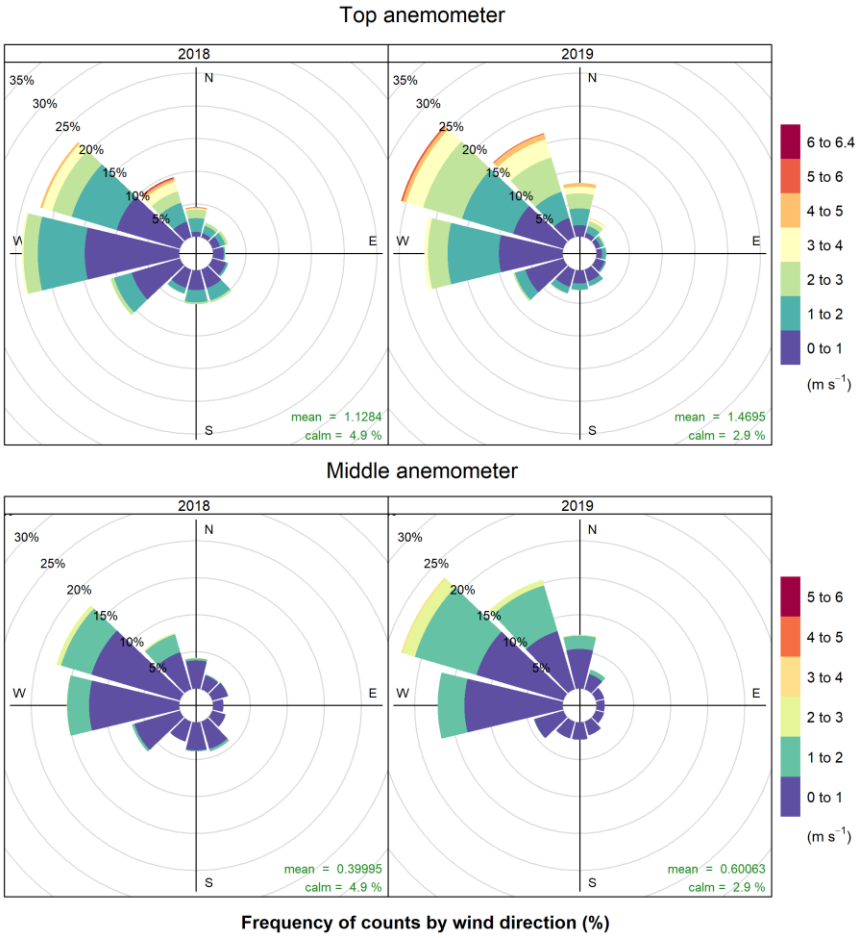

Figure 3.2: Wind roses for on-site top and middle anemometers in 2018 and 2019.

Table 3.4: Effect of the localized thinning (*Year*=2019) on the wind profile.

ws_{Top} ~	Value	CI Lower	CI Upper	Std.Error	t-value	p-value
Intercept	0.46	0.39	0.45	0.01	31.33	<0.01
ws_{Middle}	1.75	1.71	1.79	0.02	80.77	<0.01
Year (ref.=2018)	0.05	0.01	0.09	0.01	2.61	<0.01
ws_{Middle} *:Year*	-0.10	-0.15	-0.05	0.02	-3.82	<0.01

Note: The interactions between variables are shown with a colon between variables names, with lower confidence interval of the estimate (CI lower), upper confidence interval of the estimate (CI upper), standard error (Std.Error), the t-statistics (t-value) and the p-value statistics

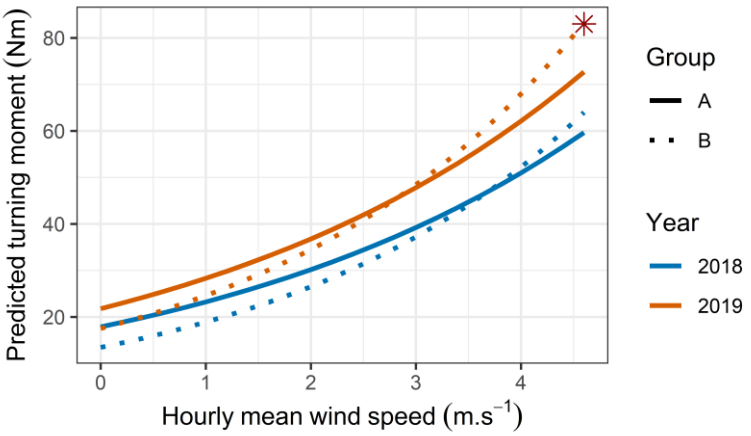

Figure 3.3: Predicted turning moment as a function of *Group* (2 levels factor: A, B) and *Year* (2 levels factor: 2018, 2019). Note: Turning moment values are only provided for an illustration of the model, because of the bias introduced in the back transformation of the logarithmic values. The red asterisk indicates the trees directly affected by the localized thinning treatment (*Group* = B, *Year* = 2019).

Table 3.5: Treatment effect by groups, model results

Log	Value	CI Lower	CI Upper	Std.Error	DF	t-value
Intercept	2.883	1.301	4.464	0.806	18955	3.573
ws	0.262	0.163	0.360	0.050	18955	5.229
Year (ref.=2018)	0.197	0.145	0.249	0.026	18955	7.450
Group (ref.=A)	-0.283	-2.484	1.918	0.988	10	-0.286
Year:Group	0.065	0.001	0.129	0.032	18955	2.001
ws:Group	0.076	-0.043	0.197	0.061	18955	1.251

Note: The results are displayed in logarithms, the interactions between variables are shown with a colon between variables names, with lower confidence interval of the estimate (CI lower), upper confidence interval of the estimate (CI upper), standard error (Std.Error), the degree of freedom (DF) and the t-statistics (t-value).

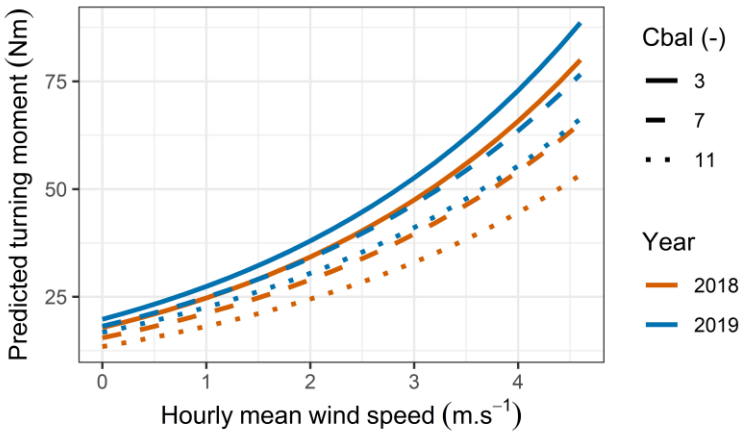

Figure 3.4: Predicted turning moment before and after the localized thinning, as a function of the selected variables: C_{BAL} (continuous, numeric) and *Year* (two-levels factor: 2018 (reference), 2019). Note: Turning moment values are only provided for an illustration of the model, because of the bias introduced in the back transformation of the logarithmic values. The thinning occurred between the 2018 and 2019 measurements.

Table 3.6: Treatment effect by tree, model results

Log	Value	CI Lower	CI Upper	Std.Error	DF	t-value
Intercept	3.018	1.387	4.649	0.832	18954	3.628
ws	0.338	0.265	0.411	0.037	18954	9.090
Year (ref.=2018)	0.046	-0.024	0.118	0.036	18954	1.278
C_{BAL}	-0.037	-0.202	0.126	0.083	18954	-0.452
Year: C_{BAL}	0.015	-0.042	0.073	0.029	18954	0.521
ws: C_{BAL}	-0.003	-0.009	0.002	0.003	18954	-1.146

Note: The results are displayed in logarithms, the interactions between variables are shown with a colon between variables names, with lower confidence interval of the estimate (CI lower), upper confidence interval of the estimate (CI upper), standard error (Std.Error), the degree of freedom (DF) and the t-statistics (t-value).

3.4 Discussion

To better anticipate the wind risk in naturally regenerated stands after a partial cut, it is important to understand how individual trees react to wind loads after having their close-competitors removed. Previous studies addressing this subject were based on a wind tunnel experiment using 1:75 scale plastic trees (Gardiner et al., 2005) or evaluated only post-thinning stands (Wallentin and Nilsson, 2014; Kamimura et al., 2017). This follow-up *in situ* study on wind loads applied to the trees after thinning was the first to monitor the trees before and after thinning. This study allows us to better understand how trees react to a sudden loss of competitors, and how these changes could affect the whole stand.

Our results show that the turning moment experienced by the sample trees was highly influenced by the localized thinning treatment, with a higher maximum hourly turning moment experienced by the treated trees following the thinning in summer 2019. The local treatment also had a significant effect on the trees which were not directly affected by the localized thinning and which retained their close competitors. These control trees also experienced a higher turning moment in summer 2019 after the thinning, but with less impact than for the treated trees. These results can be explained by the slight change in wind profile that occurred in the stand after thinning. The thinning created eight gaps in the stand canopy and even if those gaps were small and localized (radius of 3.5m) they represent 23% of the stand area, allowing the wind to flow more easily through the canopy. Therefore, this change in stand porosity changed the wind flow and increased the wind speed in the middle of the canopy confirming that even small partial cutting can have an impact on the wind profile (Cremer et al., 1982; Gardiner et al., 2005). These results confirm our hypotheses which were that even if the treatment had a bigger impact on the treated trees, the whole stand would be affected by the treatment.

The results also suggest that even if the biggest trees always experienced the highest turning moment, the increase in turning moment following the partial cut was greater for dominated trees than for dominant trees. Partial cutting would then apply a greater increase in wind stress to the less competitive trees. This tends to confirm our previous model predictions (Duperat et al., 2021) suggesting that the least competitive trees were the most at risk following a commercial thinning, highlighting the value of thinning from below in this type of stand.

To confirm a post-thinning change in wind loading on all trees in the stand, and thus intrinsically on the level of wind damage risk, we should therefore not only focus on the local change in direct competition around the treated trees, but also on the change in competition of the whole stand. The model selection we made to assess the global effect of the thinning on the stand retained the distance-

independent competition index C_{BAL} (Biging and Dobbertin, 1995) as the best variable. Our results suggest that among all the morphological variables and competition indices tested, C_{BAL} is therefore the best tool to account for a stand-wide change in competition following localized thinning in a balsam fir stand. This confirms our previous results in pre-thinning conditions (Duperat et al., 2021), and the work of Hale et al. (2012). The C_{BAL} competition index is easy to calculate with any traditional stand inventory, making its use easy to integrate into risk models and thinning simulations. It is therefore a powerful tool to predict changes in competition following a thinning, by assessing the competition status for an individual tree while reflecting any changes in competition at the stand scale.

In recent years, wind and tree studies have tended to focus increasingly on individual trees to assess the levels of risk of wind damage in stands. Our results highlight the fact that we should look at the stands in a multi-scalar way, both at the level of the individual trees and of the entire stand, in order to prevent wind damage. The importance of small changes of stand structure and level of competition within the stand following partial cut should not be overlooked during forest management planning. This is even more true during stand conversion from a homogenous stand to a more heterogeneous one (Nyland, 2003). If partial cutting tends to increase the wind speed in the stand, it could also change the level of evapotranspiration and thus influence the level of carbon fixation in the trees (Ma et al., 2012). Additionally, we know that root-grafting are common for balsam fir trees (Quer et al., 2020) but still relatively unstudied because of the difficulty of looking at what happens below the soil surface on a large scale. Those root grafts concern at least 30% of the balsam fir in the stand and should play an important role in the stability of the stand in the wind. Competition indices are already highly developed in growth monitoring (Stadt et al., 2007), we now know that they are also indicated in monitoring wind damage risk modelling, thus demonstrating the power of these tools. It would therefore be interesting to see if competition indices could provide a universal measure for forest stands that provides a method for quickly assessing potential growth, carbon fixation, wind and snow risk and a way to help compare different kinds of stands.

As was the case in previous studies using similar measurements (Hale et al., 2012; Kamimura et al., 2017; Duperat et al., 2021, 2020), the study took place in only one stand and with a small sample size. This limitation is directly linked to the amount of equipment required. With this limitation, extrapolation to other stands should be made with caution. The trees we used were also rather small for a commercial thinning operation. However, they could be considered representative of a stand conversion where the process is initiated early in the rotation (Schütz, 2001). Such a stand conversion is an important element in transitioning from plantation to continuous cover forestry (Pommerening and Murphy, 2004). Additionally, a recent study on balsam fir trees (Dupont-Leduc et al., 2020)

compared the effects of different partial cuttings on the basal area increment during a conversion thinning trial. Their results suggest that the "crop tree release" method, which consists of removing all the competitors within a 3m radius, causes a basal area increment similar to thinning from below, but with a more marked increase on the treated individuals than on the competitors. This thinning method also appears to offer a better solution for stand transition than thinning from below.

This experiment provides a first validation of using competition indices to simulate the effect of thinning on the probability of wind damage. However, it also showed that the relationship between the competition index and wind load was influenced by thinning. This means that additional research would be required to include both the tree- and the stand-level effects of such a treatment.

3.5 Conclusion

Localized thinning had both local and global impacts on the wind profile and wind loading on trees within the stand. It significantly increased the turning moment experienced by individual trees in the whole stand, but at an increased level on the trees whose close competitors were completely removed. The greatest post-thinning increase in wind stress was experienced by dominated trees, justifying the importance of thinning from below in this type of stand, to minimize wind damage risks. The distance independent competition index C_{BAL} appears to be the best tool to assess the stand-wide impact of a localized thinning. However, additional work is needed to better understand how thinning influences the relationship between competition indices and wind loading on trees.

Conclusion générale

Retour sur le projet de recherche

L'objectif global de cette thèse était d'observer l'effet de l'hétérogénéité du peuplement sur les charges imposées par le vent au niveau des arbres individuels dans une sapinière à bouleau blanc. Pour répondre à cet objectif et aux objectifs sous-jacents, une expérimentation a été mise en place dans une des sapinières de la Forêt Montmorency (Forêt d'enseignement et de recherche de l'Université Laval). Elle visait à suivre le moment de force appliqué par le vent sur un échantillon de sapins baumiers lors de trois saisons, permettant ainsi de suivre l'évolution de la réaction mécanique des sapins baumiers sous trois types de conditions : l'été 2018 pour les conditions initiales, l'hiver 2019 pour les conditions hivernales et enfin l'été 2019 pour les conditions post-éclaircie. Cette expérimentation évolutive a ainsi permis de récolter toutes les données nécessaires à l'élaboration de cette thèse.

Le but de la première saison était de comprendre la réponse mécanique des sapins baumiers en conditions « initiales » et de voir si la littérature sur le sujet était applicable à notre peuplement. Se basant sur les travaux de Hale et al (2012), notre hypothèse centrale était que l'utilisation d'indices de compétition améliore l'estimation des coefficients de moment de flexion propres à chacun de nos arbres, permettant ainsi de faire de meilleures prédictions des risques de chablis en sapinière, et le cas échéant, d'aider aux décisions sylvicoles. La seconde saison quant à elle servait d'étude pionnière pour déterminer l'impact de conditions hivernales sur la flexion des troncs. Aucune étude n'ayant, à notre connaissance, été faite sur le sujet, le but de cette saison expérimentale était de trouver les paramètres hivernaux essentiels à ajouter au modèle initial. Cette saison a permis d'observer le comportement des sapins baumiers dans un contexte de températures fortement négatives combinées à d'importantes précipitations neigeuses. Notre hypothèse centrale était que l'hiver allait augmenter le moment de force de nos arbres à cause des fortes accumulations de neige sur les houppiers. A la suite de l'hiver et juste avant notre troisième saison, une éclaircie localisée a été effectuée dans le peuplement pour laisser une partie de nos arbres face à un changement abrupt de compétition locale. Ceci nous a ainsi permis d'observer *in situ* pour la toute première fois ce qui se passerait lors d'une coupe partielle. Pour cette saison, notre hypothèse principale était que l'éclaircie localisée allait provoquer une augmentation importante du moment de force ressenti par les arbres traités pas cette éclaircie.

Les comparaisons entre les données initiales prises à l'été 2018 et les données des deux saisons suivantes ont permis de noter d'importants changements de comportement mécanique des sapins baumiers en fonction des conditions propres à chacune des saisons. Nos résultats montrent que ces changements saisonniers influencent fortement les variables à utiliser pour modéliser les peuplements hétérogènes lors de la prévision des risques de chablis. Il est important de noter le caractère innovant des deux dernières saisons d'expérimentation. Ces données étant les toutes premières à être récoltées dans ces conditions, elles permettent d'apporter de nouvelles perspectives globales sur la modélisation des risques de chablis.

L'hiver oui, mais la neige ?

Le suivi hivernal de la réaction mécanique des sapins baumiers lors d'épisodes de vent (chapitre 2), suggère que l'hiver tend à augmenter de façon générale les moments de flexion imposés sur les arbres individuels. La présence de gros blocs de neige accrochés aux houppiers des sapins laissait suggérer une augmentation importante de la masse des houppiers et donc des moments de forces associés. Cependant, et de façon surprenante, les analyses n'ont pas démontré d'effet direct de l'épaisseur de neige sur les houppiers. L'augmentation des moments de force en hiver serait donc *a priori* indépendante de la charge de neige ajoutée sur la canopée. Cela serait possiblement dû à notre façon non-optimale d'évaluer l'épaisseur de neige sur les houppiers. Il est donc difficile dans notre contexte de savoir ce qui a provoqué ce changement de réaction des sapins en hiver, mais il est imaginable que l'épaisse couverture de neige qui recouvre le sol bloque le système racinaire et empêche la diffusion de la charge appliquée sur l'arbre via une dissipation de l'énergie par le système racinaire. Cette charge serait donc augmentée sur le tronc, provoquant des moments de flexion plus importants en hiver qu'en été, pour deux charges de vent *a priori* équivalentes. La structure du peuplement change aussi énormément en hiver, notamment au niveau du profil de vent. L'épaisse couverture de neige rehausse alors le niveau du sol et les blocs de neige interceptés par les houppiers changent totalement la porosité de la canopée, perturbant ainsi le profil de vent et changeant la charge appliquée sur les arbres.

Coupe partielle, mais impact global.

Le suivi de la réaction mécanique des sapins baumiers avant et après l'éclaircie (chapitre 3) suggère qu'une perturbation même très localisée engendre des changements de réaction mécanique au niveau des arbres traités, mais engendre également un effet plus global sur l'ensemble des arbres du peuplement. A la suite de l'éclaircie localisée réalisée autour des arbres du groupe B (traité), nous avons pu constater une augmentation du moment de flexion de ces arbres, mais également une

augmentation du moment de flexion des arbres du groupe A (témoin) dont les compétiteurs n'ont pas été retirés. L'augmentation était plus marquée sur le groupe traité, cependant il est important de noter l'impact global de ce traitement localisé. Cet effet peut être facilement expliqué par la modification du profil de vent dans notre peuplement à la suite de l'éclaircie. En effet, nous avons pu enregistrer une augmentation de la vitesse de vent au milieu de la canopée, les trouées issues de l'éclaircie localisée ayant permis au vent de pénétrer plus facilement le peuplement.

Rôle des indices de compétition dans la modélisation des risques de chablis

Le premier chapitre a permis de confirmer pour la première fois les résultats de Hale et. al (2012, 2015), suggérant que l'association de la méthode FG_TMC à l'indice de compétition indépendant de la distance, C_{BAL}, présente un bon potentiel pour la prévision des risques de chablis en sapinière.

D'après les résultats du troisième chapitre, l'augmentation du moment de force à la suite de l'éclaircie localisée était plus importante pour les arbres ayant un indice de compétition élevé, soit les arbres les moins compétitifs. Ces arbres étant moins acclimatés au vent que les arbres dominants, ils sont alors plus à risque de déraciner ou briser à la suite d'une coupe partielle. Le troisième chapitre vient ainsi confirmer que l'indice de compétition C_{BAL} est la variable la plus performante pour capter les changements de compétition à la suite d'une éclaircie localisée dans ce type de peuplement. Les résultats du chapitre 3 viennent également confirmer nos simulations du premier chapitre, laissant entendre que l'éclaircie par le bas est la technique la plus adéquate pour minimiser les risques de chablis dans les sapinières à bouleau blanc. Cependant, même si les arbres ayant subi la plus forte augmentation du moment de force sont les arbres les moins compétitifs, il est important de garder en tête que l'utilisation de coupe partielle augmente le moment de force appliqué sur tous les arbres individuels, quel que soit leur niveau de compétition, et ainsi augmente le risque de chablis pour tous les arbres résiduels.

Petit bémol toutefois concernant les conditions hivernales, car les résultats du second chapitre suggèrent que c'est l'indice de compétition C_{12}, cette fois ci dépendant de la distance, qui ressort comme la meilleure variable pour capter l'hétérogénéité du peuplement. En hiver, l'environnement direct de l'arbre aurait donc plus d'importance que l'environnement global du peuplement. Une piste pouvant expliquer cela serait peut-être les « ponts » de neige qui se forment parfois entre les houppiers des arbres. Il demeure toutefois difficile de confirmer cette hypothèse, l'épaisseur de neige n'étant pas ressortie de nos modèles comme ayant un impact important sur le moment de flexion des arbres, mais ayant tout de même été maintenu dans notre sélection de variable.

Ces résultats concernant les indices de compétition sont très encourageants pour la suite des recherches en modélisation des peuplements hétérogènes. L'indice de compétition C_{BAL}, en plus de sa performance de prédiction, est extrêmement facile à calculer et est déjà utilisé dans d'autres types de modèles forestiers tels que les modèles de croissance. Sa capacité à améliorer les prédictions des modèles de risques de chablis au niveau de l'arbre individuel tout en tenant compte de la structure du peuplement, ainsi que sa simplicité d'utilisation, font de cet indice un puissant outil pour évaluer l'impact des stratégies de gestion sylvicole.

Limites de l'étude et élargissement

S'inscrivant dans la continuité des précédents travaux de recherches, ces travaux auront ainsi permis (1) d'approfondir les connaissances sur la modélisation des risques de chablis en peuplement hétérogène, (2) de fournir des données innovantes concernant la réaction mécanique des arbres individuels lors de conditions hivernales boréales et à la suite d'une coupe partielle, et, (3) de confirmer l'importance et la facilité d'utilisation des indices de compétition dans la compréhension des mécanismes induisant le chablis.

Il est toutefois important de noter les limites imputables à ce type d'expérimentation. En effet, les résultats de ces trois chapitres sont strictement basés sur une poignée d'arbres tous issus du même peuplement. Les résultats présentés ici sont donc applicables pour les sapinières à bouleau blanc présentant les mêmes conditions de croissance que la nôtre (régénération naturelle et éclaircie pré-commerciale). Le deuxième point important à prendre en compte est la taille moyenne des arbres du peuplement. Les sapins baumiers que nous avons étudiés ici sont de petits gabarits comparés à l'âge du peuplement (38-40 ans), ce type d'arbre est moins à risque que des arbres plus élancés tels qu'on peut retrouver dans des peuplements adjacents au nôtre. Les chiffres énoncés dans les résultats, notamment les risques de chablis calculés dans le premier chapitre, peuvent ainsi sembler faibles. Le plus gros défi et handicap de l'étude a résidé dans l'utilisation du matériel que nous avions à notre disposition pour mettre en place l'expérimentation, c'est notamment la taille de la tour à anémomètres qui nous a limité dans le choix de la taille du peuplement, l'anémomètre le plus haut devant se trouver à hauteur de canopée. Néanmoins, même si de plus grands arbres étudiés des conditions similaires nous auraient sans doute permis d'avoir un effet plus important de l'éclaircie sur le risque de chablis, les processus observés demeurent valides. Il serait cependant intéressant de reproduire ce type d'expérimentation dans différentes conditions de croissance et de faire le suivi de peuplements soumis à des travaux sylvicoles variés. La perturbation du sol engendrée par la circulation des machines sylvicoles serait également bonne à prendre en compte, le poids des machines pouvant influencer

l’ancrage racinaire des arbres et de ce fait impacter les risques de chablis. L’ancrage racinaire est également influencé par les nombreuses anastomoses racinaires présentes chez le sapin baumier. Il existe pour le moment relativement peu d’études sur le sujet, mais la présence d’anastomoses avec les compétiteurs proches pourrait permettre d’expliquer en partie l’efficacité des indices de compétition.

Concernant l’hiver, notre façon d’aborder cette saison peut sembler simpliste, cependant le défi résidait dans la nouveauté de ce type de données et la difficulté des travaux de terrain durant cette saison particulièrement hostile. Les conditions hivernales rendent extrêmement difficile la mise en place et le maintien d’une telle expérimentation. Le froid et la neige limitent le temps de travail extérieur et mènent à mal les équipements : les batteries se déchargent rapidement, les panneaux solaires, anémomètres et jauges de contraintes se retrouvent pris dans la glace, des animaux en quête de nourriture viennent grignoter les câbles électriques ou encore le poids de l’épaisse couverture de neige vient arracher les câbles des instruments. Pour approfondir ces premiers résultats hivernaux, les prochains travaux de recherche pourraient faire l’usage de vrais instruments de mesures d’interception de neige par les houppiers et d’un suivi plus approfondi du type de neige (densité, humidité) et du profil de vent dans la canopée. Des travaux de treuillage destructifs pourraient également être réalisés pour développer les connaissances sur l’ancrage racinaire des sapins baumiers en hiver.

Le suivi de ce dispositif se poursuivra afin de caractériser l'acclimatation aux conditions créées par la coupe partielle. Ces travaux futurs, qui s’inscrivent directement dans la continuité de notre projet, permettront d’augmenter notre capacité à comprendre et modéliser les risques de chablis post-coupe partielle dans ces peuplements, et donc, d’aider les gestionnaires forestiers dans leurs choix de traitements sylvicoles.

Bibliographie

Achim, A., Ruel, J.-C., and Gardiner, B. A. (2005a). Evaluating the effect of precommercial thinning on the resistance of balsam fir to windthrow through experimentation, modelling, and development of simple indices. *Can. J. For. Res.* 35, 1844–1853. doi:10.1139/x05-130.

Achim, A., Ruel, J.-C., Gardiner, B. A., Laflamme, G., and Meunier, S. (2005b). Modelling the vulnerability of balsam fir forests to wind damage. *Forest Ecology and Management* 204, 37–52. doi:10.1016/j.foreco.2004.07.072.

Alemdag, I. S. (1978). Evaluation of some competition indexes for the prediction of diameter increment in planted white spruce. *Information Report Forest Management Institute (Canada). no. FMR-X-108.* Available at: http://agris.fao.org/agris-search/search.do?recordID=CA19830874798 [Accessed July 11, 2019].

Anyomi, K. A., Mitchell, S. J., and Ruel, J.-C. (2016). Windthrow modelling in old-growth and multi-layered boreal forests. *Ecological Modelling* 327, 105–114. doi:10.1016/j.ecolmodel.2016.02.003.

Bastien, Y., and Gauberville, C. (2011). *Vocabulaire forestier: écologie, gestion et conservation des espaces boisés*. Forêt privée française.

Bergeron, Y., Drapeau, P., Gauthier, S., and Lecomte, N. (2007). Using knowledge of natural disturbances to support sustainable forest management in the northern Clay Belt. *The Forestry Chronicle* 83, 326–337. doi:10.5558/tfc83326-3.

Biging, G. S., and Dobbertin, M. (1995). Evaluation of Competition Indices in Individual Tree Growth Models. *Forest Science* 41, 360–377.

Blackburn, G. R. A. (1997). The growth and mechanical response of trees to wind loading.

Busby, J. A. (1965). Studies on the stability of conifer stands. *Scottish Forestry* 19, 86–102.

Butterworth, S. (1930). On the theory of filter amplifiers. *Experimental wireless*, 536–541.

Cade, B. S. (2015). Model averaging and muddled multimodel inferences. *Ecology* 96, 2370–2382. doi:https://doi.org/10.1890/14-1639.1.

Cameron, A. D., Dunham, R. A., and Petty, J. A. (1995). The effects of heavy thinning on stem quality and timber properties of silver birch (Betula pendula Roth). *Forestry: An International Journal of Forest Research* 68, 275–286. doi:10.1093/forestry/68.3.275.

Carslaw, D. C., and Ropkins, K. (2012). openair — An R package for air quality data analysis. *Environmental Modelling & Software* 27–28, 52–61. doi:10.1016/j.envsoft.2011.09.008.

Cook, N. (1985). The designer's guide to wind loading of building structures. *Butterworths, London*.

Cremer, K. W., Borough, C. J., Mckinnell, F. H., and Carter, P. R. (1982). Effects of stocking and thinning on wind damage in plantations. *New Zealand Journal of Forestry Science*, 244–265.

Deslauriers, A., Morin, H., Urbinati, C., and Carrer, M. (2003). Daily weather response of balsam fir (Abies balsamea (L.) Mill.) stem radius increment from dendrometer analysis in the boreal forests of Québec (Canada). *Trees - Structure and Function* 17, 477–484. doi:10.1007/s00468-003-0260-4.

Díaz-Yáñez, O., Mola-Yudego, B., González-Olabarria, J. R., and Pukkala, T. (2017). How does forest composition and structure affect the stability against wind and snow? *Forest Ecology and Management* 401, 215–222. doi:10.1016/j.foreco.2017.06.054.

Duperat, M., Gardiner, B., and Ruel, J.-C. (2020). Wind and snow loading of balsam fir during a Canadian winter: A pioneer study. *Forests* 11, 1089. doi:10.3390/f11101089.

Duperat, M., Gardiner, B., and Ruel, J.-C. (2021). Testing an individual tree wind damage risk model in a naturally regenerated balsam fir stand: potential impact of thinning on the level of risk. *Forestry: An International Journal of Forest Research* 94, 141–150. doi:10.1093/forestry/cpaa023.

Dupont-Leduc, L., Schneider, R., and Sirois, L. (2020). Preliminary Results from a Structural Conversion Thinning Trial in Eastern Canada. *Journal of Forestry* 118, 515–533. doi:10.1093/jofore/fvaa022.

Gardiner, B. A., Stacey, G. R., Belcher, R. E., and Wood, C. J. (1997). Field and wind tunnel assessments of the implications of respacing and thinning for tree stability. *Forestry (Lond)* 70, 233–252. doi:10.1093/forestry/70.3.233.

Gardiner, B., Berry, P., and Moulia, B. (2016). Review: Wind impacts on plant growth, mechanics and damage. *Plant Science* 245, 94–118. doi:10.1016/j.plantsci.2016.01.006.

Gardiner, B., Blennow, K., Carnus, J.-M., Fleischer, P., Ingemarsson, F., Landmann, G., et al. (2010). Destructive storms in European forests: past and forthcoming impacts. European Forest Institute Available at: https://hal.inrae.fr/hal-02824530 [Accessed February 16, 2021].

Gardiner, B., Byrne, K., Hale, S., Kamimura, K., Mitchell, S. J., Peltola, H., et al. (2008). A review of mechanistic modelling of wind damage risk to forests. *Forestry* 81, 447–463. doi:10.1093/forestry/cpn022.

Gardiner, B., Marshall, B., Achim, A., Belcher, R., and Wood, C. (2005). The stability of different silvicultural systems: a wind-tunnel investigation. *Forestry (Lond)* 78, 471–484. doi:10.1093/forestry/cpi053.

Gardiner, B., Peltola, H., and Kellomäki, S. (2000). Comparison of two models for predicting the critical wind speeds required to damage coniferous trees. *Ecological Modelling* 129, 1–23. doi:10.1016/S0304-3800(00)00220-9.

Gardiner, B., Schuck, A., Schelhaas, M.-J., Orazio, C., Blennow, K., and Nicoll, B. (2013). *Living with Storm Damage to Forests What Science Can Tell Us What Science Can Tell Us*. doi:10.13140/2.1.1730.2400.

Gardiner, B., Suárez, J., Achim, A., Hale, S., and Nicoll, B. F. (2004). a PC-based wind risk model for British Forests (User's Guide). *Forestry Commission, Edinburgh*.

Gauthier, S. (2009). *Ecosystem Management in the Boreal Forest*. PUQ.

Hale, S. E., Gardiner, B. A., Wellpott, A., Nicoll, B. C., and Achim, A. (2012). Wind loading of trees: influence of tree size and competition. *Eur J Forest Res* 131, 203–217. doi:10.1007/s10342-010-0448-2.

Hale, S. E., Gardiner, B., Peace, A., Nicoll, B., Taylor, P., and Pizzirani, S. (2015a). Comparison and validation of three versions of a forest wind risk model. *Environmental Modelling & Software* 68, 27–41. doi:10.1016/j.envsoft.2015.01.016.

Hale, S., Nicoll, B., and Gardiner, B. (2015b). ForestGALES - A wind risk decision support tool for forest management in Britain. User manual, Version 2.5. Forestry Commission, Edinburgh, U.K., pp58.

Hanewinkel, M., and Peyron, J. L. (2013). The economic impact of storms. *Living with Storm Damage to Forests. What Science Can Tell Us* 3, 55–63.

Hegyi, F. (1974). A simulation model for managing jack-pine stands. *Growth models for tree and stand simulation* 30, 74–90.

Jactel, H., Bauhus, J., Boberg, J., Bonal, D., Castagneyrol, B., Gardiner, B., et al. (2017). Tree Diversity Drives Forest Stand Resistance to Natural Disturbances. *Curr Forestry Rep* 3, 223–243. doi:10.1007/s40725-017-0064-1.

Jarvis, P. G., James, G. B., and Landsberg, J. J. (1976). "Coniferous Forest," in *Vegetation and the Atmosphere Vol 2*, ed. J. L. Monteith (London: Academic Press), 171–240.

Jessome, A. P. (1977). Strength and related properties of woods grown in Canada. *Forestry Technical Report, Eastern Forest Products Laboratory, Canada*, 37 pp.

Kamimura, K., Gardiner, B. A., and Koga, S. (2017). Observations and predictions of wind damage to Larix kaempferi trees following thinning at an early growth stage. *Forestry (Lond)* 90, 530–540. doi:10.1093/forestry/cpx006.

Kamimura, K., Gardiner, B., Dupont, S., and Finnigan, J. (2019). Agent-based modelling of wind damage processes and patterns in forests. *Agricultural and Forest Meteorology* 268, 279–288. doi:10.1016/j.agrformet.2019.01.020.

Kamimura, K., Gardiner, B., Dupont, S., Guyon, D., and Meredieu, C. (2015). Mechanistic and statistical approaches to predicting wind damage to individual maritime pine (Pinus pinaster) trees in forests. *Can. J. For. Res.* 46, 88–100. doi:10.1139/cjfr-2015-0237.

Keller, H. M. (1978). *Snow cover in forest stands*.

Kiernan, D. H., Bevilacqua, E., and Nyland, R. D. (2008). Individual-tree diameter growth model for sugar maple trees in uneven-aged northern hardwood stands under selection system. *Forest Ecology and Management* 256, 1579–1586. doi:10.1016/j.foreco.2008.06.015.

Larouche, C., Guillemette, F., Raymond, P., and Saucier, J.-P. (2013). *Le guide sylvicole du Québec - Tome II : Les concepts et l'application de la sylviculture*. Québec: Publications du Québec Available at: https://acces.bibl.ulaval.ca/login?url=https://search.ebscohost.com/login.aspx?direct=true&db=nlebk&AN=1485651&lang=fr&site=ehost-live.

Lavoie, S., Ruel, J.-C., Bergeron, Y., and Harvey, B. D. (2012). Windthrow after group and dispersed tree retention in eastern Canada. *Forest Ecology and Management* 269, 158–167. doi:10.1016/j.foreco.2011.12.018.

Lundqvist, L. (1996). Stem diameter growth of scots pine trees after increased mechanical load in the crown during dormancy and (or) growth. *Annals of Botany* 77, 59–62. doi:10.1006/anbo.1996.0007.

Ma, Z., Peng, C., Zhu, Q., Chen, H., Yu, G., Li, W., et al. (2012). Regional drought-induced reduction in the biomass carbon sink of Canada's boreal forests. *PNAS* 109, 2423–2427. doi:10.1073/pnas.1111576109.

Mazerolle, M. J. (2019). *AICcmodavg: Model selection and multimodel inference based on (Q)AIC(c)*. Available at: https://cran.r-project.org/package=AICcmodavg.

Meunier, S. (2002). Comparaison de la résistance au renversement du sapin baumier et de l'épinette blanche sur site mésique en sapinière boréale.

Mitchell, S. (2008). Forest Science Program – Final Technical Report 2007/08 : Improvement of a mechanistic risk model for estimating windthrow losses. University of British Columbia, Dept of Forest Sciences.

Mitchell, S. J. (2013). Wind as a natural disturbance agent in forests: a synthesis. *Forestry* 86, 147–157. doi:10.1093/forestry/cps058.

Moore, J. R., Gardiner, B. A., Blackburn, G. R. A., Brickman, A., and Maguire, D. A. (2005). An inexpensive instrument to measure the dynamic response of standing trees to wind loading. *Agricultural and Forest Meteorology* 132, 78–83. doi:10.1016/j.agrformet.2005.07.007.

Morimoto, J., Nakagawa, K., Takano, K. T., Aiba, M., Oguro, M., Furukawa, Y., et al. (2019). Comparison of vulnerability to catastrophic wind between Abies plantation forests and natural mixed forests in northern Japan. *Forestry: An International Journal of Forest Research* 92, 436–443. doi:10.1093/forestry/cpy045.

Mortensen, N. G., Landberg, L., Troen, I., and Petersen, E. L. (1993a). Wind analysis and application program (WASP). *Roskilde, Denmark, Risø National Laboratory*.

Mortensen, N. G., Landberg, L., Troen, I., and Petersen, E. L. (1993b). *Wind Atlas Analysis and Application Program (WAsP)*. 1st ed. Roskilde, Denmark.: Risø National Laboratory.

Mugasha, A. G. (1989). Evaluation of simple competition indices for the prediction of volume increment of young jack pine and trembling aspen trees. *Forest Ecology and Management* 26, 227–235. doi:10.1016/0378-1127(89)90123-0.

Nicoll, B. C., Connolly, T., and Gardiner, B. A. (2019). Changes in Spruce Growth and Biomass Allocation Following Thinning and Guying Treatments. *Forests* 10, 253. doi:10.3390/f10030253.

Normales climatiques canadiennes (2011). Available at: http://climat.meteo.gc.ca/climate_normals/ [Accessed April 9, 2019].

Novak, M. D., Warland, J. S., Orchansky, A. L., Ketler, R., and Green, S. (2000). Wind Tunnel And Field Measurements Of Turbulent Flow In Forests. Part I: Uniformly Thinned Stands. *Boundary-Layer Meteorology* 95, 457–495. doi:10.1023/A:1002693625637.

Nykänen, M.-L., Peltola, H., Quine, C., Kellomäki, S., and Broadgate, M. (1997). Factors affecting snow damage of trees with particular reference to European conditions. *The Finnish Society of Forest Science and The Finnish Forest Research Institute*.

Nyland, R. D. (2003). Even- to uneven-aged: the challenges of conversion. *Forest Ecology and Management* 172, 291–300. doi:10.1016/S0378-1127(01)00797-6.

Offenthaler, I., Hietz, P., and Richter, H. (2001). Wood diameter indicates diurnal and long-term patterns of xylem water potential in Norway spruce. *Trees* 15, 215–221. doi:10.1007/s004680100090.

Peltola, H., Kellomäki, S., Hassinen, A., and Granander, M. (2000). Mechanical stability of Scots pine, Norway spruce and birch: an analysis of tree-pulling experiments in Finland. *Forest Ecology and Management* 135, 143–153.

Peltola, H., Kellomäki, S., and Väisänen, H. (1999). A mechanistic model for assessing the risk of wind and snow damage to single trees and stands of Scots pine, Norway spruce, and birch. 29, 15.

Pinheiro, J., Bates, D., DebRoy, S., Sarkar, D., and R Core Team (2018). *nlme: Linear and Nonlinear Mixed Effects Models*. Available at: https://CRAN.R-project.org/package=nlme.

Poëtte, C., Gardiner, B., Dupont, S., Harman, I., Böhm, M., Finnigan, J., et al. (2017). The Impact of Landscape Fragmentation on Atmospheric Flow: A Wind-Tunnel Study. *Boundary-Layer Meteorol* 163, 393–421. doi:10.1007/s10546-017-0238-1.

Pommerening, A., and Murphy, S. T. (2004). A review of the history, definitions and methods of continuous cover forestry with special attention to afforestation and restocking. *Forestry: An International Journal of Forest Research* 77, 27–44. doi:10.1093/forestry/77.1.27.

Prévosto, B. (2005). Les indices de compétition en foresterie : exemples d'utilisation, intérêts et limites. *Revue Forestière Française* LVIII, 413–430.

Puettmann, K. J., Coates, K. D., and Messier, C. C. (2008). *A Critique of Silviculture: Managing for Complexity*. 1 edition. Washington, DC: Island Press.

Quer, E., Baldy, V., and DesRochers, A. (2020). Ecological drivers of root grafting in balsam fir natural stands. *Forest Ecology and Management* 475, 118388. doi:10.1016/j.foreco.2020.118388.

Quine, C. (1994). An improved understanding of windthrow: moving from hazard towards risk. *Forestry*.

Quine, C. P., and Gardiner, B. A. (2007). "Understanding How the Interaction of Wind and Trees Results in Windthrow, Stem Breakage, and Canopy Gap Formation," in *Plant Disturbance Ecology* (Elsevier), 103–155. doi:10.1016/B978-012088778-1/50006-6.

R Core Team (2018). *R: A Language and Environment for Statistical Computing*. Vienna, Austria: R Foundation for Statistical Computing Available at: https://www.R-project.org/.

Raupach, M. R. (1994a). Simplified expressions for vegetation roughness length and zero-plance displacement as functions of canopy height and area index. *Boundary-Layer Meteorology* 71, 211–216.

Raupach, M. R. (1994b). Simplified expressions for vegetation roughness length and zero-plane displacement as functions of canopy height and area index. *Boundary-Layer Meteorol* 71, 211–216. doi:10.1007/BF00709229.

Raupach, M. R., Finnigan, J. J., and Brunet, Y. (1996). Coherent eddies and turbulence in vegetation canopies: the mixing-layer analogy. *Springer* Boundary-Layer Meteorology 25th Anniversary Volume, 351–382.

Riopel, M., Bégin, J., and Ruel, J.-C. (2010). Probabilités de pertes des tiges individuelles, cinq ans après des coupes avec protection des petites tiges marchandes, dans des forêts résineuses du Québec. *Can. J. For. Res.* 40, 1458–1472. doi:10.1139/X10-059.

Robitaille, A., and Saucier, J. P. (1998). *Paysages régionaux du Québec méridional.* Publication du Québec. Québec: Direction de la gestion des stocks forestiers et Direction des relations publiques, Ministère des Ressources Naturelles du Québec.

Rouvinen, S., and Kuuluvainen, T. (1997). Structure and asymmetry of tree crowns in relation to local competition in a natural mature Scots pine forest. *Canadian Journal of Forest Research*, 890–902.

Rudnicki, M., Lieffers, V. J., and Silins, U. (2003). Stand structure governs the crown collisions of lodgepole pine. *Canadian Journal of Forest Research* 33, 1238–1244.

Rudnicki, M., Meyer, T. H., Lieffers, V. J., Silins, U., and Webb, V. A. (2008). The periodic motion of lodgepole pine trees as affected by collisions with neighbors. *Trees* 22, 475–482.

Rudnicki, M., Silins, U., Lieffers, V. J., and Josi, G. (2001). Measure of simultaneous tree sways and estimation of crown interactions among a group of trees. *Trees* 15, 83–90.

Ruel, J.-C. (1995). Understanding windthrow: Silvicultural implications. *The Forestry Chronicle* 71, 434–445. doi:10.5558/tfc71434-4.

Ruel, J.-C. (2000). Factors influencing windthrow in balsam fir forests: from landscape studies to individual tree studies. *Forest Ecology and Management*.

Saad, C., Boulanger, Y., Beaudet, M., Gachon, P., Ruel, J.-C., and Gauthier, S. (2017). Potential impact of climate change on the risk of windthrow in eastern Canada's forests. *Climatic Change* 143, 487–501. doi:10.1007/s10584-017-1995-z.

Sakamoto, Y., Ishiguro, M., and Kitagawa, G. (1986). Akaike information criterion statistics. *Dordrecht, The Netherlands: D. Reidel* 81.

Schelhaas, M. J., Kramer, K., Peltola, H., van der Werf, D. C., and Wijdeven, S. M. J. (2007). Introducing tree interactions in wind damage simulation. *Ecological Modelling* 207, 197–209. doi:10.1016/j.ecolmodel.2007.04.025.

Schindler, D., Fugmann, H., Schönborn, J., and Mayer, H. (2012). Coherent response of a group of plantation-grown Scots pine trees to wind loading. *European Journal of Forest Research* 131, 191–202.

Schütz, J.-P. (2001). Opportunities and strategies of transforming regular forests to irregular forests. *Forest Ecology and Management* 151, 87–94. doi:10.1016/S0378-1127(00)00699-X.

Seidl, R., Rammer, W., and Blennow, K. (2014). Simulating wind disturbance impacts on forest landscapes: Tree-level heterogeneity matters. *Environmental Modelling & Software* 51, 1–11. doi:10.1016/j.envsoft.2013.09.018.

signal developers (2013). *signal: Signal processing*. Available at: http://r-forge.r-project.org/projects/signal/.

signal developers (2014). *signal: Signal processing*. Available at: http://r-forge.r-project.org/projects/signal/.

Silins, U., Lieffers, V. J., and Bach, L. (2000). The effect of temperature on mechanical properties of standing lodgepole pine trees. *Trees* 14, 424–428. doi:10.1007/s004680000065.

Silva, G. (1996). Étude de la résistance mécanique d'arbres soumis à une simulation de l'action du vent dans la région de l'Outaouais au Québec.

Stadt, K. J., Huston, C., Coates, K. D., Feng, Z., Dale, M. R. T., and Lieffers, V. J. (2007). Evaluation of competition and light estimation indices for predicting diameter growth in mature boreal mixed forests. *Ann. For. Sci.* 64, 477–490. doi:10.1051/forest:2007025.

Taylor, A. R., Dracup, E., MacLean, D. A., Boulanger, Y., and Endicott, S. (2019). Forest structure more important than topography in determining windthrow during Hurricane Juan in Canada's Acadian Forest. *Forest Ecology and Management* 434, 255–263. doi:10.1016/j.foreco.2018.12.026.

Valinger, E. (1996). Wind and snow damage in a thinning and fertilization experiment in Picea abies in southern Sweden. *Forestry* 69, 25–34. doi:10.1093/forestry/69.1.25.

Valinger, E., and Fridman, J. (1997). Modelling probability of snow and wind damage in Scots pine stands using tree characteristics. *Forest Ecology and Management* 97, 215–222.

Valinger, E., Lundqvist, L., and Bondesson, L. (1993). Assessing the Risk of Snow and Wind Damage from Tree Physical Characteristics. *Forestry* 66, 249–260. doi:10.1093/forestry/66.3.249.

Vitkova, L., and Dhubháin, Á. N. (2013). Transformation to continuous cover forestry - a review. *Irish Forestry*, 119–140.

Wallentin, C., and Nilsson, U. (2014). Storm and snow damage in a Norway spruce thinning experiment in southern Sweden. *Forestry (Lond)* 87, 229–238. doi:10.1093/forestry/cpt046.

Wellpott, A. (2008). The stability of continuous cover forests.

Wickham, H. (2016). *ggplot2: Elegant Graphics for Data Analysis*. Springer-Verlag New York Available at: https://ggplot2.tidyverse.org.

Zhu, J., Matsuzaki, T., Lee, F., and Gonda, Y. (2003). Effect of gap size created by thinning on seedling emergency, survival and establishment in a coastal pine forest. *Forest Ecology and Management* 182, 339–354. doi:10.1016/S0378-1127(03)00094-X.